Air Separation on Carbon Molecular Sieves, 4A and 5A Zeolites by Pressure Swing Adsorbtion

by

Manzoor Zahur

A Thesis Presented to the

FACULTY OF THE COLLEGE OF GRADUATE STUDIES

KING FAHD UNIVERSITY OF PETROLEUM & MINERALS

DHAHRAN, SAUDI ARABIA

In Partial Fulfillment of the
Requirements for the Degree of

MASTER OF SCIENCE

In

CHEMICAL ENGINEERING

January, 1991

Air Separation on Carbon Molecular Sieves, 4A and 5A Zeolites by Pressure Swing Adsorption

BY

Manzoor Zahur

A Thesis Presented to the

FACULTY OF THE COLLEGE OF GRADUATE STUDIES

KING FAHD UNIVERSITY OF PETROLEUM & MINERALS

DHAHRAN, SAUDI ARABIA

In Partial Fulfillment of the

Requirements for the Degree of

MASTER OF SCIENCE

In

CHEMICAL ENGINEERING

January, 1991

KING FAHD UNIVERSITY OF PETROLEUM & MINERALS

DHAHRAN, SAUDI ARABIA

This thesis, written by

MANZOOR ZAHUR

under the direction of his thesis committee, and approved by all the members, has been presented to and accepted by the Dean, College of Graduate Studies, in partial fulfillment of the requirements for the degree of

MASTER OF SCIENCE IN CHEMICAL ENGINEERING

Thesis Committee

Mirza Maniful Hassan
Chairman (Dr. Mirza M. Hassan)

Kevin F. Loughlin
Member (Dr. Kevin F. Loughlin)

Shafkat Ali Beg.
Member (Dr. Shafkat A. Beg)

Dr. Mazen A. Shalabi
Department Chairman

Dr. Ala H. Rabeh
Dean College of Graduate Studies

Date : 15-5-91

This thesis is dedicated

To

My beloved parents, sisters, brothers and wife

for the sacrifices they made to educate me.

ACKNOWLEDGEMENT

Praise and gratitude be to Allah Almighty, with whose gracious help it was possible to accomplish this work. Acknowledgement is due to King Fahd University of Petroleum and Minerals for extending all facilities and providing financial support.

I would like to offer my indebtedness and sincere appreciation to my committee chairman Dr. Mirza M. Hassan, who has been a constant source of help and encouragement during this work. I also greatly appreciate the invaluable co-operation and support extended by Dr. Shafkat A. Beg, who served as one of the committee members. Thanks are due to Dr. Kevin F. Loughlin, who also served as a member of thesis committee.

I wish to acknowledge the assistance given by Mr. John Chapman, Mr. Bashir Ahmed, Mr. Jim Butcher, and Mr. Syed Kamal Ahmed for their help during experiments. I also express my thanks to my friends, Mr. Salman Ahmed Chishty, Mr. Yaqoub Mohamed, Mr. Imaduddin S. Javed, Mr. Aqil Jamal, Mr. Azam Baig, Mr. Ashraf Fatehi and Mr. Yusuf Jani, for their help and co-operation.

I owe my parents and relatives an expression of gratitude for their patience understanding and encouragement. I would like to thank my beloved wife Asma, for her patience and support throughout the course of this work.

Lastly, but not least, I am thankful to all faculty, colleagues and friends who made my stay at the university a memorable and valuable experience.

TABLE OF CONTENTS

Page

LIST OF TABLES

LIST OF FIGURES

THESIS ABSTRACT

NAME OF STUDENT : *MANZOOR ZAHUR*

TITLE OF STUDY : *Air Separation on Carbon Molecular Sieves, 4A and 5A Zeolites by Pressure Swing Adsorption.*

MAJOR FIELD : *Chemical Engineering*

DATE OF DEGREE : *January, 1991*

This work describes the results of a chromatographic study of sorption equilibria and kinetics of nitrogen and oxygen in carbon molecular sieves. The temperature dependence of the experimental equilibrium constants and micropore diffusivity is correlated by the Van't Hoff and Arrhenius equations respectively.

A single column pressure swing adsorption (PSA) unit has been designed and constructed to study the separation of air on carbon molecular sieves (CMS), 4A and 5A zeolites. The effect of various operating parameters on the performance of the unit is reported. The results from the analysis of PSA air separation on CMS show that a fairly high purity nitrogen product (> 98 %) can be easily obtained. Experimental studies of PSA air separation on 5A-zeolite reveal that efficient separation can be achieved to yield a oxygen product containing 4-5 % residual nitrogen. In case of 4A-zeolite using oxygen as purge the results show that a product containing 88 % oxygen can be obtained. If nitrogen is used as purge, for the production of nitrogen on 4A-zeolite a product concentration containing 0.8% oxygen can be achieved. It was observed that an increase in purge to feed ratio, L/v_H *ratio and desorption time increase the product purity. On the other hand pressure ratio and cycle time shows some optimum values for all three systems.*

The theoretical model of Farooq and Ruthven [69] was used after minor modification to predict the results for air separation on carbon molecular sieve. The model predictions agree reasonably well with the experimental data.

MASTER OF SCIENCE DEGREE

KING FAHD UNIVERSITY OF PETROLEUM AND MINERALS

Dhahran , Saudi Arabia

January 1991

ملخص رسالة ماجستير

إســـــم الطالب : منظور ظهور

عنوان الدراسة : فصل الهواء على الكربون الجزيئي المنخل (٤أ ، ٥أ زيوليت) باستعمال الامتصاص تحت الضغط المتيغر .

التخصـــــص : الهندسة الكيميائية .

تاريخ الورقـــة : يناير ١٩٩١م

إن هذا العمل يصف نتائج الدراسة الكروموتجرافية لتوازن الامتصاص وطبيعة حركة النيتروجين والاكسجين في الكربون الجزيئي المنخل . وقد وجد ان معادلات فانت هوف وارهينيور تمثل جيداً ثوابت الاتزان والانتشار الدقيق على الترتيب .

ولقد تم تصميم وبناء عمود واحد لدراسة فصل الهواء على الكربون الجزيئي المنخل من الأنواع (٤أ ، ٥أ زيوليت) وقد تمت دراسة تأثير المتغيرات التشغيلية على أداء العمود ، وتبين من الدراسة التحليلية ان النيتروجين المفصول ذو نقاوة عالية ٩٨٪ وكذلك احتوى الاكسجين المفصول على زيوليت $أ على أ٤ - ٥) ٪ من النيتروجين المتبقي وفي حالة ٥أ زيولايت وباستعمال الاكسجين كمنظف فان النتائج اظهرت انه يمكن الحصول على ناتج نقاوة ٨٨٪ .

وفي حالة استعمال النيتروجين كمنظف فان النيتروجين المفصول به ٠.٨٪ فقط من الاكسجين .

وقد لوحظ أنه بزيادة نسبة تدفق الغاز المنظف الى تدفق الهواء وكذلك زيادة وقت الامتصاص يزيد من نقاوة المنتج . ومن ناحية أخرى فان نسب الضغط ووقت الدورة أظهرا قيم فضلي للأنظمة الثلاثة . وقد تم استعمال موديل فاروق و روتفن [77] بعد تعديلات طفيفة للتنبؤ بفصل الهواء على الكربون الجريز المنخل وقد كانت قدرة الموديل على التنبؤ عالية بحيث وافقت النتائج المخبرية .

درجة الماجستير في العلوم

جامعج الملك فهد للبترول والمعادن

الظهران - المملكة العربية السعودية

يناير ١٩٩١م

CHAPTER 1

INTRODUCTION AND OBJECTIVES

1.1 GENERAL INTRODUCTION:

Separation processes have been studied, developed and utilized in practically all disciplines of science, engineering and medicine. The reason for this development is due to the fact that although elements, mixtures and compounds do exist in nature and materials are synthesized, they are not in the required degree of purity. In most cases what is available and what is needed seldom match, hence the importance of separation science and technology. A separation process can be as simple as sedimentation or as elaborate as isotope separation. In deciding a particular separation process, the important consideration is usually the economic factor, when there is a choice available. This selection process continues with time, since ongoing research and development may alter the economic viability of a process.

Gas separation processes are witnessing significant technological innovation [1]. At present liquefaction processes used for gas separation are now facing competition from adsorptive separation processes. Most of the gas separation processes used can be broadly put under the headings of purification, wherein

small quantities of undesired components are to be removed, or bulk separations wherein two or more components are to be recovered. In the former case where small amounts of material are to be removed from the bulk of the gas, the adsorption process is suitable.

Adsorption is primarily a physical phenomena where molecules of various fluids get trapped into the porous structure of some solids. Due to the difference in polarity and molecule size between fluid and solid, molecules of gas or liquid, as soon as they come into contact with the solid surface, adhere to it. Large scale adsorption processes are in operation either as a cyclic batch system in which the adsorbent bed is alternatively saturated and regenerated in a cyclic manner or as continuous flow systems which are normally counter current contactors between the feed and the adsorbent. Cyclic batch systems are preferred where the separation factor is high and mass transfer resistance is low due to their low capital cost.

Selectivity forms the basis of the adsorption process. This depends either on the ratio of the adsorption equilibrium or adsorption kinetics. For equilibrium selectivity a separation factor (α_{AB}) may be defined, which measures the relative affinity for the components [2].

$$\alpha_{AB} = \frac{X_A/X_B}{Y_A/Y_B} \qquad \text{----------(1.1)}$$

where :

X_A and Y_A are respectively, the mole fractions of component A in adsorbed and fluid phases at equilibrium.

A simple example is the separation of oxygen-nitrogen mixture which exhibits a good equilibrium selectivity when the adsorbent used is 5A and close to unity when the adsorbent is CMS. In the case of kinetic selectivity the ratio of micropore or intracrystalline diffusivities for the components determines the selectivity. Kinetic separations are feasible in molecular sieve adsorbents such as zeolites or CMS where the diameter of the micropore is comparable with that of the diffusing molecule.

The requirement for adequate adsorptive capacity restricts the choice of adsorbents for practical separation processes to microporous adsorbents with pore diameters ranging from a few Angstroms to tens of Angstroms. This includes both the traditional microporous adsorbents such as silica gel, activated alumina, and activated carbon as well as the recently developed crystalline aluminosilicates or zeolites, or carbon molecular sieves.

The development of CMS and synthetic zeolites [3], stimulated the research of separating gas mixtures by adsorption [4]. A relatively new trend has been the use of pressure swing adsorption (PSA) for gas separation, originally developed in 1959. This process is sometimes called heatless adsorption to differentiate it from the thermal swing adsorption process. Pressure swing adsorption was first introduced by Skarstrom [5], for separation of air.

Nowadays pressure swing units are widely used for air separation, both small scale for production of medical oxygen and, increasingly, on a large scale as an alternative to the cryogenic process for production of industrial oxygen and nitrogen. There are two different types of process in common use. Processes which utilize a zeolite adsorbent depend on the preferential adsorption of nitrogen under equilibrium conditions, where as processes which use a carbon molecular sieve depend on a kinetic separation in which oxygen, the faster diffusion species, is preferentially adsorbed. The type of cycles, the conditions of operation, and the product purities are quite different for these two types of process.

The process was initially used commercially for air drying and other purification processes [1]. Many process developments have been implemented based on the Skarstrom cycle. Presently, PSA is used commercially for hydrogen purification, hydrogen production, n-paraffin separation, air separation, and more newly implemented applications [6].

1.2 OBJECTIVES OF THIS STUDY:

The present study is undertaken to determine the kinetic and equilibrium parameters for the sorption of oxygen and nitrogen on CMS. A literature search reveals that little information is available on the kinetic and equilibrium parameters for the sorption of oxygen and nitrogen on CMS [7,8,9,10]. The literature survey also reveals that the kinetic and equilibrium properties vary for different CMS samples. In this study experiments are carried out to determine

the micropore diffusivities and adsorption equilibrium constants of oxygen and nitrogen in CMS for wide ranges of temperatures by the chromatographic method, to evaluate the activation energies and isosteric heats of adsorption.

An experimental study is also undertaken in order to assess the feasibility of separating air by PSA on CMS, 4A and 5A zeolites. In CMS oxygen having smaller diameter diffuses faster than nitrogen. This system represents the kinetic separation case. On the other hand for air separation on 5A zeolite, both oxygen and nitrogen diffuse very easily in the wider lattice of 5A zeolite indicating negligible intracrystalline diffusional resistance. Nitrogen being more strongly adsorbed on 5A as compared to oxygen serves as the basis for equilibrium separation. In the case of 4A zeolites, while diffusion favours the sorption of oxygen, equilibrium favours the sorption of nitrogen and therefore represents a mixed phenomena. We, therefore have taken two extreme cases of kinetic separation (as in CMS) and equilibrium separation (as in 5A), and a mixed case (as in 4A). These adsorbents were selected because little work has been done in considering the two extreme cases of selectivity, such as kinetic as in CMS, equilibrium as in 5A and the mixed case (kinetic+equilibrium) as in 4A zeolite.

The research investigation also focuses on the effect of various operating parameters (e,g length/velocity, purge to feed ratio, cycle time, pressure ratio) on the performance of the system for all three adsorbents at room temperature.

CHAPTER 2

LITERATURE REVIEW

2.1 SELECTION OF ADSORBENT:

Selectivity forms the basis of the adsorption process. This depends either on the ratio of the adsorption equilibrium or adsorption kinetics. For equilibrium selectivity a separation factor (α_{AB}) may be defined by Equation (1.1), which measures the relative affinity for the components [2].

Unlike the distillation process, where the selectivity is a function of the components concerned, the sorption selectivity also depends on the adsorbent in use. Hence even for a two component system each adsorbent will exhibit a particular selectivity thereby giving the designer a wider choice.

Kinetic separations are in general possible only with molecular sieve adsorbents such as zeolites or carbon sieves. The kinetic selectivity is measured by the ratio of the micropore or intracrystalline diffusivities for the components considered. Differences in diffusion rates between molecules of comparable molecular weight may become large enough to provide a useful separation only when diffusion is hindered by steric effects. This require that the diameter of the micropore be comparable with the dimension of the diffusing molecule.

2.2 DESCRIPTION OF ADSORBENT :

The primary requirement for economic separation process is an adsorbent that has sufficient selectivity, capacity and stability. Selectivity depends on a difference in either adsorption kinetics or adsorption equilibrium. To be practically useful an adsorbent must have a reasonably high capacity; otherwise the size of the equipment needed for the separation process becomes uneconomically large. To achieve the required capacity the adsorbent must have a high specific surface area which requires highly porous material with fine pores.

Various adsorbents are used in industry for various applications. A summary of the adsorbents along with the application is given in Table 2.1. We will discuss here only CMS, 4A and 5A zeolite, which will be used in the present study.

2.2.1 CARBON MOLECULAR SIEVES (CMS) :

It has been produced since about the mid 1970's. It interests researches because of its unique ability to perform a kinetic separation based on the different pore diffusion rates of different gas molecules. The earliest examples of CMS appear to have been prepared by decomposition of polyvinyldene dichloride (Saran) but a wide variety of starting materials have also been used [11,12]. Most commercial carbon sieves are prepared from anthracite or hard coal by controlled oxidation and subsequent thermal treatment [13]. The pore

Table 2.1. Representative Commercial Gas-Adsorption Separations [2]

Separation	Adsorbent
I. Gas bulk separation	
Normal paraffins/iso-paraffins, aromatics	zeolite
N_2 / O_2	zeolite
O_2 / N_2	CMS
CO, CH_4, CO_2, N_2, A, NH_3/H_2	zeolite, activated carbon
Acetone/vent streams	activated carbon
C_2H_4/*vent streams*	activated carbon
II. Gas purification	
H_2O/*olefin-containing cracked gas, natural gas,* air synthesis gas, etc.	silica, alumina, zeolite
CO_2/C_2H_4, *natural gas, etc.*	zeolite
Organics/vent streams	activated carbon,others
Sulfur compounds/natural gas, hydrogen,	zeolite
liquefied petroleum gas(LPG), etc solvents/air	activated carbon
Odors/air	activated carbon
NO_x/N_2	zeolite
SO_2/*vent streams*	zeolite
Hg/chlor-alkali cell gas effluent	zeolite

Adsorbates are listed first.

structure may be modified to some extent by subsequent treatments including controlled cracking of hydrocarbon within the micropore system and partial gasification under carefully regulated conditions [14,15].

By these means it is possible to prepare carbon sieves with effective micropore diameters ranging from about 4 to 9 A°. The micropore size distribution of such sieves is much narrower than in a typical activated carbon and the porosity and therefore the adsorptive capacity are generally very much smaller. The ability to modify the effective pore size by adjusting the condition of the manufacturing process makes it relatively easy to tailor a carbon sieve to achieve a particular separation.

A review of proposed applications of CMS has been given by Juntgen [16]. At present the most important large-scale application is in air separation.

2.3. ZEOLITES:

Zeolites show high selectivity toward polar molecules and molecules with high quadrupole moments. This is due to the fact that the zeolite crystal is an ionic structure and therefore has large electrostatic field gradients within the micropores. Polar molecules and molecules with quadrupole moments can interact energetically with this electrostatic field and are therefore more strongly adsorbed than nonpolar molecules. It is this property which makes the zeolites very good dessicants as well as selective sorbents for separation of compounds.

2.3.1. STRUCTURE AND CHEMICAL COMPOSITION OF ZEOLITES :

The structure of many zeolites have been described and discussed extensively by Barrer [17], Breck [18], Shoemaker and Seff [19], Reed and Breck [20], and Shoemaker and Broussard [21]. Molecular sieves are synthetic crystalline aluminosilicates, honeycombed with cavities which are interconnected by micropores varying from about 3 to 10 A° in diameter. Smith [22], has defined a zeolite as an "aluminosilicate with a framework structure enclosing cavities, occupied by large ions and water molecules, both of which have considerable freedom of movement, permitting ion exchange and reversible dehydration". The generalized structural formulae is given by:

$$M_{x/n}\left[(AlO_2)_x\ (SiO_2)_y\right]\ W\,H_2O \qquad \text{----------(2.1)}$$

where 'M' denotes a cation of valence n, W is the number of water molecules, x and y are the number of aluminium and silicon tetrahedra respectively. The term in the square bracket in the above formula gives the framework structure of the zeolites.

The fundamental building units in zeolites are tetrahedra of SiO_4 and AlO_4, where the small Si and Al are surrounded by four oxygen ions as shown in Figures 2.1 and 2.2. Each SiO_4 tetrahedron is electrically neutral whereas each

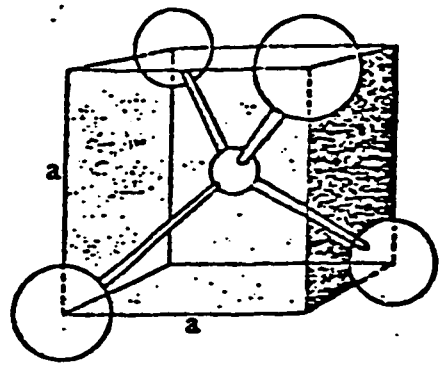

Figure 2.1 Tetrahedron of Oxygen Coordinate with Silicon [2].

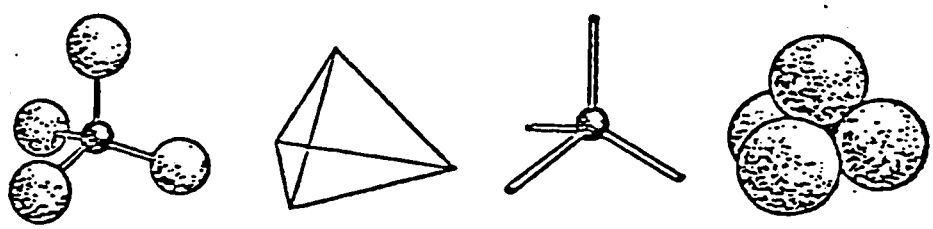

Figure 2.2 Method of Representing the Tetrahedral Coordination of Oxygen Ions with Aluminium and Silicon [2].

AlO_4 unit has one excess negative charge which must be balanced by an exchangeable cation. The structures of most zeolites can be more easily visualized in terms of polyhedra (secondary building units) which are themselves assemblages of tetrahedra. One of the polyhedra usually used to describe types A, X, or Y type of zeolite is known as the sodalite cage. This unit, shown in Figure 2.3, is a truncated octahedron with eight hexagonal and six square faces. Each edge of the sodalite unit represents an oxygen ion located near the centre of the edge with silicon or aluminium ions at the corners. The sodalite structure encloses a spherical cavity having internal diameter of about 6.6 A° and is sometimes referred to as the β cage. The six membered oxygen ring giving access to this cavity has a pore diameter of about 2.2 A°.

2.3.2 ZEOLITE-A :

The structure of zeolite-A is made up from sodalite cages placed at the corners of a 12.3 A° cube and joined together by four membered oxygen bridges. The cage contains a nearly spherical cavity of approximate volume 776 A° and free diameter of 11.4 A° and is shown in Figure 2.4. These cavities are interconnected through eight membered oxygen rings of free diameter about 4.2 A°. The large cages of the type A structure are sometimes referred to as the α cages. The six-membered oxygen rings which give access to the sodalite cages are too small to admit all except the smallest of molecules, (like NH_3 , H_2O) so most adsorbed species are confined to the central cavity and the sodalite cage can be

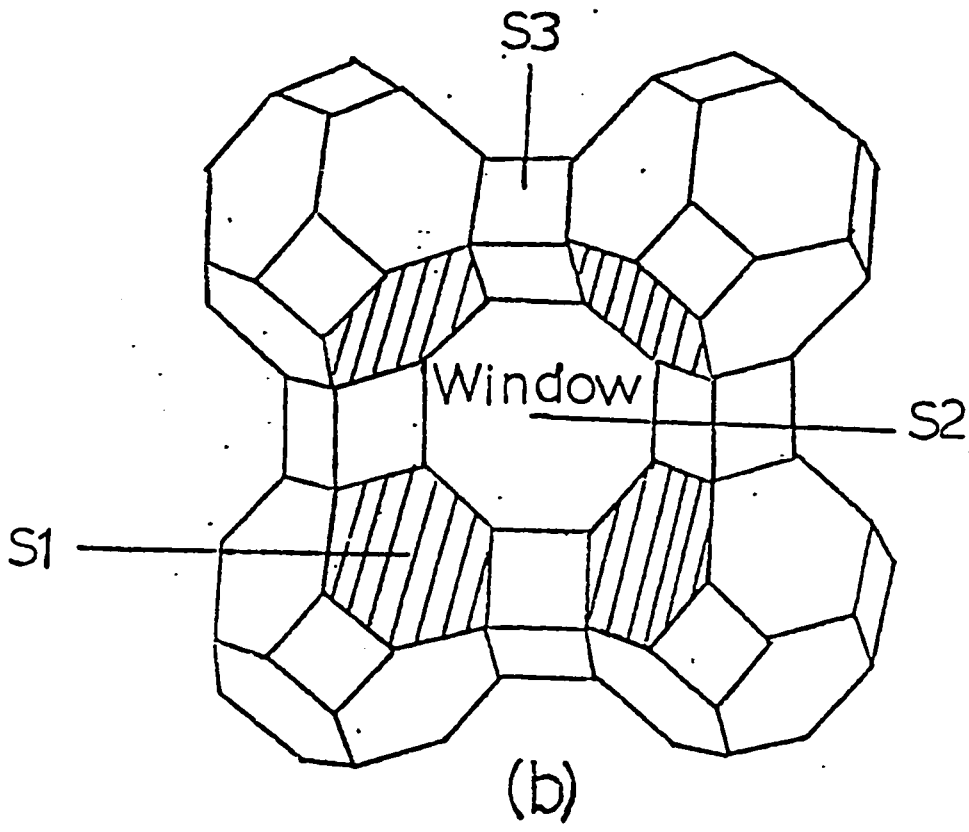

Array of Sodalite Cages in the framework of zeolite A

S1 - First principal cation sites(8 per cavity)
S2 - Second preferential cation sites(3 per cavity
S3 - Third preferential cation sites (3 per cavity)

Figure 2.3 Array of Sodalite Cages in the Framework Zeolite-A [22].

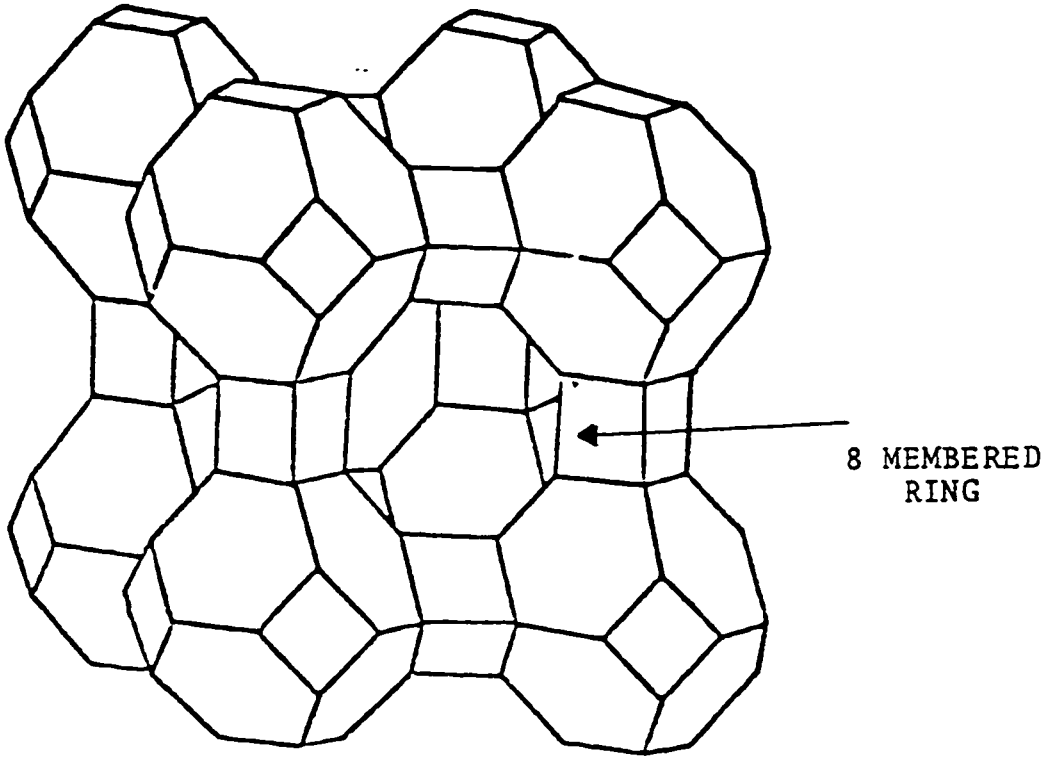

Figure 2.4 Unit Cell of A Type Zeolite Showing Eight-Membered Ring [22]

considered simply as a building block for the crystal structure. A diagram of (110) section of this structure is shown in Figure 2.5.

2.3.3 CATION DISTRIBUTION IN ZEOLITE-A :

The cation positions in type A zeolites are well known [24]. The ideal chemical composition of NaA zeolite per pseudo unit cell is given by :

$$Na_{12}\left[(AlO_2)_{12}\ (SiO_2)_{12}\right] \qquad \text{----------(2.2)}$$

In a well dehydrated sieve the most energetically favorable positions (Type I site) are at the centres of the eight hexagonal windows in the corners of the α cage. The next most favorable site is within the eight-membered oxygen ring (type II) and the least favorable site is close to the four-membered oxygen ring (type III site). Since there are six divalent Ca^{++} ions in calcium A zeolite, all these ions can be accommodated in the most favorable sites (at the centre of the six rings) and away from the eight-membered oxygen ring. The diffusion path is therefore unobstructed. The free aperture is about 4.3 A° and the unobstructed sieve is known as 5A (CaA) zeolite. Because of the effect of molecular vibration it can admit molecules with critical diameter of about 5 A° , which includes normal but not branched or cyclic hydrocarbons. However, in the case of NaA zeolite there are twelve monovalent sodium ions, having ionic radius of 0.97 A°,

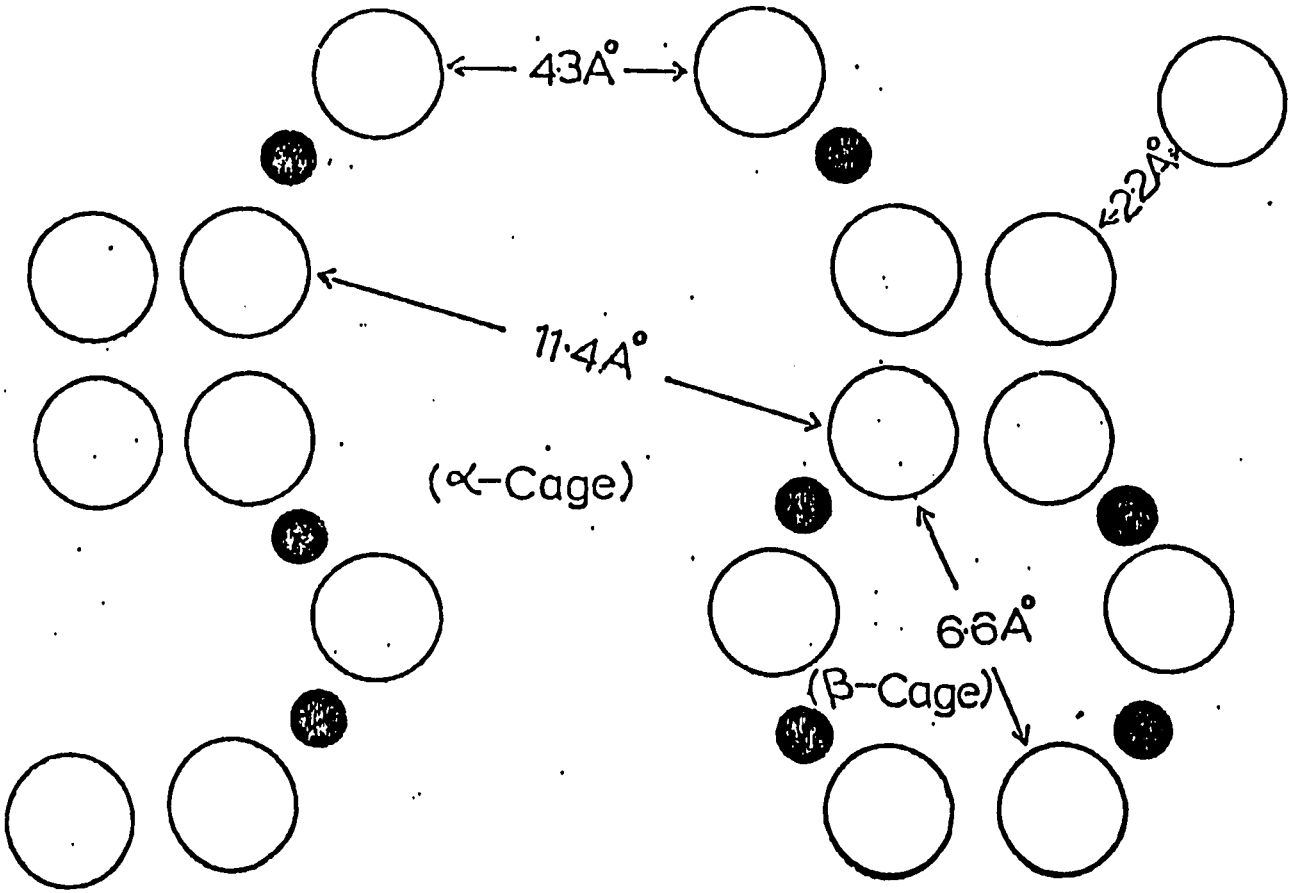

Figure 2.5 A Diagram of (110) Section of Zeolite-A Structure [22].

eight of which are accommodated in sites of type I and three in sites of type II (there are three eight-membered oxygen rings per cavity since each window is shared between two cavities) and one cation in a type III site as shown in Figure 2.3b. The presence of cations within the eight-membered oxygen ring reduces the free diameter of the windows between the cavities. Thus the 4A sieve can admit only molecules with critical diameters less than 4 A°.

2.4 DIFFUSION IN ADSORBENT

In commercial adsorbent pellets there are three distinct resistances to mass transfer: external fluid film, macropore diffusion and micropore (intracrystalline) diffusion as sketched in Figure 2.6. Depending on the relative magnitude either a single resistance may be controlling or more than one resistance may be significant.

2.4.1 TRANSPORT IN EXTERNAL FILM :

The mass transfer rate from bulk fluid phase to the exterior of the particle is correlated by the linear driving force rate expression as,

$$\frac{\partial q}{\partial t} = k_f a_p (c - c^{*}) \qquad \text{----------(2.3)}$$

The mass transfer coefficient for a single sphere surrounded by stagnant fluid is given by [25];

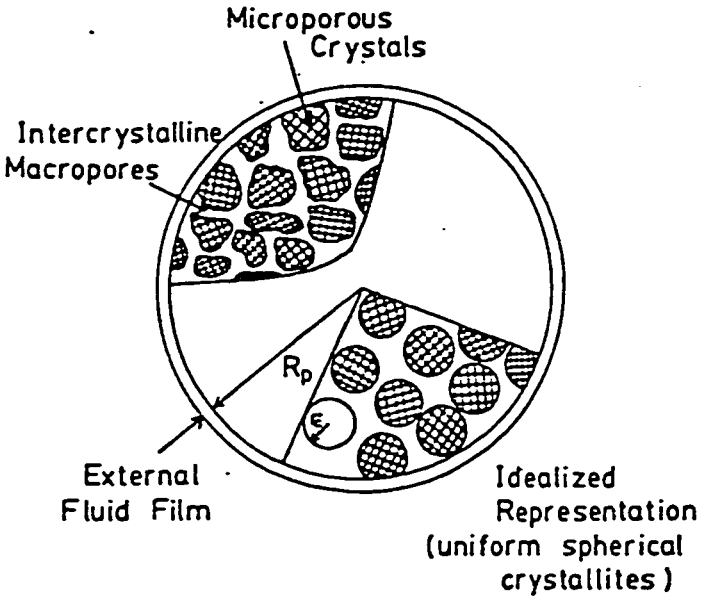

Figure 2.6 **Schematic Diagram of Composite Adsorbent Pellet [2].**

$$\frac{k_f(2R_p)}{D_m} = 2.0 \qquad \text{----------(2.4)}$$

In analogy to the correlation of the heat transfer coefficient for forced convection around a sphere, the following correlation for mass transfer coefficient has been proposed [26].

$$N_{AB} = Sh = 2.0 + 0.6\,(Re)^{1/2}\,(Sc)^{1/3} \qquad \text{----------(2.5)}$$

where the Nusselt number for mass transfer is defined as :

$$N_{AB} = \frac{2R_p k_f}{D_{AB}} \qquad \text{----------(2.6)}$$

2.4.2 TRANSPORT IN MACROPORES :

The mechanism by which the solute is transported within the macropore structure of a porous solid such as a zeolites and CMS adsorbent can be described by molecular diffusion, Knudsen diffusion, and diffusion due to

Poiseulle flow. Molecular diffusion in a porous material becomes dominant when the molecules collide more often with each other, than with the pore walls. This situation arises when the mean free path of the molecule is smaller than the pore diameter of the sorbent. The molecular diffusivity, can be calculated using the well known correlation of Chapman-Enskog [27] as given by :

$$D_{AB} = \frac{.0018583 \times T^{3/2} \sqrt{\frac{M_A + M_B}{M_A M_B}}}{P\sigma^2_{AB}\Omega} \qquad \text{----------(2.7)}$$

where M_A and M_B are the molecular weights of two species of gases, T is the absolute temperature, P is the total pressure (atm), Ω is the collision integral, and σ is the force constant in the Lennard-Jones potential function. If the molecules in the pore collide more frequently with the walls than among themselves, transport occurs mainly by Knudsen diffusion, This situation arises when the mean free path of the molecule is larger than the pore diameter. The expression for Knudsen flow has been derived from the kinetic theory of gases and is given by:

$$D_K = 9700\, r_A \sqrt{T/M} \qquad \text{----------(2.8)}$$

where D_K is Knudsen diffusivity, r_A is macropore radius, T is the absolute temperature, and M is the molecular weight of the species.

Another kind of diffusive transport can occur due to Poiseulle flow and its contribution may be significant in large pores and at high pressure. However for most gas-solid systems this contribution is very small and can generally be neglected.

2.4.3 TRANSPORT IN MICROPORES :

Five diffusion coefficients have been defined for two species of diffusing molecules by Crank [28] given by, D_{AB} mutual diffusion coefficient, D_A intrinsic or self diffusion coefficient for component A and D_B ,self diffusion coefficient of B, and two tracer diffusion coefficients D_A^*, D_B^*. In the case of the gas CMS system, if one considers component A to be the gas and B to be the CMS and if the particle of CMS can be considered as rigid, the intrinsic and tracer diffusion D_B, D_B^* are effectively zero. The expression for D_{AB} then reduces simply to D_A. In the above situation one is left with two diffusivities given by D_A , and D_A^*,

The relationship between the intrinsic diffusion coefficient, D_A and tracer diffusion coefficient D_A^*, was deduced by Ash and Barrer [29], and Karger [30], by considering the chemical potential as the driving force for diffusion instead of concentration gradient and using the principles of irreversible thermodynamics:

$$D^{*} = D\left[1 - \frac{C L_{AA^{*}}}{C^{*} L_{AA}}\right] \frac{\partial \ln C}{\partial \ln a} \qquad \text{----------(2.9)}$$

where 'a' is the activity of the diffusion at a point where its concentration is C, $L_{AA^{*}}$ is the cross-coefficient between traced and untraced molecule of A having same mobility in the irreversible thermodynamic formulation of diffusion, and C^{*} is the concentration of labelled species at a point where the concentration of the unlabeled species is C. Since the cross coefficient arises from direct interaction between A and A^{*}, it should be significant whenever the sorbate is sufficiently concentrated for such encounters to become frequent. However, within the Henry's law region the concentration is low and such encounters occur relatively infrequently and under these condition the interference effect can be neglected ($L_{AA^{*}} = 0$) and Equation (2.9) reduces to :

$$D^{*} = D \frac{\partial \ln C}{\partial \ln a} \qquad \text{----------(2.10)}$$

and is known as Darkens[31] relation. In the Henry's law region, the concentration correction factor, $\frac{\partial \ln C}{\partial \ln a}$ reduces to unity. The intrinsic diffusion coefficient becomes equal to the tracer diffusion coefficient and the tracer diffusion coefficient may be replaced by limiting diffusivity at zero sorbate

concentration, D_o. Under these circumstances Equation (2.10) reduces to:

$$D = D_o \frac{\partial \ln a}{\partial \ln C} \qquad \text{----------(2.11)}$$

Since at low concentration $a \propto p$, Equation (2.11) can be written as:

$$D = D_o \frac{\partial \ln P}{\partial \ln C} \qquad \text{----------(2.12)}$$

2.5. TEMPERATURE DEPENDENCE OF SORPTION PARAMETERS :

The temperature dependence of the equilibrium constants, K_p is correlated, by Van't Hoff types of equation given by:

$$K_p = K_o Exp(-\Delta U_o / RT) \qquad \text{----------(2.13)}$$

where U_o is related to the limiting heat of sorption by

$$\Delta U_o = \Delta H_o + RT \qquad \text{----------(2.14)}$$

Experimental results are plotted as K_p vs. 1/T in semi-logarithmic coordinates and the values of K_o , ΔU_o derived from the slope and intercept.

The temperature dependence of micropore diffusivity can be adequately described by the Arrhenius type of equation by,

$$D = D_o \, Exp(-E/RT) \qquad \text{----------(2.15)}$$

The values of D_o and E are derived from the slope and intercept of the diffusivity values plotted against the reciprocal temperature in semi-logarithm coordinates.

CHAPTER 3

THEORETICAL MODEL AND ANALYSIS OF CHROMATOGRAPHIC EXPERIMENTS

3.1 INTRODUCTION:

The problem of modelling the packed column consists of writing and solving fluid mass balance partial differential equations. Lapidus and Amundson [32] made an early theoretical contribution to the analysis of the dynamic response of an adsorption column. They obtained an analytical solution for the step response of a column subject to a step change in sorbate concentration at the bed inlet. Their model included both finite mass transfer resistance with linear equilibrium. Kubin [33] and Kucera [34] provided major contributions by deriving the relationship between the second moment of the pulse response and the external film mass resistance and intraparticle diffusion. The model of Suzuki and Smith[35] is applicable to particles having unimodel pore size distribution. If this model is used to determine the rate parameters in a biporous solid, such as zeolite and CMS the results may be in error. Hence for accurate interpretation of pulse data in these solids, a model which is based on bidisperse pore size distribution should be applied. Hashimoto and Smith [36], and Haynes and Sharma [37,38] presented such a model for bimodal pore structure relating

the moments of the pulse response to axial dispersion, macropore diffusivity, micropore diffusivity and external fluid to particle surface diffusional process in zeolite. Their correlation was simplified by Ruthven and Shah [39] for high values of equilibrium constant ($K_p >> 1.0$). In a biporous system a single effective diffusion coefficient cannot properly describe the mass transfer when the contribution from both macro and micropore are important. If a single resistance model is to be used the experimental conditions must be selected to ensure that either macro or micropore resistance is controlling.

3.1.1 EXTERNAL FILM MASS TRANSFER RESISTANCE :

The external diffusional mass transfer resistance is given by the terms $(\varepsilon/(1-\varepsilon))(R_p/3k_f)$ and in film theory the entire diffusional resistance is assumed to be concentrated in the fictitious film around the particle. The mass transfer coefficient depends in general on the velocity and diameter of the particle as given by Equation (2.5 and 2.6). Roberts and York [40] have also shown that a similar form of correlation is satisfactory for data in packed beds at low Reynolds number. They proposed the following correlation :

$$Sh = \frac{2 R_p k_f}{D_{AB}} = 2.0 + 1.45\,(\mathrm{Re})^{1/2}\,(Sc)^{1/3} \qquad \text{----------(3.1)}$$

at Re < 100.

At low Reynold number, the two equations give identical results, i.e., $Sh = \frac{2 R_p k_f}{D_{AB}} = 2.0$ and the mass transfer coefficient is given by :

$$R_p k_f = D_{AB} \qquad \text{----------(3.2)}$$

It becomes clear from Equation (3.2) that the mass transfer coefficient at low Reynolds number is independent of velocity and is inversely proportional to the particle size. Since all the experimental runs in this study were performed at low Reynolds number, the highest Reynolds number being 0.5, Equation (3.2) was used to estimate the external film mass transfer resistance coefficient. The value of k_f obtained in such a calculation was relatively high, giving very small values of external film diffusional resistance and consequently contributing very little to the second moment or variance of the pulse-response curve and therefore can be neglected.

3.1.2 MACROPORE MASS TRANSFER RESISTANCE :

The macropore resistance to mass transfer is given by the term $(\varepsilon/(1-\varepsilon))\ (R^2_p/15\varepsilon_p D_p)$. The macropores of the CMS sieve are relatively large and if it is assumed that the dominant transport mechanism in macropores of CMS is by molecular diffusion, then the macropore diffusivity, D_p can be related to molecular diffusion by :

$$D_p \leq D_{AB}/\tau \qquad \text{----------(3.3)}$$

Hence an approximate estimate can be obtained for the value of D_p from Equation (3.3) using the value of τ of 2-3 as given by Roberts and York [40], Sargent and Whitford [41] and Lee and Ruthven [42]. From this approximate value of D_p, the contribution of macropore resistance can be estimated; it is found to be small for the present experimental conditions, and therefore can be neglected.

3.1.3 MICROPORE MASS TRANSFER RESISTANCE :

The micropore diffusional resistance is normally expressed by the term $1/(15D_c/r_c^2)$. This is very important for diffusion in molecular sieves when the size of the diffusing molecule is comparable with the micropore diameter of the sorbent.

3.1.4 CORRELATION FOR AXIAL DISPERSION COEFFICIENT :

When a fluid flows through packed beds axial mixing may occur. For modelling purpose the effect of such mixing is represented by an axial dispersion coefficient. The two main mechanisms which contribute to axial dispersion are molecular diffusion and turbulent mixing. The following equation may be used to make an approximate estimation of the axial dispersion coefficient [2],

$$D_L = \gamma_1 D_m + \gamma_2 2R_p v \qquad \text{----------(3.4)}$$

where γ_1 and γ_2 are constants which normally have values of 0.7 and 0.5 respectively. The first term represents the contribution from molecular diffusion and the second term arises from turbulent mixing.

3.2 THEORETICAL MODEL :

A column packed with zeolite subjected to a pulse or step input can be modelled by writing fluid phase mass balance equations and appropriate boundary conditions. The assumptions of the model in this work :

(*i*) Pressure drop across the bed is negligible

(*ii*) The operation is isothermal

(*iii*) The isotherm is linear

(*iv*) Instantaneous adsorption/desorption on crystal surface

(*v*) Spherical particle

(*vi*) Axially dispersed plug flow.

A mass balance across the differential elements of crystal, pellet and packed bed results in the following set of partial differential equations with associated

boundary conditions:

$$D_C\left(\frac{\partial^2 q}{\partial r^2} + \frac{2}{r}\frac{\partial q}{\partial r}\right) = \frac{\partial q}{\partial t} \qquad \text{----------(3.5)}$$

The appropriate initial and boundary conditions are :

$$q\,(r_c\,,\,t) = K_c\,\bar{c}\,(R\,,\,t) \qquad \text{----------(3.6)}$$

$$\frac{\partial q}{\partial r}\,(0\,,\,t) = 0 \qquad \text{----------(3.7)}$$

The average concentration through the particle is defined by :

$$\bar{q}(R\,,\,t) = \frac{3}{r_c^3}\int_0^{r_c} r^2\,q\,(r\,,\,t)\,dr \qquad \text{----------(3.8)}$$

The appropriate form of diffusion equation for macropore controlled system may be obtained from a differential mass balance on a spherical shell element :

$$\varepsilon_p D_p\left(\frac{\partial^2 \bar{c}}{\partial R^2} + \frac{2}{R}\frac{\partial \bar{c}}{\partial R}\right) = \omega\,(1-\varepsilon)\frac{\partial \bar{q}}{\partial t} + \frac{\partial \bar{c}}{\partial t} \qquad \text{----------(3.9)}$$

$$\frac{\partial \bar{Q}}{\partial t} = \frac{3k_f}{R_p}\left[c\,(z\,,\,t) - \bar{c}(R_p\,,\,t)\right] \qquad \text{----------(3.10)}$$

$$\frac{\partial \bar{c}}{\partial R}\,(0\,,\,t) = 0 \qquad \text{----------(3.11)}$$

$$\bar{Q} = \frac{3\omega\,(1-\varepsilon)}{R_p^3}\int_0^{R_p} \bar{q}\,R^2\,dR + \frac{3\varepsilon}{R_p^3}\int_0^{R_p} \bar{c}\,R^2\,dR \qquad \text{----------(3.12)}$$

$$D_L\frac{\partial^2 c}{\partial z^2} - v\frac{\partial c}{\partial z} - \left(\frac{1-\varepsilon}{\varepsilon}\right)\frac{\partial \bar{Q}}{\partial t} = \frac{\partial c}{\partial t} \qquad \text{----------(3.13)}$$

$$c\,(z\,,0) = c\,(R\,,0) = q\,(r\,,0) = 0 \quad (\textit{or constant}) \qquad \text{----------(3.14)}$$

$$c\,(0\,,t) = c_o\,\delta\,(t) \text{ for } \textit{pulse input} \;\; ; c\,(0\,,t) = c_o \text{ for } \textit{step input} \qquad \text{----------(3.15)}$$

$$c\,(\infty\,,t) = 0 \qquad \text{----------(3.16)}$$

This system of differential equations with associated boundary condition (3.5 to 3.16) was transformed into the Laplace domain and solved for $C_L(S,L)$. The method of solution is similar to that of Suzuki and Smith [35], for monodisperse porous particle and Haynes and Sharma [38], for bidisperse porous particles. It is not necessary to invert the transform because the n^{th} absolute moment of the peak is correlated with the transformed exit concentration by:

$$m_n = (-1)^n \lim_{s\to 0}\frac{d^n \bar{c_L}}{ds^n} \qquad \text{----------(3.17)}$$

and the n^{th} absolute moment is given by :

$$m_n = \int_o^{\infty} c\,t^n\,dt \qquad \text{----------(3.18)}$$

The first moment is defined by :

$$\mu = \frac{\int_0^\infty ctdt}{\int_0^\infty cdt} \qquad \text{----------(3.19)}$$

The second moment is defined by :

$$\sigma^2 = \frac{\int_0^\infty c(t-\mu)^2 dt}{\int_0^\infty cdt} \qquad \text{----------(3.20)}$$

Haynes and Sharma [37,38], by applying the above procedure obtained the following set of equations :

$$\mu = L/v\left[1+(\frac{1-\varepsilon}{\varepsilon})K_p\right] \qquad \text{----------(3.21)}$$

where :

$$K_p = \varepsilon_p + (1-\varepsilon_p)K_c \qquad \text{----------(3.22)}$$

$$\frac{\sigma^2 L}{2\mu^2 v} = \frac{D_L}{v^2} + (\frac{\varepsilon}{1-\varepsilon})\left[\frac{R_p}{3k_f} + \frac{R_p^2}{15\varepsilon_p D_p} + \frac{r_c^2}{15K_p D_c}\right] \qquad \text{----------(3.23)}$$

The first, second, third and fourth terms on the right hand side of Equation (3.23) represent the contribution of axial dispersion, external film resistance, macropore and micropore resistance respectively.

3.2.1 PLATE THEORY OF CHROMATOGRAPHY:

An alternative approach, originally developed by Martin and Synge [43], has also been widely used. This approach, which is directly analogous to the 'tank in series' model for a nonideal flow reactor, depends on representing the column by a finite number of hypothetical well-mixed stages, the number of stages being a direct measure of the axial dispersion and mass transfer resistance in the system. Although physically less realistic, this model gives results which are very similar to those obtained from the continuous theory.

The definition of the height equivalent to a theoretical plate (HETP) follows naturally :

$$HETP = \frac{\sigma^2 L}{\mu^2} = \frac{2D_L}{v} + 2v\left(\frac{\varepsilon}{1-\varepsilon}\right)\frac{1}{kK_p}\left[1 + \frac{\varepsilon}{(1-\varepsilon)K_p}\right]^{-2} \qquad \text{------(3.24)}$$

where :

$$\frac{1}{k K_p} = \frac{R_p}{3k_f} + \frac{R_p^2}{15\varepsilon_p D_p} + \frac{r_c^2}{15K_p D_c} \qquad \text{----------(3.25)}$$

When micropore diffusion is significant $k = 15\ D_c/r_c^2$. For large values of K_p, combining Equation (3.24) for the case of micropore diffusion control, with Equation (3.4) for D_L yields an expression of the same general form as the van Deemter equation :

$$HETP = A_2 + 2\nu\left(\frac{\varepsilon}{1-\varepsilon}\right)\left[\frac{r_c^2}{15K_pD_c}\right] \qquad \text{----------(3.26)}$$

where :

$A_2 = 2\gamma_1 D_m$, and we have assumed $K_p >> 1.0$.

3.3 METHODS OF EXTRACTION OF RATE PARAMETERS FROM CHROMATOGRAPHIC DATA :

There are three different methods by which the rate parameters of a column subjected to pulse input can be extracted, they are:

(*i*) Time domain analysis.

(*ii*) Frequency domain analysis.

(*iii*) Moment analysis.

Time domain analysis is preferable, but the analytical solution cannot easily be obtained for most cases and hence requires tedious numerical calculations.

Frequency domain analysis has some advantages and disadvantages over both the time domain analysis and the moment analysis. The advantages of frequency domain analysis lie in the fact that the frequency domain solution can be easily obtained, but the analytical inversion to time domain solution is difficult. Even if the inversion can be accomplished, the solution is likely to contain definite integrals of untabulated functions that have to be solved numerically. Another disadvantage of this method is that for a lumped parameter model there is no change in the frequency solution as the value of the parameter changes but the time domain solution changes as the roots of characteristic equation change from real to multiple to complex. In the Fourier analysis unlimited numbers of equations can be obtained in a series of frequency, as the amplitude ratio and phase lags are derived as function of the process parameters. But because of the interaction of the parameter at low frequencies and the amplification of experimental errors at high frequencies when the output signal is transposed to the Fourier domain the advantages of the Fourier analysis over moment analysis are not substantial.

3.3.1 MOMENT METHOD OF ANALYSIS :

The method yields reliable results provided that certain precautions are taken. Moreover when only two parameters are involved the moment method is adequate. The most important drawback of the moment method is that the second moment is sensitive to any tailing of the peak. In such situations, it is preferable to use time domain analysis for extracting rate parameters.

3.3.2 TIME DOMAIN ANALYSIS :

To avoid the errors associated with moments analysis various more sophisticated methods such as Fourier transformation and combination of Fourier transform and moments method have been developed [44,45]. The advantages of such method have, however, been largely eliminated by the availability of full analytic solution for the general model in the time domain [46], and by the development of improved numerical techniques which allow the time domain solutions to be calculated rapidly, directly from the model Equations [47]. With these developments the best approach appears to be a combination of moments method to determine the initial estimates of the parameters values coupled with a final optimization by direct matching of the response curves in the time domain.

3.4 MEASUREMENT OF MICROPORE DIFFUSIVITY :

Different methods are in use for the measurement of the kinetic and equilibrium parameters in adsorption. Some common methods which are currently being used are discussed below:

3.4.1 VOLUMETRIC METHOD :

In this method, the quantity of gas admitted to the system is determined from measurements of known volumes, pressure and temperature. After exposing this gas to activated adsorbent the pressure eventually drops to a steady state value. From volumetric knowledge of the mole of gas present in the

gas phase before and after adsorption, the quantity adsorbed can be easily calculated after equilibrium is attained.

3.4.2 GRAVIMETRIC METHOD :

This method measures the amount of gas or vapor adsorbed by weighing the sample in a closed system on a balance, generally of the quartz spring type.

The experimental setup consists of a Cahn RG electrobalance, which is enclosed in a special pyrex glass cover. The vacuum section is comprised of a two stage oil diffusion pump and a liquid nitrogen trap. A small amount of adsorbent is placed in the pan. Differential steps of sorbate are introduced into the system. When the system comes to equilibrium i.e. no change in weight of sample is observed, equilibrium weight of the sorbent and sorbate is monitored, recorded and analysed.

3.4.3 CHROMATOGRAPHIC METHOD :

In this method the adsorbent is contained in a packed column and a sample of gas to be studied is introduced as a pulse or step input into the column, which is equipped with a thermal conductivity detector (TCD) or other type of composition analyzer to monitor the exit concentration. The response is then analyzed to evaluate the sorption properties.

The chromatographic method of measuring equilibrium constant and diffusivities offers certain advantages.

(*i*) The chromatographic method offers advantages of speed and simplicity over more conventional methods of studying adsorption kinetics and equilibria.

(*ii*) It is particularly useful for studying the behavior of weakly adsorbed and relatively fast diffusing species for which the intracrystalline sorption rates may be too fast to permit reliable uptake rate measurement.

(*iii*) It is relatively quick and easy to derive the equilibrium constant from the first moment of the chromatographic response.

(*iv*) The method can be easily applied to high temperature studies and the effect of trace impurities can be easily investigated by dosing the carrier stream.

The disadvantages of the chromatographic method are ;

(*i*) It is difficult to determine the isotherm.

(*ii*) In the chromatographic method more resistances are present.

(*iii*) Axial dispersion is always present.

3.5. EXPERIMENTAL MEASUREMENT OF MICROPORE DIFFUSIVITY BY THE CHROMATOGRAPHIC METHOD :

3.5.1 INTRODUCTION :

A small pulse or step input is introduced into a column packed with CMS and from the response curve the equilibrium and kinetic parameters are extracted by moments analysis. Special care must be taken in the choice of column length, diameter, particle size, dead volume in the system, pulse size and gas velocity. The column should be long enough so that equilibrium is attained between the sorbate and sorbent. The particle size and diameter of the column must be chosen such that the ratio of the column to the particle diameter is more than about 10. In this way channeling can be avoided and axial dispersion minimized. The pulse size must be small enough so that the isotherm does not deviate significantly from linearity.

The external film mass transfer resistance encountered in a chromatographic experiment can be minimized or eliminated by using sufficiently high gas velocity but the velocity should not be so high as to give a large pressure drop through the column.

3.5.2 APPARATUS AND EXPERIMENTAL PROCEDURE:

Standard chromatographic method is employed. A schematic diagram of the experimental set up of a chromatographic study is shown in Figure 3.1. The carrier gas helium first went to the reference side of thermal conductivity detector (TCD) block, then to the gas sampling loop. The detector was a four filament GOWMAC. 10-454 thermal conductivity detector. The filament current was in general set at 295 mA. By using the carrier gas as its own reference gas it is expected that the susceptibility of the TCD output to carrier

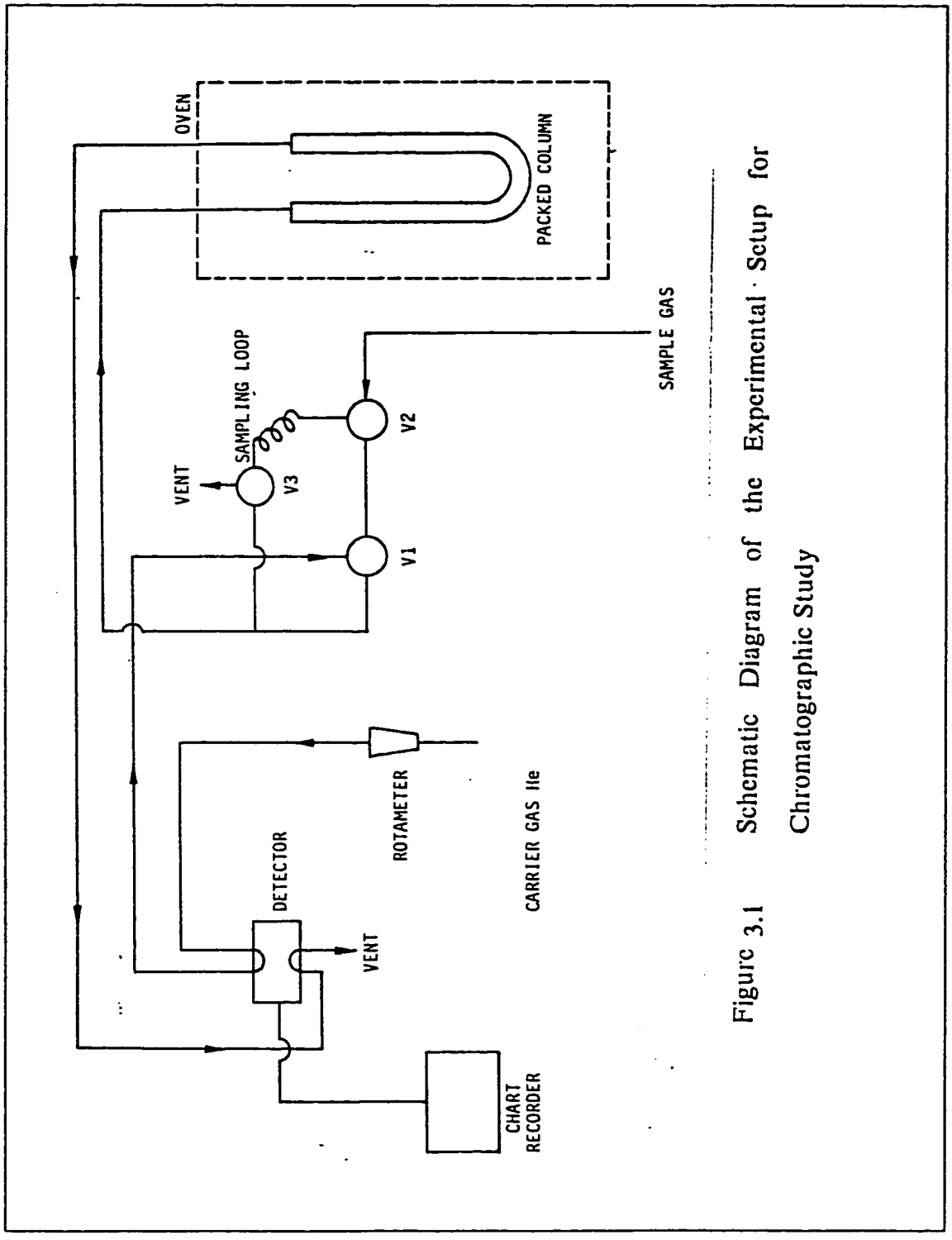

Figure 3.1 Schematic Diagram of the Experimental Setup for Chromatographic Study

flow and pressure fluctuations would be minimized.

The flow direction through the sampling loop was set by the use of three solenoid valves. At the start of the run, the carrier gas flow is set in a way such that it can pick up the sample gas from the sampling loop before flowing through the column. The output from the TCD is recorded on a chart recorder as shown in Figure 3.2, which is then analyzed to obtain the equilibrium and kinetic parameters. Prior to an experimental run, the adsorbent column is regenerated overnight at 250°C under a stream of He and then cooled to the required temperature. The details of the adsorbent column used for the chromatographic experiments of oxygen and nitrogen are given in Table 3.1.

The voidage of the bed is calculated from the known adsorbent particle density and the weight of the packed column, as shown in Appendix-A. Linearity of the system will be confirmed by measuring the response for two different sizes of injection pulses.

3.6 ANALYSIS OF EXPERIMENTAL DATA

3.6.1 METHOD OF DETERMINATION OF EQUILIBRIUM CONSTANT:

The equilibrium constant, K_p based on pellet volume is determined from the first moment of the response curve, with allowance being made for the dead volume determined experimentally. In order to determine the dead volume accurately the following experiments were performed. The system was subjected

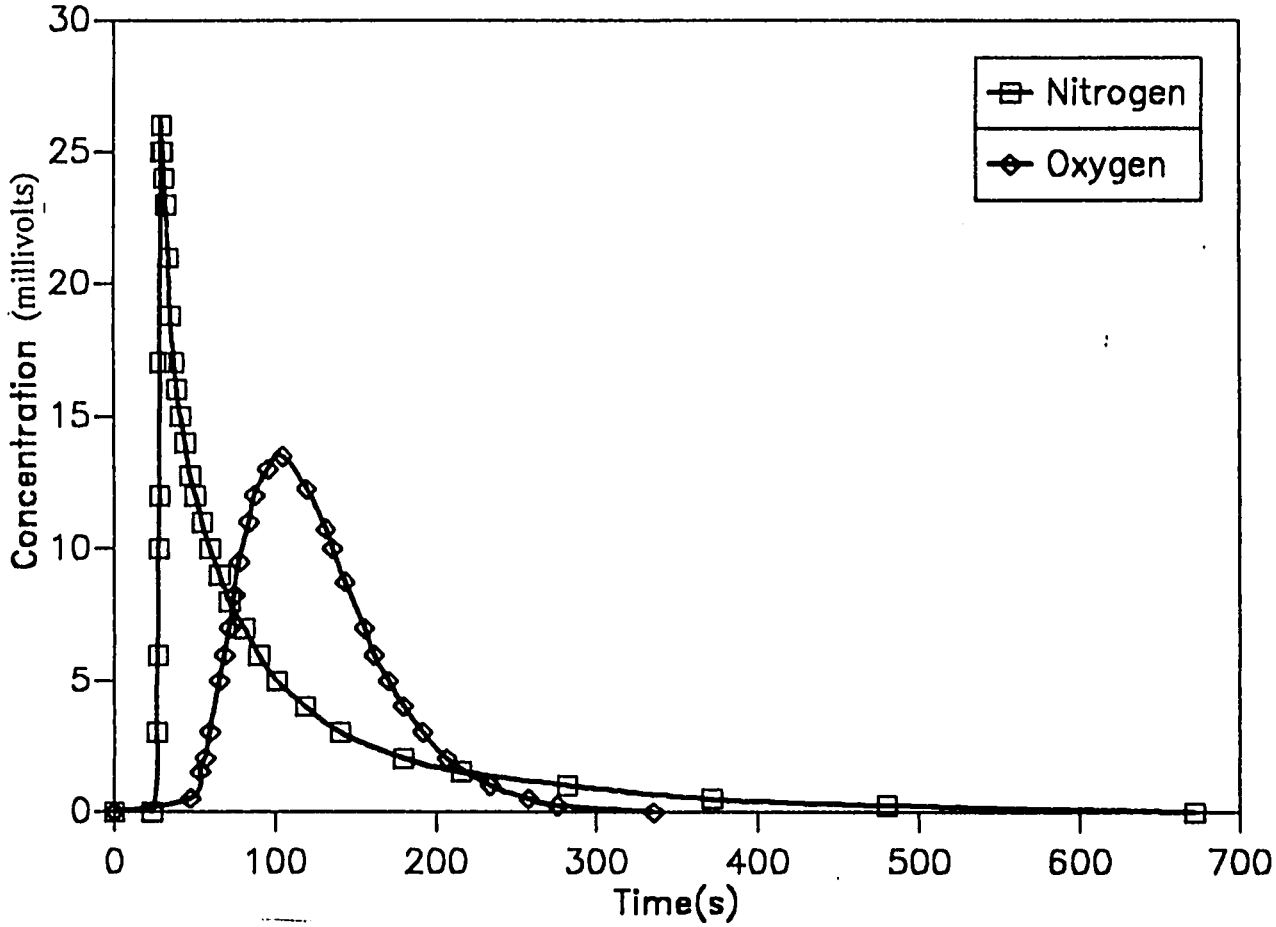

Figure 3.2 Typical Chromatographic Response Curves for O_2 and N_2 on CMS at 50°C (v=4.85 cm/s for O_2 and v=4.81 cm/s for N_2)

Table 3.3 Details of Adsorbent and Chromatographic Column

Adsorbent	Carbon Molecular Sieve (Bergbau Forschung)
Length of column	49.0 cm
Internal diameter of column	1.00 cm
Voidage	0.433
Weight of adsorbent	28.1 gm
Density of adsorbent	1.21 gm/cc
Macropore volume	0.278 cc/gm
Macropore pore radius	1.32 micron
Porosity of macropore	0.366

to oxygen pulses at 100°C in the absence of the adsorption column at various flow rates. The peak was analyzed and μ' was plotted against 1/ v as shown in Figure 3.3. μ' at experimental conditions were then subtracted from actual first moment to obtain μ.

Experimentally the value of K_p can be determined by the least squares method from plot μ vs. 1/v according to Equation (3.23). A plot of μ vs.1/v passes through the origin, with a slope of $L\left[1+(\frac{1-\varepsilon}{\varepsilon})K_p\right]$ from which K_p can be obtained. The temperature dependence of the equilibrium constant, K_p for these gases may be correlated by by Van't Hoff type of equation given by (2.13). From this correlation the preexponential factor K_o and limiting heats of sorption ΔH_o can be calculated.

3.6.2 METHOD OF DETERMINATION OF DIFFUSIONAL MASS TRANSFER RESISTANCE :

The relative importance of the different mass transfer resistances was determined by performing replicate experiments with two particle sizes. If both particle sizes give the same value of the time constant, then micropore diffusional resistance must be dominant. The micropore diffusional and axial dispersion resistance for these systems can be obtained respectively from the intercept and slope of plots, $\sigma^2 L/2\mu^2 v$ vs. $1/v^2$ as given by Equation (3.23). The calculated diffusivity may be correlated by the Arrhenius type of Equation given

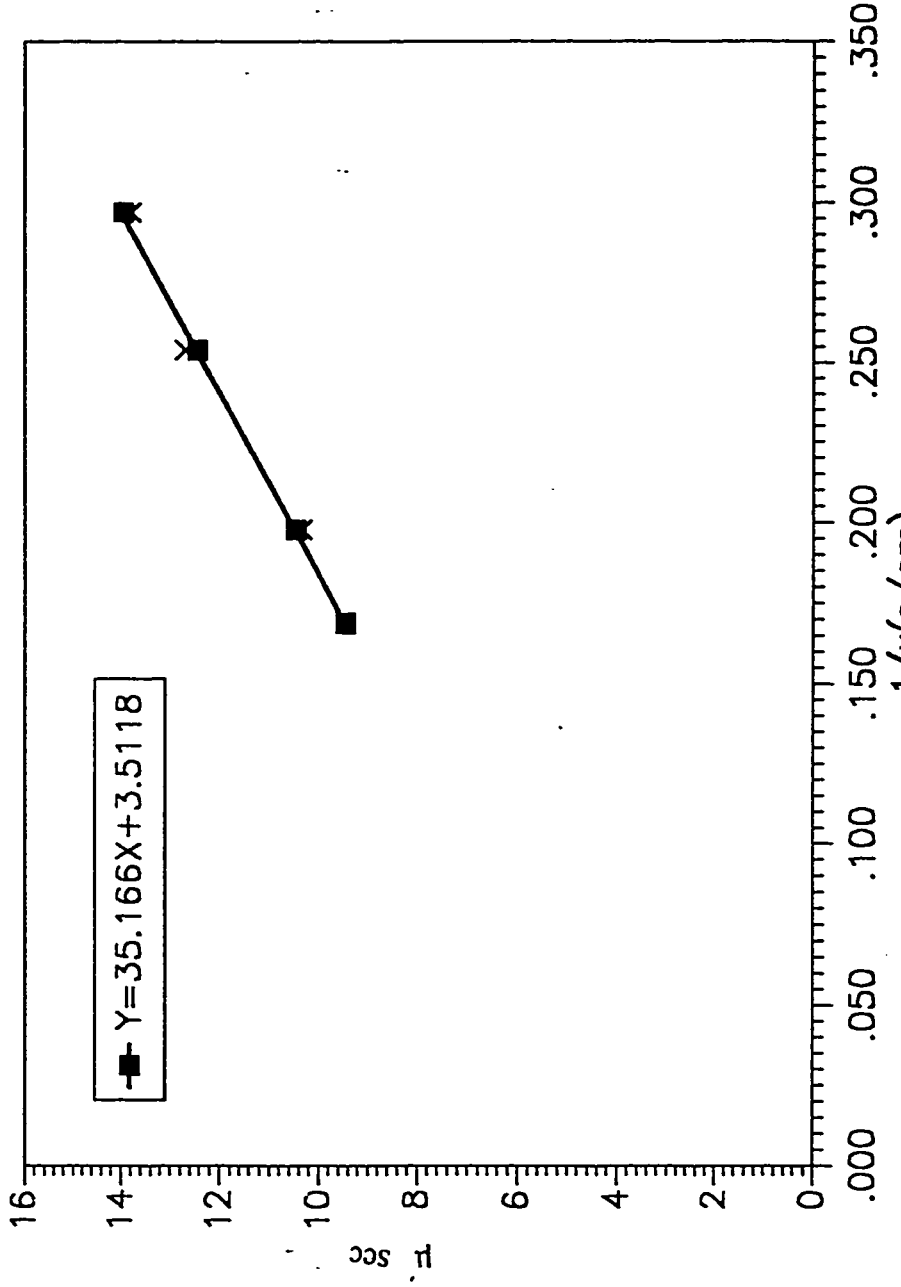

Figure 3.3 Plot of μ' *versus* $1/v$ to Determine the Dead Volume

by Equation (2.15).

3.7 RESULTS AND DISCUSSION OF CHROMATOGRAPHIC STUDY :

The sorption and diffusion measurements for nitrogen, oxygen on CMS were performed at different temperatures. The linearity of the equilibrium isotherm was checked by varying the pulse size. In order to find the importance of the different mass transfer resistance, experiments were performed with two different particle sizes. Results of such replicate experiments are shown in Figures 3.4 as plots of $\sigma^2 L/2\mu^2 v$ vs. $1/v^2$. These plots give the same intercept for the two particle sizes implying that the external film and macropore mass transfer resistance can be neglected and peak broadening was due to the combined effects of axial dispersion and micropore diffusion only.

The equilibrium constants for nitrogen and oxygen were estimated in CMS by the method described in section 3.4.1. The first moments for nitrogen and oxygen as functions of the inverse of interstitial velocity are shown in Figures 3.5 and 3.6 respectively for various temperatures. From the slopes of these plots K_p values were calculated using Equations (3.23) and are reported in Table 3.2. The present experimental results for nitrogen and oxygen are plotted as K_p vs. 1/T in semi logarithmic co-ordinates in Figures 3.7. These data are correlated by the Van't Hoff type of equation given by Equation (2.13).

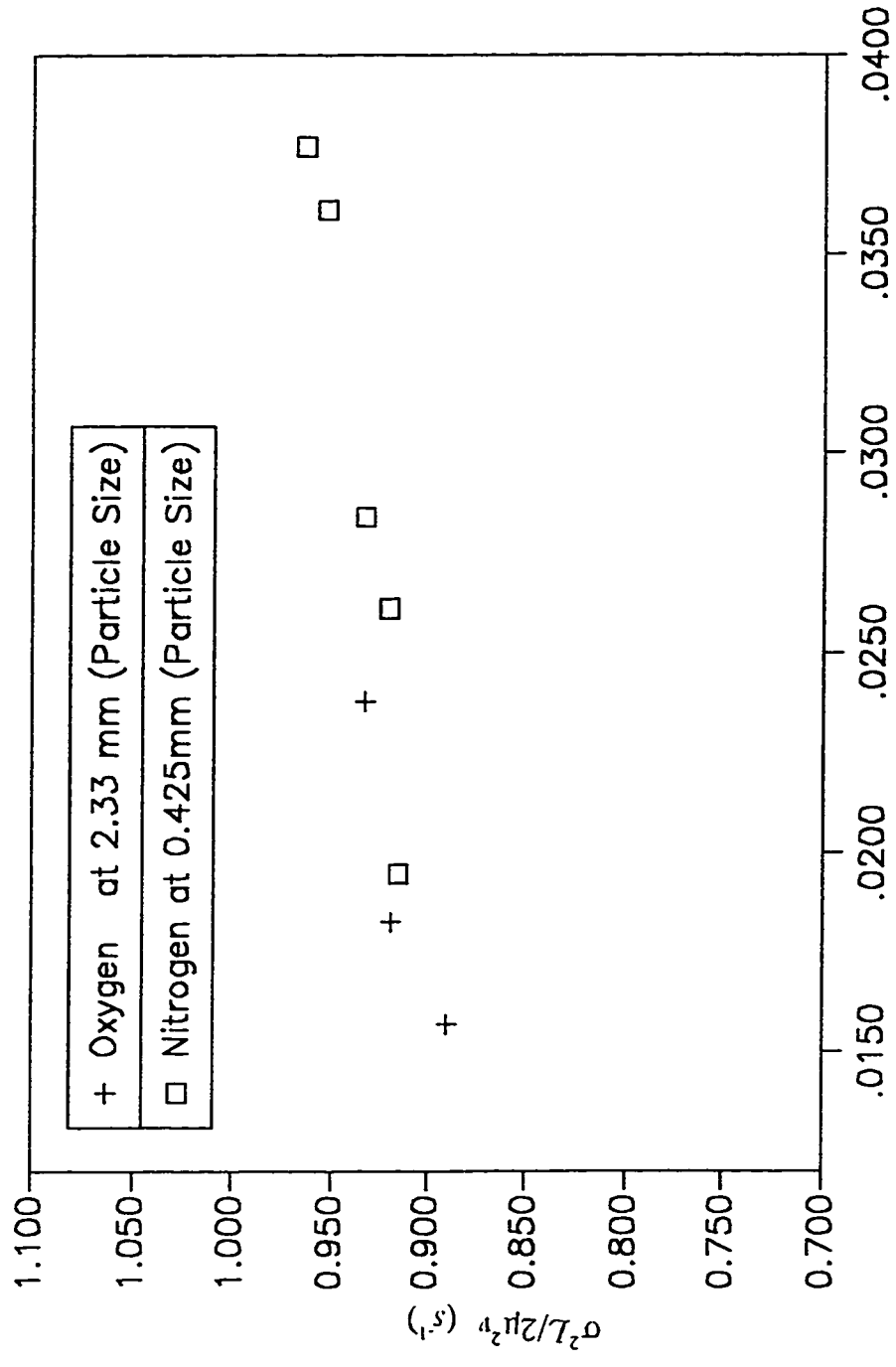

Figure 3.4 Plot of $\sigma^2 L/2\mu^2 v$ versus $1/v^2$ for O_2 and N_2 on CMS at 100° C for Different Particle Sizes

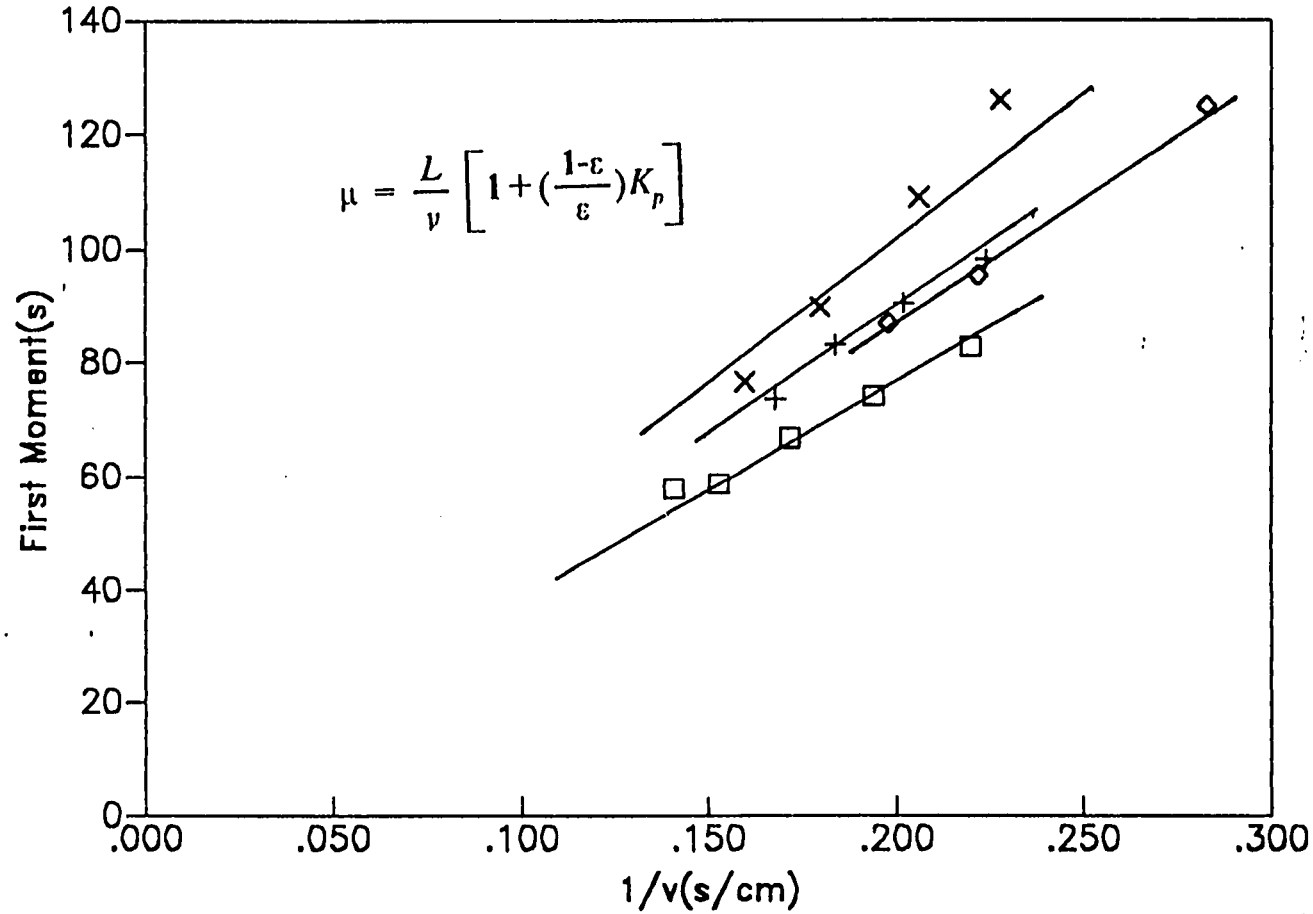

Figure 3.5 **Plots of First Moment versus 1/v for N_2**

(×,50°C;+,75°C;◇,80°C;□,100°C)

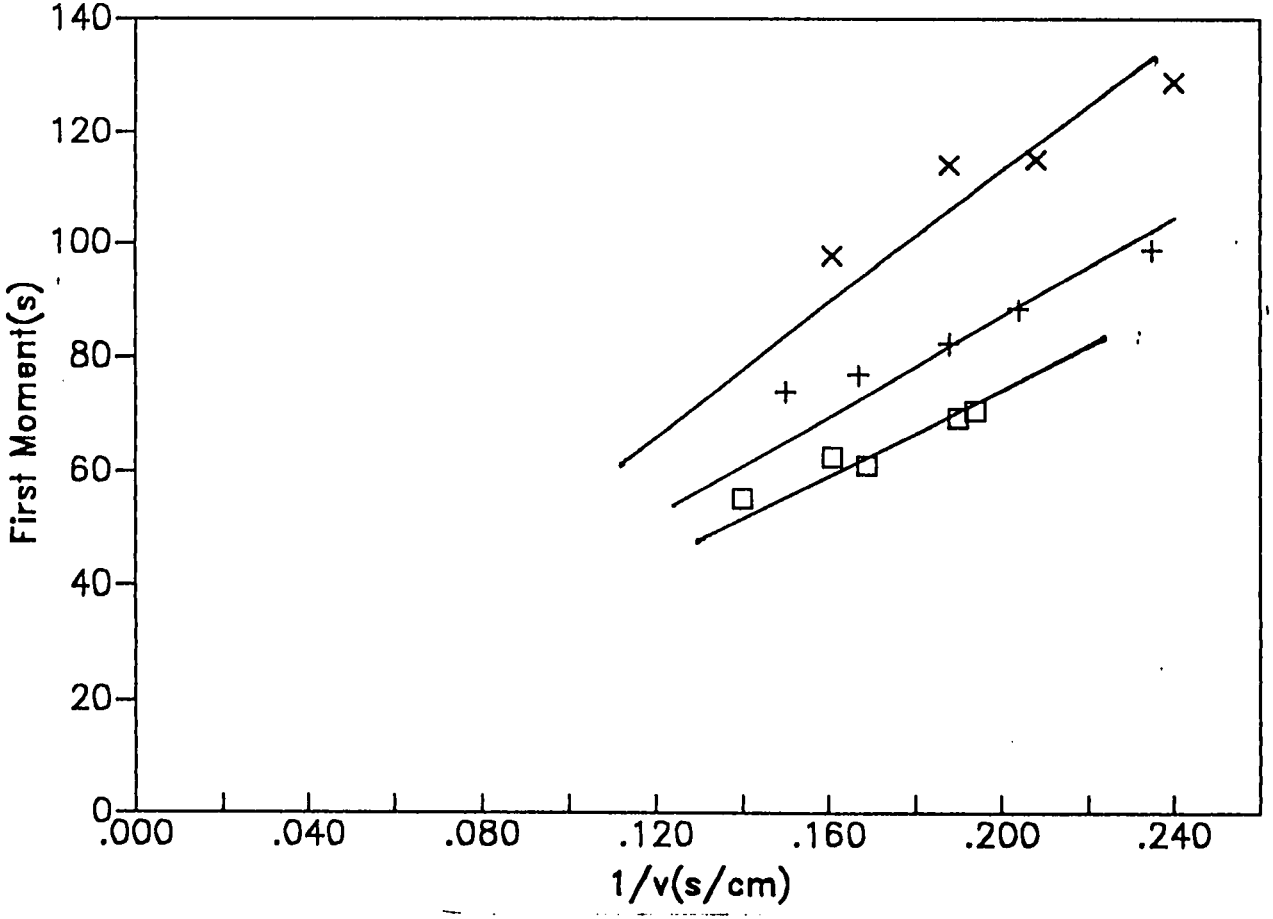

Figure 3.6 Plots of First Moment versus 1/v for O_2

(× ,50°C; + ,75°C; □ ,100°C)

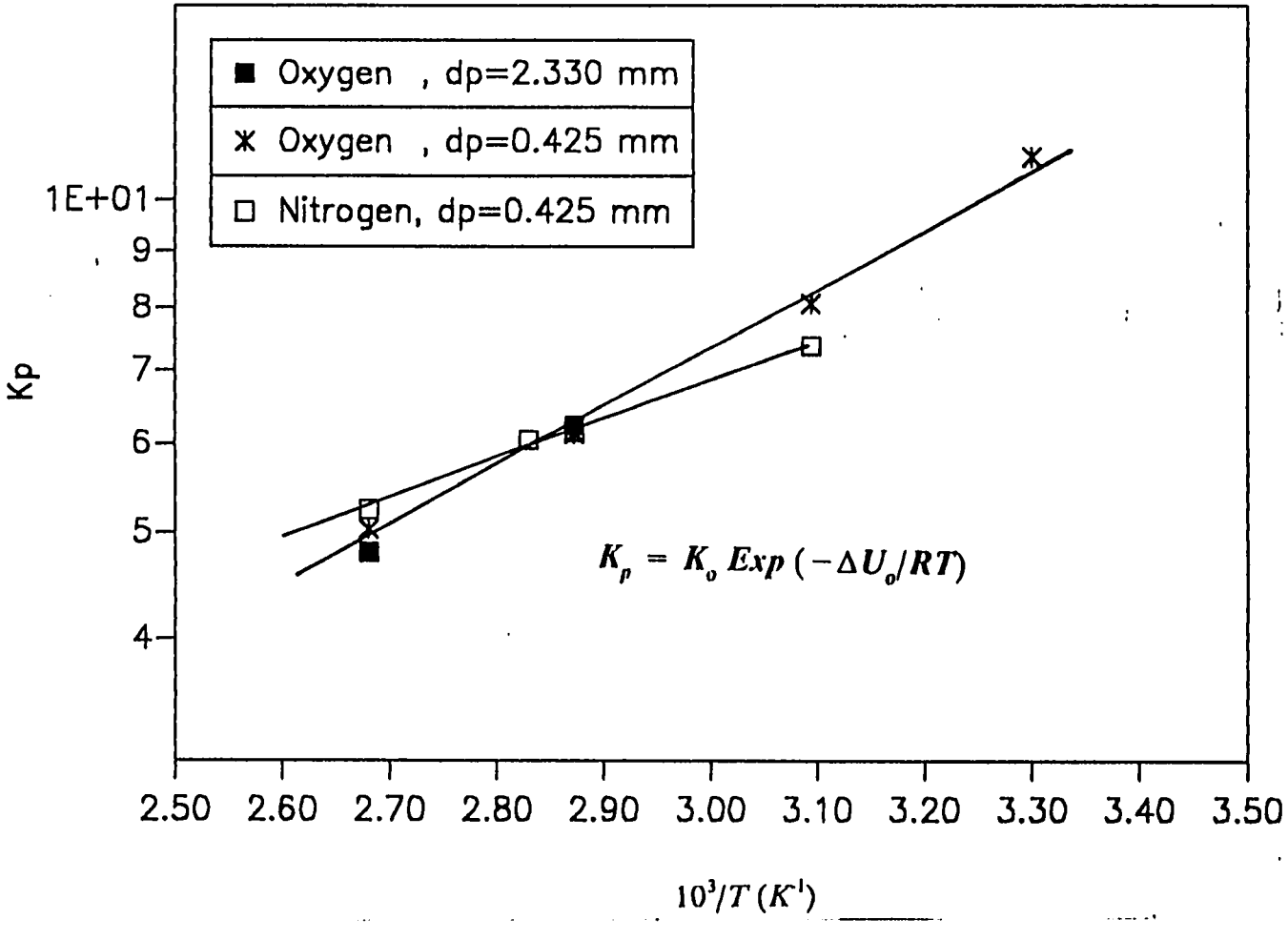

Figure 3.7 Plot of K_p versus 1/T for N_2 and O_2 in CMS

The pre-exponential factors K_o and limiting heat of sorption, U_o were calculated and are listed in Table 3.2.

In order to evaluate the micropore diffusional resistance of nitrogen and oxygen, the plots of $\sigma^2 L/2\mu^2 v$ vs. $1/v^2$ were prepared as shown in Figures 3.8 and 3.9 respectively for various temperature. From the intercepts of these plots D_c/r_c^2 values were calculated and are also tabulated in Table 3.2. The calculated CMS diffusivity was correlated by the Arrhenius type of equation and plots are shown in Figure 3.10. The pre exponential factor D_o/r_c^2 and activation energy are tabulated in Table 3.2. The other approach to calculate the micropore diffusional resistance is by HETP analysis as described by Equation (3.26). The plot of HETP vs. v for Nitrogen and Oxygen at different temperature are shown in Figures 3.11 and 3.12 respectively.

A time domain analysis as described in section 3.3.2 was also performed in the present study. The experimental pulse responses were integrated to yield the experimental breakthrough curves, which were then compared with the numerical solution of the model equation for an adsorber subjected to a step input. The micropore diffusivity was varied to get a good match of the theoretical and experimental breakthrough curves, while using the same value of Henry's constant as obtained from the moment method. Such a comparison is shown in Figure 3.13 for both Oxygen and Nitrogen. The micropore diffusivity obtained by this method have been compared with values obtained from the

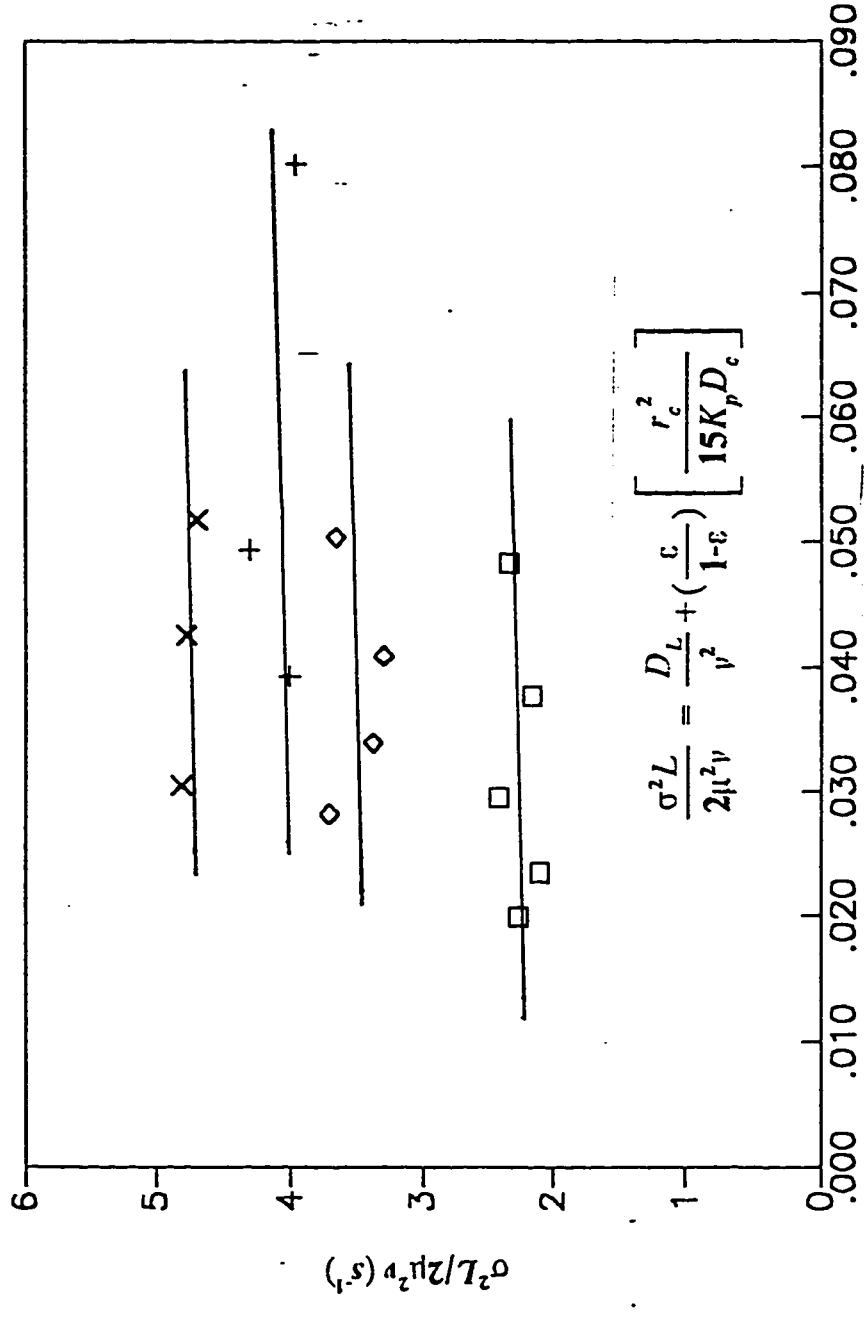

Figure 3.8 Plots of $\sigma^2 L/2\mu^2 \nu$ versus $1/\nu^2$ for N_2 (×,50°C;+,75°C;◇,80°C;□,100°C)

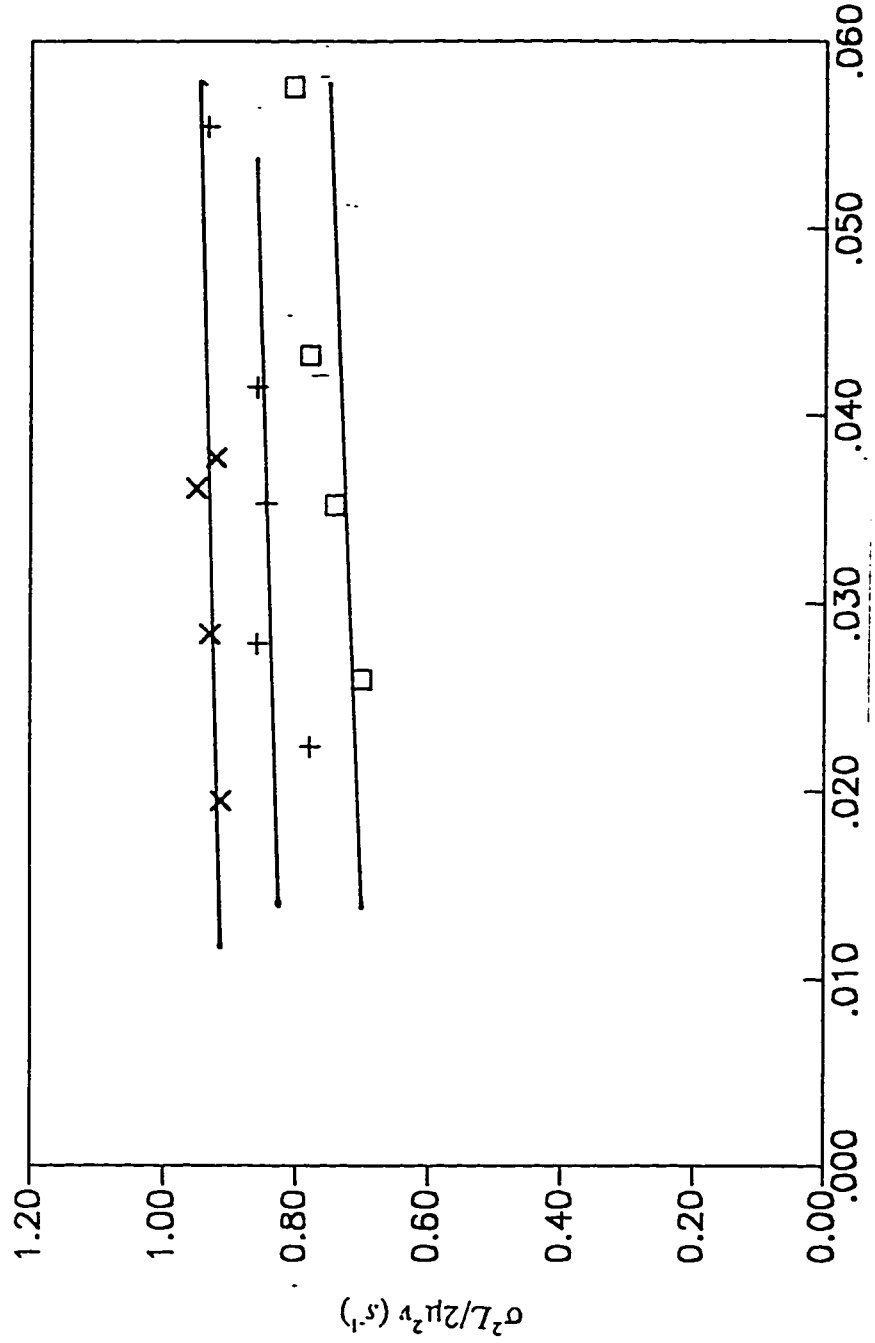

Figure 3.9 Plots of $\sigma^2 L/2\mu^2 v$ versus $1/v^2$ for O_2

(× ,50°C; + ,75°C; □ ,100°C)

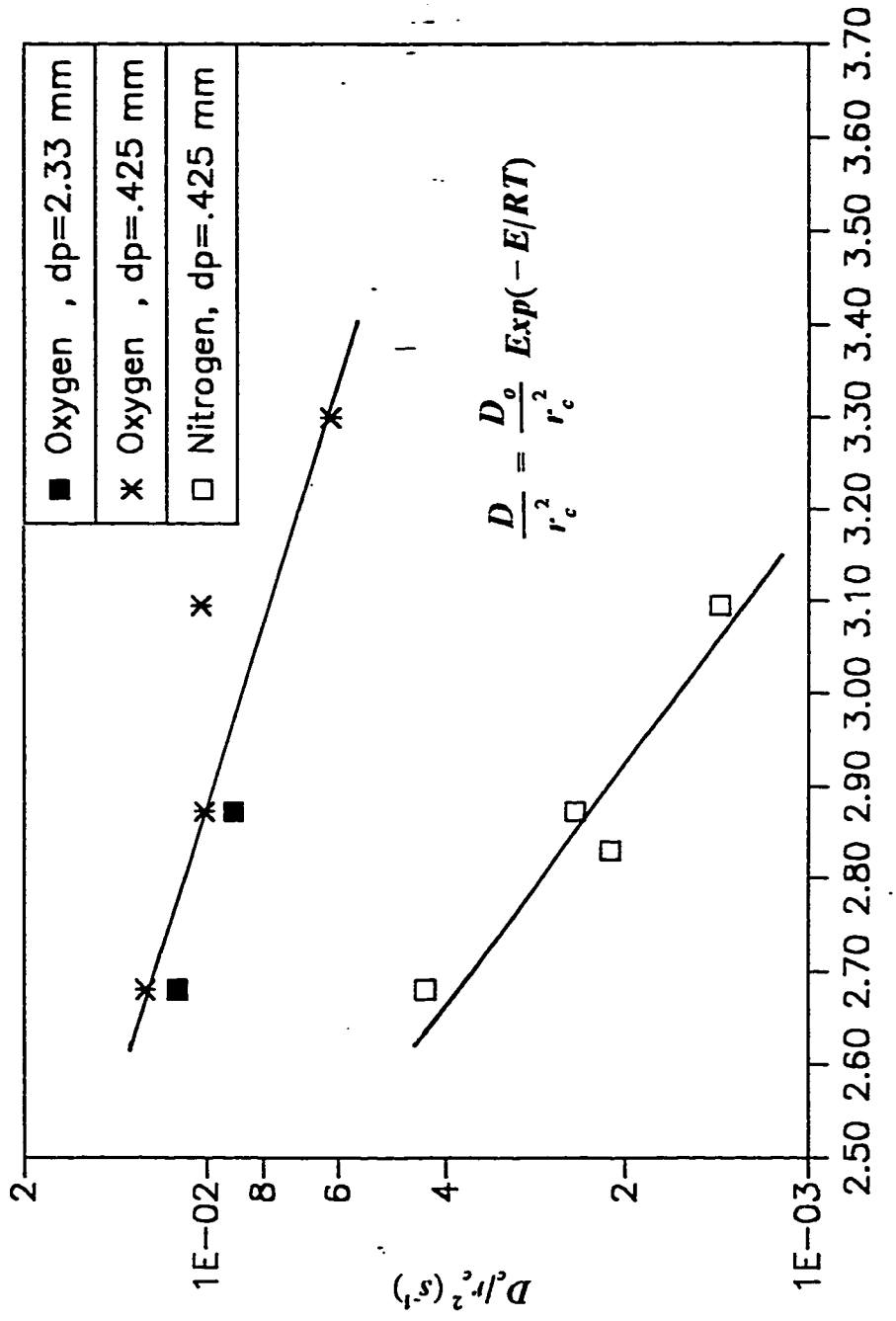

Figure 3.10 Plot of D_e/r_c^2 versus 1/T for N_2 and O_2 in CMS

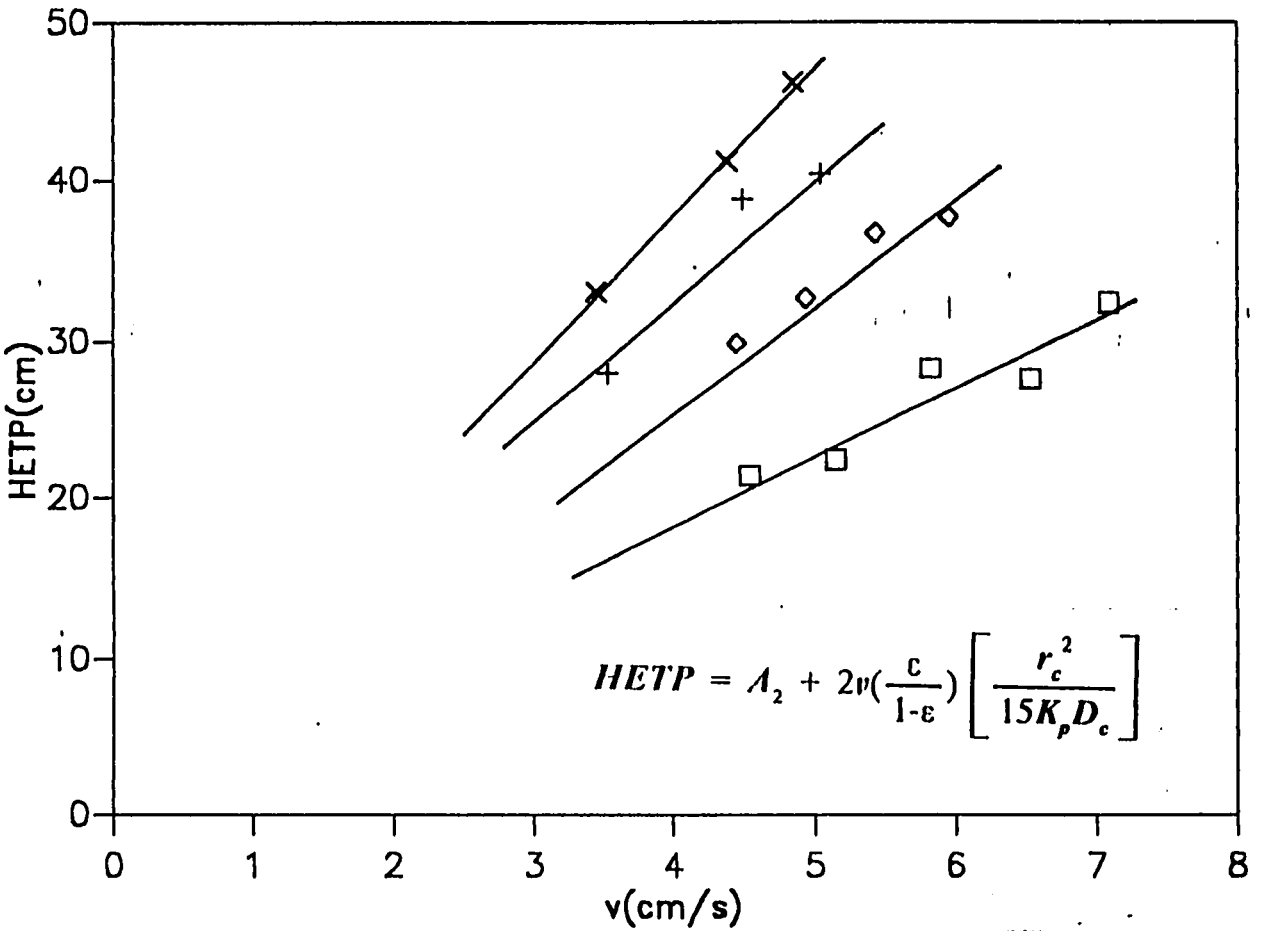

Figure 3.11 **Plots of HETP versus v for N_2**

(X,50°C;+,75°C;◇,80°C;□,100°C)

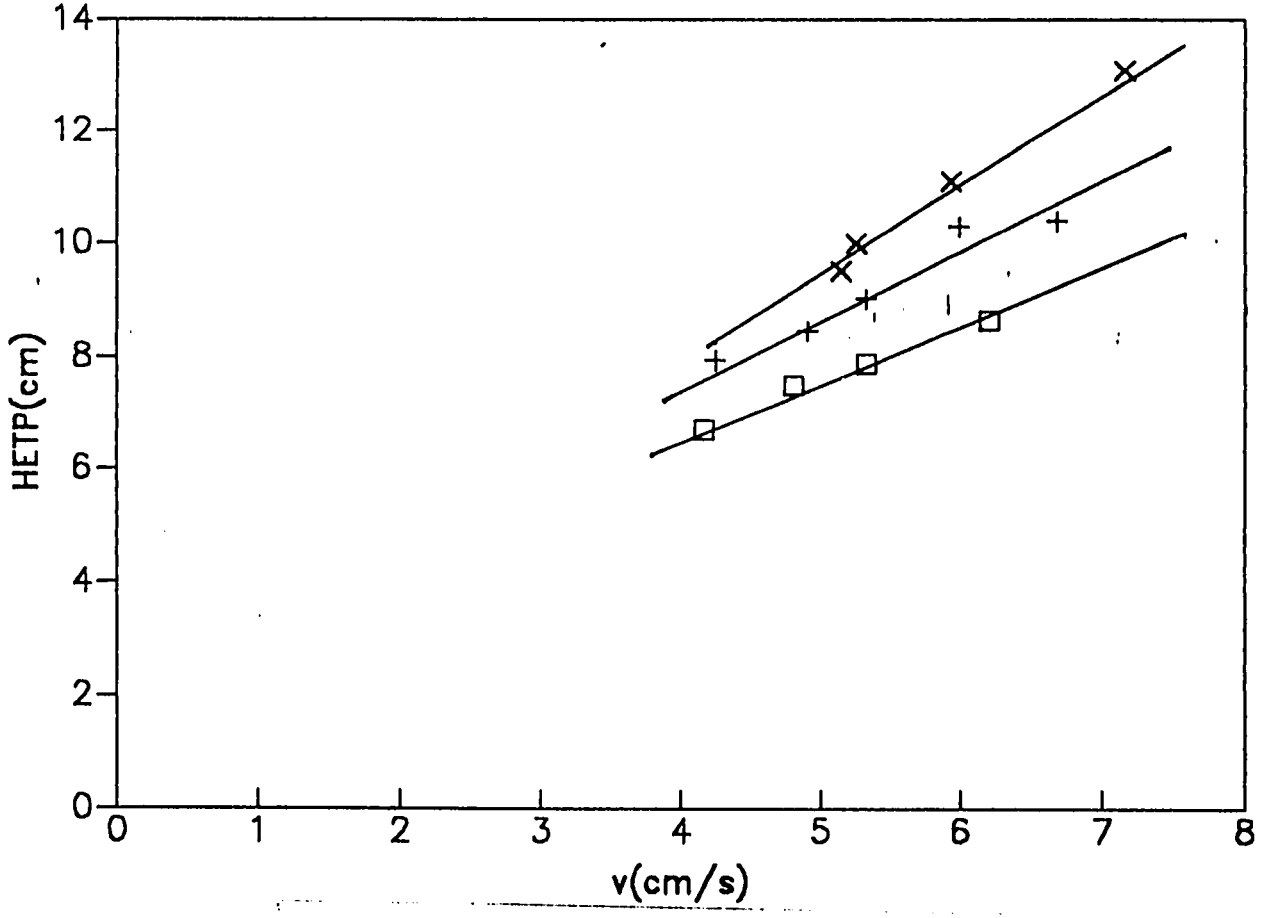

Figure 3.12 Plots of HETP versus v for O_2

(× ,50°C;+ ,75°C;□ ,100°C)

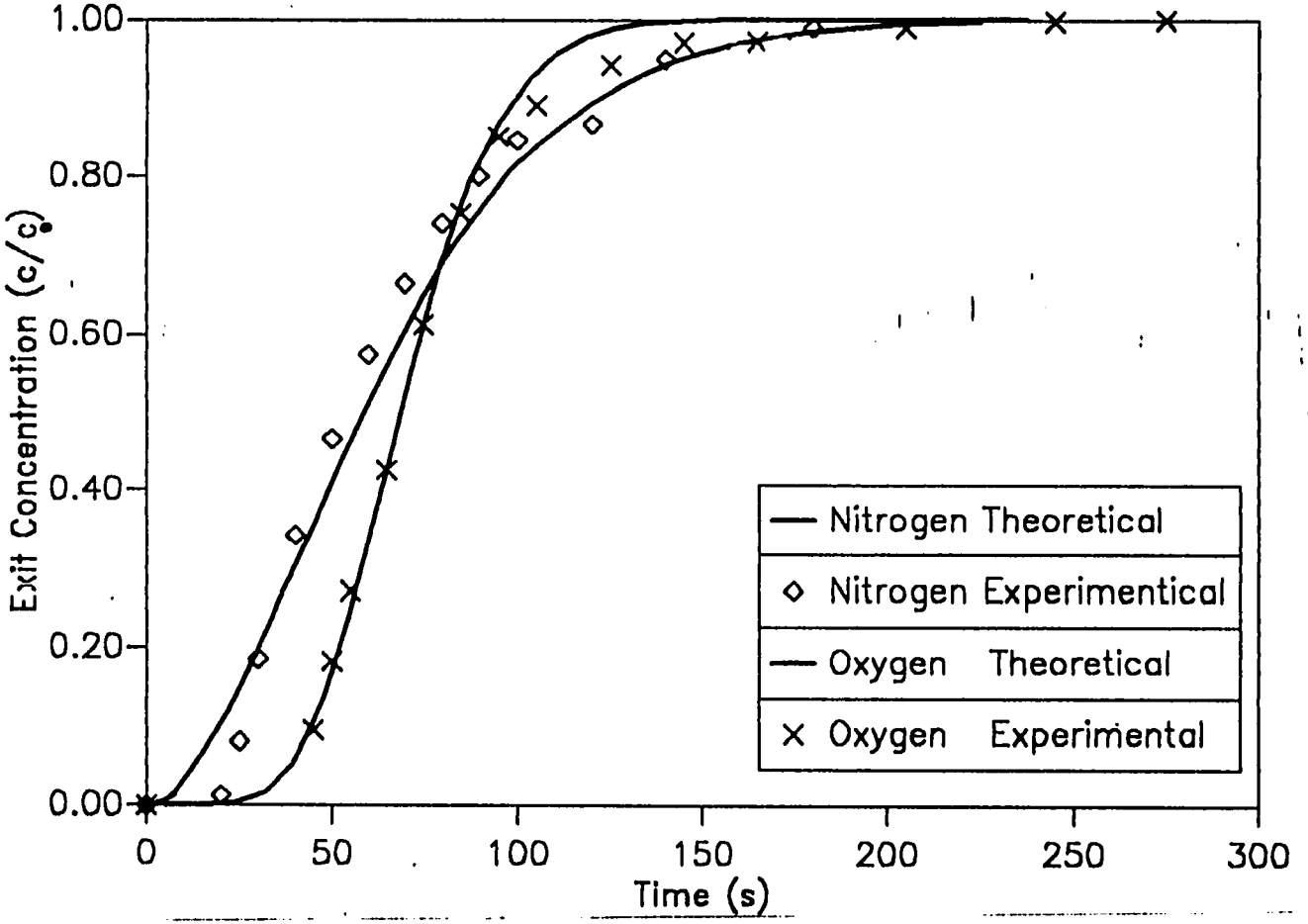

Figure 3.13 **Comparison of Theoretical and Experimental Breakthrough Curves for N_2 at v = 6.53 cm/s and O_2 at v = 6.19 cm/s in CMS at 100°C**

moment method and HETP analysis as shown in Table 3.3. It is evident from this table that micropore diffusivity obtained from different methods described above are broadly consistent.

The values derived for the sorption parameters have been compared in Table 3.4 with the values available in the literature. It is observed that the values of the equilibrium constants are in very good agreement with the values reported by Ruthven et al. [7] and Knoblauch [9]. However, the reciprocal time constants (D_c/r_c^2) for both oxygen and nitrogen are different. The apparent differences in (D_c/r_c^2) values may be attributed to the difference in samples used.

3.7.1 CONCLUSIONS OF CHROMATOGRAPHIC STUDY:

The pulse chromatographic technique was used to measure the sorption and kinetic behavior of oxygen and nitrogen in CMS. The micropore diffusivity obtained from moment method, HETP analysis and time domain analysis were broadly consistent. The Henry's law constants, limiting heats of sorption, diffusion coefficients and activation energies of both gases have been compared with previously reported data and was found to agree well as shown in Table 3.4.

The values of equilibrium constants agree well with the previously reported data [7,9]. The kinetic selectivity D_{O_2} / D_{N_2} at $303^{\circ}K$ was found to be about 7.4, which is much lower than the kinetic ratio reported earlier. The limiting heats of adsorption and activation energy respectively were found to be 2.33 kcal/mole and 2.39 kcal/mole for O_2 and 2.54 kcal/mole and 5.50 kcal/mole for N_2.

Table 3.2 Summary of the results obtained for sorption of O_2 and N_2 on CMS by moment method of analysis.

TEMP $T°C$	$\frac{D_c}{r_c^2}(10^3)$ (s^{-1})	K_P	K_0	$-\Delta U_0$ $\frac{kcal}{mole}$	$-\Delta H_0$ $\frac{kcal}{mole}$	E $\frac{kcal}{mole}$	$\frac{D_0}{r_c^2}$ (s^{-1})	Gas (Particle Size)
50	1.40	7.38						
75	2.12	6.15	0.40	1.87	2.54	5.50	6.82	NITROGEN
80	2.43	6.16						(0.425 mm)
100	4.32	5.24						
30	5.48	10.92						
50	9.00	8.08	0.61	1.63	2.33	2.39	0.37	OXYGEN
75	10.1	6.12						(0.425 mm)
100	12.6	5.04						
75	9.00	6.24						OXYGEN
100	11.2	4.80						(2.3 mm)

Table 3.3 Comparison of D_c/r_c^2 Obtained by Different Methods of Analysis.

Temp °C	$[D_c/r_c^2\ (s^{-1})] \times 10^3$			
	Moment Method of Analysis	Time Domain Analysis	Plate Theory Analysis	Gas (Particle Size)
50	1.40	2.10	1.43	Nitrogen
75	2.12	2.95	2.06	(0.425mm)
80	2.43	3.00	2.47	
100	4.32	4.75	4.50	
30	5.84	7.70	5.55	Oxygen
50	9.00	8.00	8.95	(0.425mm)
75	10.10	9.50	10.21	
100	12.60	15.00	11.18	
75	9.00	8.50	7.98	Oxygen
100	11.20	11.17	9.87	(2.30mm)

Table 3.4 Comparison of equilibrium and diffusivity data for O_2 and N_2 in Carbon Molecular Sieves at 303 ° K.

		O_2	N_2	D_{O_2}/D_{N_2}
Present Data	$D_c/r_c^2(s^{-1})$ (Chromat.)	5.40×10^{-3}	7.35×10^{-4}*	7.4
	K (Chromat.)	10.92	8.93*	
	E (kcal/mol)	2.39	5.50	
Ruthven [7]	$D_c/r_c^2(s^{-1})$ (Chromat.)	3.7×10^{-3}	1.2×10^{-4}	30
	K (Chromat.)	8.2	9.6	
	E (kcal/mol)		6.5	
Knoblauch [9]	$D_c/r_c^2(s^{-1})$	1.7×10^{-4}	7.0×10^{-6}	24
	K	9.25	8.9	
Chihara and Suzuki [8] -Regen. Sieve	$D_c/r_c^2(s^{-1})$	0.19	0.034	5.6
	K	12	12	
	E (kcal/mol)	1.4	2.6	
	$-\Delta H_o$ (kcal/mol)	3.8	3.8	
Chihara and Suzuki [8] -Treated Sieve	$D_c/r_c^2(s^{-1})$	4.5×10^{-3}	1.1×10^{-3}	4.1
	K	5.0	5.0	
	E (kcal/mol)	6.6	7.4	
	$-\Delta H_o$ (kcal/mol)	2.8	2.8	

* Found by extrapolation.

CHAPTER 4

PRESSURE SWING ADSORPTION STUDY

4.1 LITERATURE SURVEY:

The phenomenon of adsorption has been understood for over 100 years. The early adsorption processes used either activated carbon, or silica gel adsorbents. The potential of adsorption as a separation process was greatly enhanced by the invention of molecular sieves by Union Carbide in the late 1950's [1,3]. Molecular sieves are crystalline materials having uniformly sieved pores whose dimensions are similar to those molecules found in such streams as atmospheric gases, or light hydrocarbons. Several types of molecular sieves were invented having a very specific pore size.

The invention of molecular sieves, initiated research work on the development of processes to take advantage of their unique properties.

One of the many processes which have been developed in the field of adsorption is the pressure swing adsorption (PSA) process. The process was invented by Skarstrom in 1959 [4]. It is also known as the adiabatic or heatless adsorption process to differentiate it from the thermal swing adsorption process. The use of PSA processes for separation of gas mixtures has considerably

developed since their invention.

A brief description of the adsorption separation processes is given in the following section.

4.1.1 ADSORPTION SEPARATION PROCESSES :

Large scale adsorptive separation processes may be broadly classified as cyclic batch system and continuous flow systems. In a cyclic batch system the adsorbent beds go through adsorption and desorption steps alternately in a cyclic manner. On the other hand, a continuous flow system normally involves continuous countercurrent contact between feed and adsorbent, thereby maximizing the driving force for mass transfer. For systems where the separation factor is high and mass transfer resistance small, cyclic processes are generally employed because of advantages of simplicity and cost. Continuous countercurrent operation is generally used only where selectivities are low and mass transfer resistance high as it is only under these conditions that the additional capital cost of a countercurrent system can be justified.

4.1.2 CYCLIC SEPARATION PROCESSES :

In a cyclic process the bed is loaded in the adsorption step which is followed by a desorption step in which the bed is again regenerated; examples of adsorption cyclic separation processes are listed in Table 4.1. The following methods are commonly used for the regeneration of the loaded column.

TABLE 4.1. Examples of Cyclic Adsorption Separation Processes [2]

Process	Liquid (L) or Gas Phase (G)	Adsorbent	Selectivity	Regeneration Method
Drying of gas streams	G	13X, 4A, or 3A mol. sieve	Equilib.	T swing or P swing
Drying of solvents	L	4A sieve	Equilib.	T swing
Solvent recovery	G	Act. carbon	Equilib.	Steam stripping
H_2 recovery	G	Mol. sieve	Equilib.	P swing
Air separation	G	Carbon mol. sieve	Kinetic	P swing
		Zeolite	Equilib.	P swing
Linear paraffins separation	G	5A mol. sieve	Shape selective sieving	Displacement or vacuum
Waste water purification	L	Act. carbon	Equilib.	Steam stripping

(*i*) ***PURGE GAS STRIPPING*** :

Regeneration of the bed is achieved in this case by purging the column with a nonadsorbing carrier gas at essentially constant temperature and pressure. This method is relatively uncommon since such a process is applicable only for very weakly adsorbed components. Purge gas stripping is generally combined with pressure swing or temperature swing in order to reduce the purge gas requirement.

(*ii*) ***DISPLACEMENT DESORPTION*** :

In this type of process, an adsorbable material which displaces the adsorbed species already present in the adsorbent, is used instead of an inert, as in purge gas stripping. It is useful for the separation of strongly adsorbed species where conditions of adsorbent stability or reactivity of the sorbate make temperature swing operation unsuitable. The use of displacement desorption makes the product recovery somewhat more complex as additional separation steps are required to remove the displacing component.

(*iii*) ***TEMPERATURE SWING*** :

Since at a given pressure the equilibrium loading is greater at low temperature, desorption may be achieved by raising the temperature of the column. In a temperature swing process the column temperature is generally raised either by passing a stream of hot gas or by using heating coils within the bed. Drying of air, natural gas, or other process streams are example of

processes which employ thermal swing cycles.

(iv) PRESSURE SWING :

In a pressure swing process the separation of gas mixtures is achieved by alternate adsorption and desorption using the pressure as the thermodynamic variable which controls the equilibrium loading. The pressure swing cycle, therefore operates between two pressures, adsorbing at higher pressure and desorbing at lower, essentially at constant temperature. Processes such as small scale air drying, separation of oxygen and nitrogen from air and hydrogen purification commonly use pressure swing cycles.

4.1.3 PRESSURE SWING vs. THERMAL SWING ADSORPTION PROCESSES :

The basic difference between the pressure swing adsorption (PSA), and the thermal swing adsorption (TSA) processes is in the method of regeneration of the adsorbent.

Two equilibrium adsorption isotherms are shown in Figure 4.1. As shown in the Figure, the loading of a given adsorbate increases with the partial pressure of the adsorbate at a fixed temperature. The loading of a given adsorbate decreases as the temperature increases at a fixed pressure. It is obvious that the net effect is more or less the same as far as the loading is concerned.

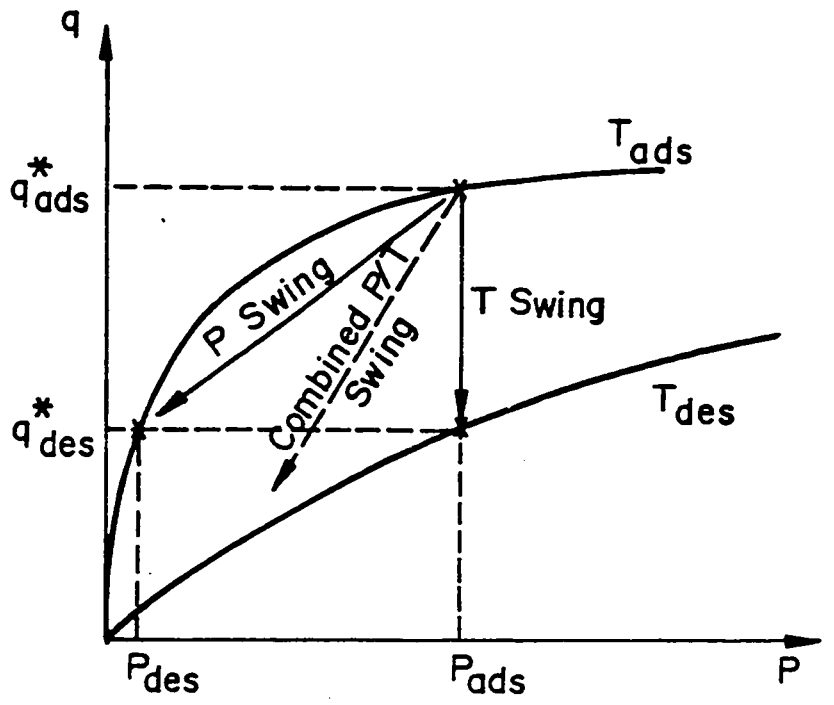

Figure 4.1 Schematic Isotherm showing Pressure Swing, Thermal Swing and Combined Pressure-Temperature Swing Operation for an Adsorption Process

A PSA cycle operates between two pressures, adsorbing at the higher pressure, and desorbing at the lower one, with a minimal change in the temperature which may result from the heat of adsorption. A TSA cycle operates between two different temperatures, but at the same pressure, adsorbing at the lower temperature, and desorbing at the higher one. Various combinations may exist, and in fact, some TSA cycles are operated at two different pressures. PSA may appear more preferable than TSA which requires an external heat source plus the means of removing the heat from the adsorbent [47].

4.1.4 SELECTION OF PROCESS :

All the cyclic processes described earlier have advantages and disadvantages. The final decision to select the most suitable process depends on the system under consideration and the availability of resources. A thermal swing process is good for strongly adsorbed species and may be advantageous if a cheap source of heat is available. However, the energy cost involved may sometimes be significant. Moreover, the time delays in heating and cooling do not permit rapid cycling, thus limiting maximum throughput. On the other hand, the throughput in a pressure swing process is higher as a result of more rapid response of gas-solid system to pressure changes than to temperature change. This allows the use of shorter cycle times, increasing the throughput. The raffinate product (the less strongly adsorbed species) can be recovered at high purity in general but only at relatively low fractional recovery. Such

processes are therefore most useful for the separation of mixtures in which the feed is relatively inexpensive and the required product is the less strongly adsorbed species.

4.1.5 APPLICATION OF PRESSURE SWING ADSORPTION PROCESS :

Cryogenic processes, which can produce ultrapure oxygen as well as nitrogen and inert gases remain the most economical process for large scale production. For many applications of oxygen, however a high purity is not required and the daily requirement is not large. Under these circumstances PSA processes have proved more economical than cryogenic processes. Some of the application requiring low-grade oxygen (below 95%) are biological treatment of waste water, feed to ozonator for waste water treatment, basic oxygen furnace in steel making, nonferrous metals smelting, paper & pulp industry, medical application and various partial oxidation process.

The goal of research in the 1950's and 1960's, as well as the original invention of the PSA process, was oxygen separation from air. The commercialization of the oxygen process was realized in 1970. In 1983 about 200 PSA oxygen systems were installed world wide in the 1-36 tons per day size range. There were also approximately 40,000 small units installed per year with capacities between 2 & 4 litres per minutes, for use by patients with chronic pulmonary dysfunction (e,g emphysema). The small units for medical oxygen were commercialized in the mid 1970's. These are two bed systems, each containing 1-2 pounds of zeolite which basically operate on the original

Skarstrom cycle. The product purity is 85-95% at only 10-30% oxygen recovery [37].

Much like oxygen production, PSA has also been found to be more economical for small to medium scale production of nitrogen at purities of about 99%. Such a market exists in inert gas generating needs such as purging, inert blanketing of fuel tanks and nitrogen based controlled atmosphere in food , metallurgical, and other industries. A more recent use of nitrogen is enhanced oil recovery.

4.2. THE BASIC DESCRIPTION OF PSA PROCESS:

The basic PSA process consists of two adsorption beds connected together as shown on Figure 4.2. There are four distinct steps involved in the PSA process as shown in Figure 4.3. The first step consists of passing feed gas into column 2 with a portion of product purging column 1. In step 2, column 2 which is originally at feed pressure is reduced to a lower pressure (blowdown), and column 1 is pressurized to feed pressure (repressurization). In step 3, the feed flows into column 1, with a portion of the product purging column 2. In the fourth step, blowdown of column 1 and repressurization of column 2 occurs.

The changes of pressure and flow rates occurring simultaneously in columns 1 and 2 during one full cycle is illustrated in Figure 4.4.

Steps 2 and 4 are short in duration and are somewhat exaggerated on the diagrams for clarity. Steps 1,2,3, and 4 represent low pressure flow,

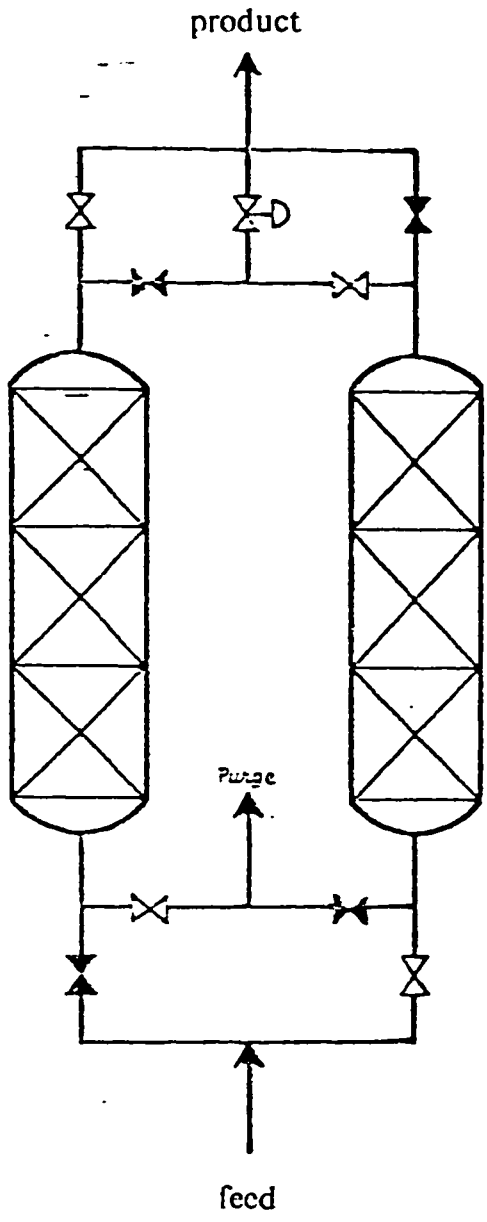

Figure 4.2 - The basic two bed PSA system

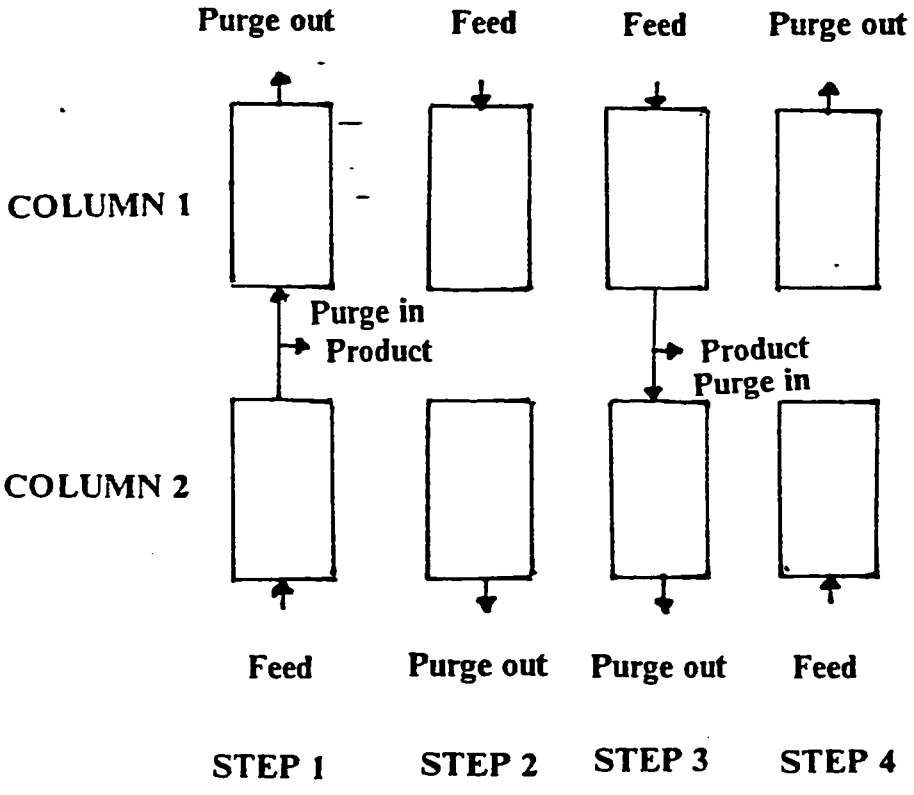

Figure 4.3 Four steps involved in PSA

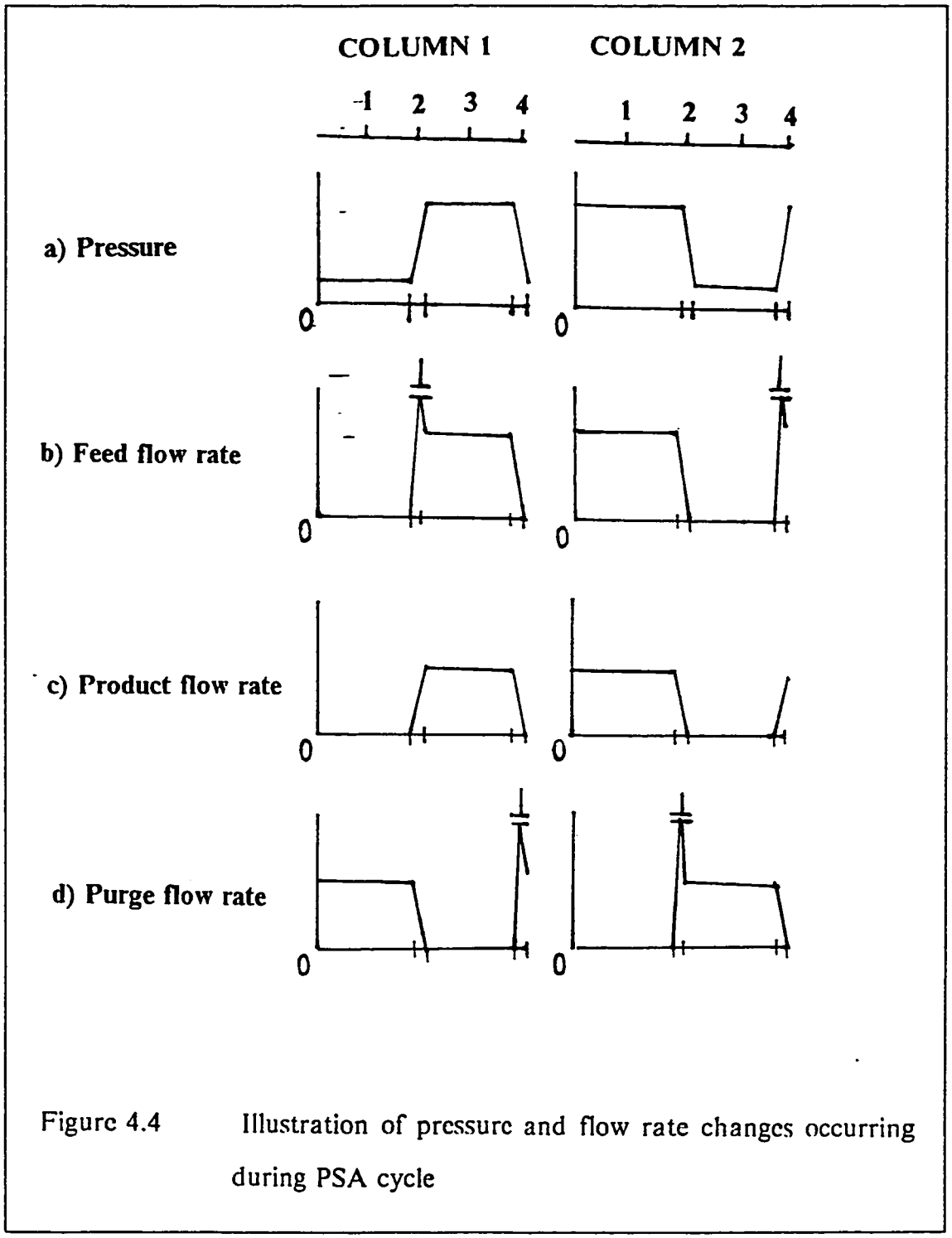

Figure 4.4 Illustration of pressure and flow rate changes occurring during PSA cycle

repressurization, high pressure flow, and blowdown respectively. In the Figures shown, no quantitative values are given to any flow rate except for flow rates equal to zero. Figure 4.4a indicates column 1 is at low pressure during step 1 . The pressure increases rapidly in step 2 up to some high value and remains there through step 3. Step 4 results in a pressure reduction back to the low value. During step 1, the feed flow rate is zero as indicated by Figure 4.4b. Then it increases rapidly as step 2 begins and drops to some positive value. The feed rate remains constant at a positive value during step 3, then drops back to zero as step 4 occurs. Figure 4.4c shows that the product flow rate has a value of zero during step 1 and then increases to some positive value during step 2. The product flow rate remains constant in step 3 and then drops to zero during step 4. Figure 4.4d shows that the purge flow rate is constant in step 1 and then decreases to zero during step 2. The purge rate remains at zero during step 3, then as step 4 occurs, it increases rapidly and then drops back to some positive value.

A characteristic of pressure swing adsorption cycle is the loss of recovery caused by blowdown and purging losses. The amount of blowdown losses depend on the pressure difference between the feed and the purge streams, and the cycling rate. However, the purging step is essential for an efficient separation. Reverse flow purge ensures that the more strongly adsorbed components are pushed back towards the bed inlet and that they do not contaminate the product stream in the next cycle. It is essential that sufficient purge is used to flush the void spaces within the bed, as well as to desorb most

of the more strongly adsorbed components from the outlet region of the bed. Product purity increases as the purge is increased, but after a certain point the gain becomes marginal [48].

4.2.1 SINGLE COLUMN PRESSURE SWING ADSORPTION :

A modified type of PSA cycle [49], utilizing a single adsorbent column was suggested by Turnock and Kadlec [50]. At one end of the column pressurized feed is alternately applied and the blow down, containing the more strongly adsorbed species exhausted on a rapid cycle; the other end either is used to obtain more or less continuous stream of the less strongly adsorbed component in the adsorption step, and also to introduce purge in the desorption step. Successful operation requires a careful choice of particle size and cycle time to obtain a proper dynamic response with sufficient pressure drop to prevent break through of the more strongly adsorbed species. However the very rapid pressure cycling may reduce adsorbent life and the overall economic comparison is not yet established [49]. Hence the important parameters that effect the process are the length of column to velocity ratio, cycle time, purge to feed ratio and pressure ratio.

4.2.2 CURRENT STATUS OF PSA RESEARCH :

Pressure swing adsorption is an active research area at present, and many papers are being published in this field. The aim of the research work in the area of pressure swing adsorptions is the utilization of the process for new

separation schemes as well as the simulation of the separation performance.

Mitchell and Shendalman [51] studied the purification of He from a feed blend containing CO_2. In their studies, they used silica gel as an adsorbent and they reported on the dynamic behavior of the pressure swing cycle. In their experiment they investigated the effects of space velocity, dynamic capacity, and purge to feed ratio. Using an equilibrium model they predict an exponential diminution of CO_2 concentration with time when the purge ratio exceeds one; however the actual observed concentration levels decrease monotonically but not rapidly. Their analytical solution is obtained from a mathematical model with linear isotherm for a trace component by the method of characteristics. In their second paper, they present a non-equilibrium model by including a mass transfer resistance. This allows them to bracket the behavior during pressure changes in the adsorption columns. They also found that large space velocity has a deleterious effect on process performance; increasing the dynamic capacity improves the rate of product clean up and that higher purge to feed ratios have a profound effect on initial product purification.

In 1973 three review papers by Lee and Stahl [52], Landolt and Kerr [53] and Wankat [54] appeared stressing the need for further investigation in this new area of gas separation. Bird and Granville [55] studied the separation of nitrogen from helium using the pressure swing adsorption process. In their experiments, they used three bed heights of .286, .584,and .889 m, respectively. In each case, the bed diameter was .025 m and the adsorbent was activated

carbon. As a conclusion of their study, they found that for operation at ambient temperature, mass transfer efficiencies were enhanced by reducing either the flow rate or cycle time. Weaver and Hamrin [56] separated hydrogen isotopes using a single staged pressure swing adsorber packed with metallic palladium on alumina. They performed eleven heatless adsorption runs to examine the effect of the purge to feed ratio and cycle time. They also developed a mass balance model to predict the effect of these parameters on separation. Additional runs were made to determine the breakthrough at the two operating pressures of 19.7 and 114.7 psi. As a conclusion of their study, they found that as the purge to feed ratio increased from 0 to 3, better separations were achieved but the quantity of product decreased. A critical value of purge to feed ratio is in the range of 1.0 to 1.2; as the cycle time increase from 1 to 8 min, the quantity of product increased, but the magnitude of separation decreased.

Wong and Hill [57] studied the separation of hydrogen isotopes by a pressure swing adsorption process. In their first paper, they used a single column pressure swing adsorption process. Vanadium monohydride was used as adsorbent and the feed was hydrogen containing a trace of HT. They observed that the separations were controlled by a kinetic isotope effect. In the second paper by Wong et al. [58] a two-column pressure swing adsorption process was used. The columns were packed with vanadium hydride. They observed that for process operation solely within the monohydride phase, a postulated isotope effect in the rates of hydrogen adsorption and desorption appeared to control the process performance. For the case when process operation involved

transitions back and forth between the monohydride and dihydride phases, they found that the performance is mainly controlled by an equilibrium isotope effect.

Fernandez and Kenney [59] investigated the separation of oxygen and nitrogen in air on 5A zeolite by a single column pressure swing gas separation process. They were able to adequately represent the process by an " approximate" solution of an equilibrium model taking into account the changes in mass flow due to adsorption. Comparison of theory and data obtained using molecular sieve adsorbent indicate accuracy of 10% for prediction of concentrations, 15% for predictions of feed flows and 12% for estimation of recovery. Carter and Wyszynski [60] studied the drying of compressed air by pressure swing adsorption using a granular silica gel adsorbent under different operating conditions. In their experiment, portion of the dried air expanded to lower pressure to purge the saturated bed for regeneration purposes. The effect of the volume ratio of purge flow to feed flow on the dry air humidity when the process has reached quasisteady state was investigated over the range 0.58-1.48. They used a simplified dynamic adsorption model that takes into account previously determined equilibrium and rate data to predict the measured humidities.

The separation of mixtures of helium and methane using a single column of activated carbon in a pressure swing adsorption process was studied experimentally by Cheng and Hill [61] in 1985. A local-equilibrium well stirred

cell model in which dead volumes at the feed and product ends of the column were accounted for, was used to predict the process performance. The systematic differences between the experiment and model were attributed to omission from the model of flow resistance and heat release. Whitley and Hamrin [62] studied the separation of hydrogen sulfide-hydrogen mixtures by heatless adsorption. They used two brass columns having dimensions of 0.94 cm inside diameter and 87.6 cm length. The columns were packed with Union Carbide molecular sieve type 4A, 8 × 12 mesh beads. The purge to feed ratio, cycle time, and total feed rate were all proved to be important factors affecting the degree of removal of the hydrogen sulfide. The investigators used an equilibrium model and assume that the adsorption isotherm is linear to predict the data.

Tondeur and Wankat [63] reviewed gas purification on pressure swing adsorption. The objective of their review was to present a comprehensive, flow sheet oriented review of PSA processes, emphasizing general principles and offering possibly new conceptual tools for comparison, analysis and evaluation of these processes. The processes were restricted to those where a separation is based on decreasing the pressure and usually purging at low pressure with the pure gas produced by the process. Old separations such as air drying, enrichment of air in oxygen, and hydrogen purification were mentioned but in recent years, PSA has raised renewed interest, relating to new needs in gas separations on one hand and to a better knowledge of the basic processes involved on the other hand. A great variety of operating schemes has resulted, comprising sometimes a large number of columns and complex flow sheeting. In

particular, they mention the use of two adsorbents for hydrogen and methane recovery and removal of C^{+}_{2} from the effluent gas of a hydrodesulfurization plant. The two adsorbents used were activated carbon and coke.

Cen et al. [64] conducted an experimental and theoretical study for the bulk separation of a ternary gas mixture by pressure swing adsorption. Each cycle encompassed four steps: pressurization, adsorption, cocurrent blowdown, and countercurrent vacuum desorption. The experimental data were satisfactorily predicted and simulated by an equilibrium model and a linear driving force model. A feed mixture containing 49.5/49.5/1.0, $H_2/CH_4/H_2S$ was separated into three useful products : a clean H_2($>99H_2$, $< 0.01 H_2S$) a clean CH_4($>95CH_4$, $< 0.01 H_2S$) product, and a H_2S product (over 10%). Cocurrent blowdown was a crucial step for recovering the medium product (CH_4). Vacuum desorption and pressurization by H_2 were important in recovering the heavy product (H_2S) and cleaning the bed for high purity H_2 product.

Ruthven et al. in three papers [65,66,67] reported on theoretical and experimental modelling of PSA processes. In their first paper, they present a dynamic model for a simple two-bed PSA system. The dynamic model equations, incorporating dispersion in the gas phase, were solved by the method of orthogonal collocation to yield a useful simulation which, using independently measured rate and equilibrium constants, was shown to provide a good representation of the experimental data reported by Mitchell and Shendalman

(1973). In their second paper, the model was adapted to a non-linear Langmuir isotherm for ethylene adsorption on 4A and 5A zeolites. The model successfully simulated the slow intracrystalline diffusion in the 4A sieve, and the fast macropore diffusion in the 5A sieve. In their third paper, the model was adapted to the situation in which both kinetic effects and changes in flow rate are significant.

4.3 THEORETICAL MODEL :

Two distinct approaches to modelling the simple PSA cycles described earlier have been developed. In the first, the equilibrium model, it is assumed that the solid and gas phases during adsorption or desorption steps remain at equilibrium. In the second analysis, the presence of significant mass transfer resistance is allowed for. This approach will be referred to here as the dynamic model.

The equilibrium model provides valuable information concerning the maximum purge/feed ratio and column length required to produce a pure raffinate product for any specified separation factor and pressure ratio. However, in a real system the effect of mass transfer resistance and axial dispersion are generally important and therefore in order to obtain a more realistic model these effects have to considered.

Chihara and Suzuki[68] proposed a simple method for evaluation of cyclic steady profile of the amount adsorbed by assuming equivalency of the PSA in a

which consists mainly of adsorption step, reverse flow desorption step and the counter current continuous flow (CCF) contacting system. The operation scheme of the basic PSA is illustrated in Figures 4.5a and 4.5b.

Pressurizing and blowdown steps (steps 1 and 3 in Figure 4.5a) are considered rapid enough and the profile of the amount adsorbed in the column during these steps remain unchanged (frozen profile) when the cycle time of pressure swing is far smaller than the time constant of saturation of the column i.e. throughput ratio is far smaller than unity. Profiles of the amount adsorbed in the column during adsorption and purge steps stay almost unchanged. Figure 4.6, shows this concept. In the cyclic steady state, the profile of the adsorbed amount of i, q_i moves between curve H and L in Figure 4.6a. The curves H and L respectively, shows the profiles at the end of the adsorption step (step 2) and the one at the end of desorption step (step 4). The fractional area of the shaded part surrounded by the curves H and L correspond to throughput ratio. Also partial pressure of component i, p_i in the gas phase moves gradually during the adsorption step from profile 1 to 2 and during purge desorption step from 3 to 4. When cycle time of PSA becomes small, the shaded area diminishes and the curves H and L coincide to give the bold curve in Figure 4.6b. In this case, the gas phase concentration profile during the adsorption step and desorption step are approximately unchanged.

The assumption of the establishment of frozen profile suggests that it may be estimated by means of the CCF analogy. Figure 4.5 shows the basic idea of

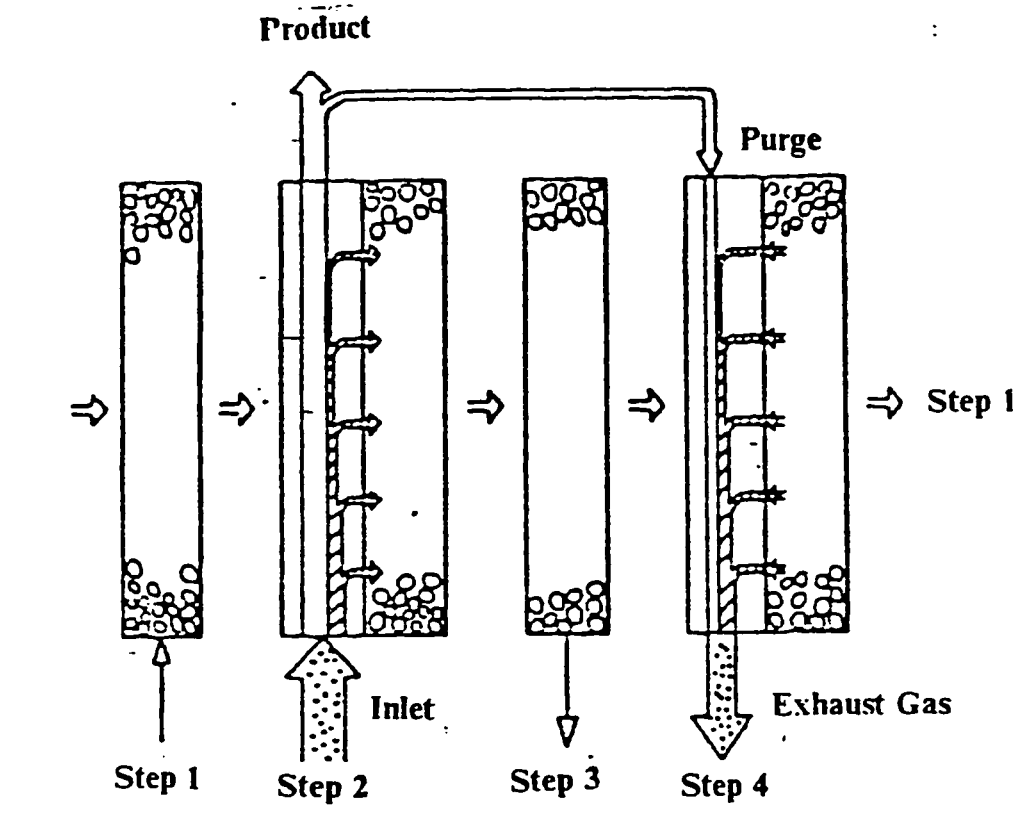

Figure 4.5(a) Conceptual scheme of PSA operation

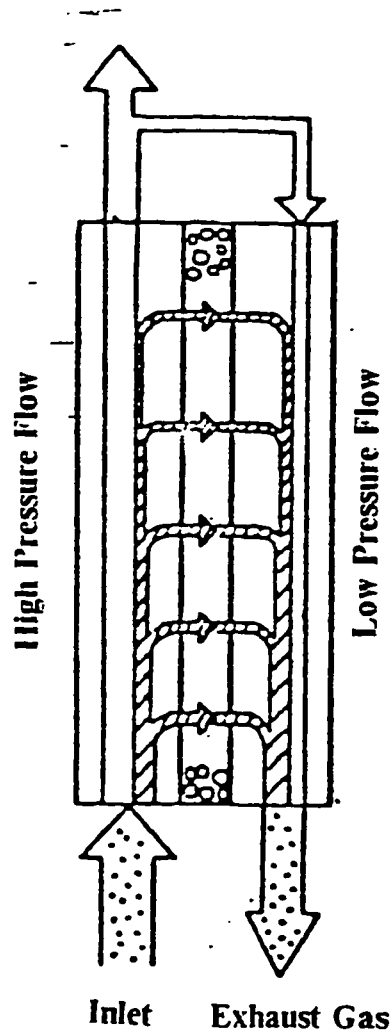

Figure 4.5(b) Conceptual scheme of steady cocurrent flow contactor

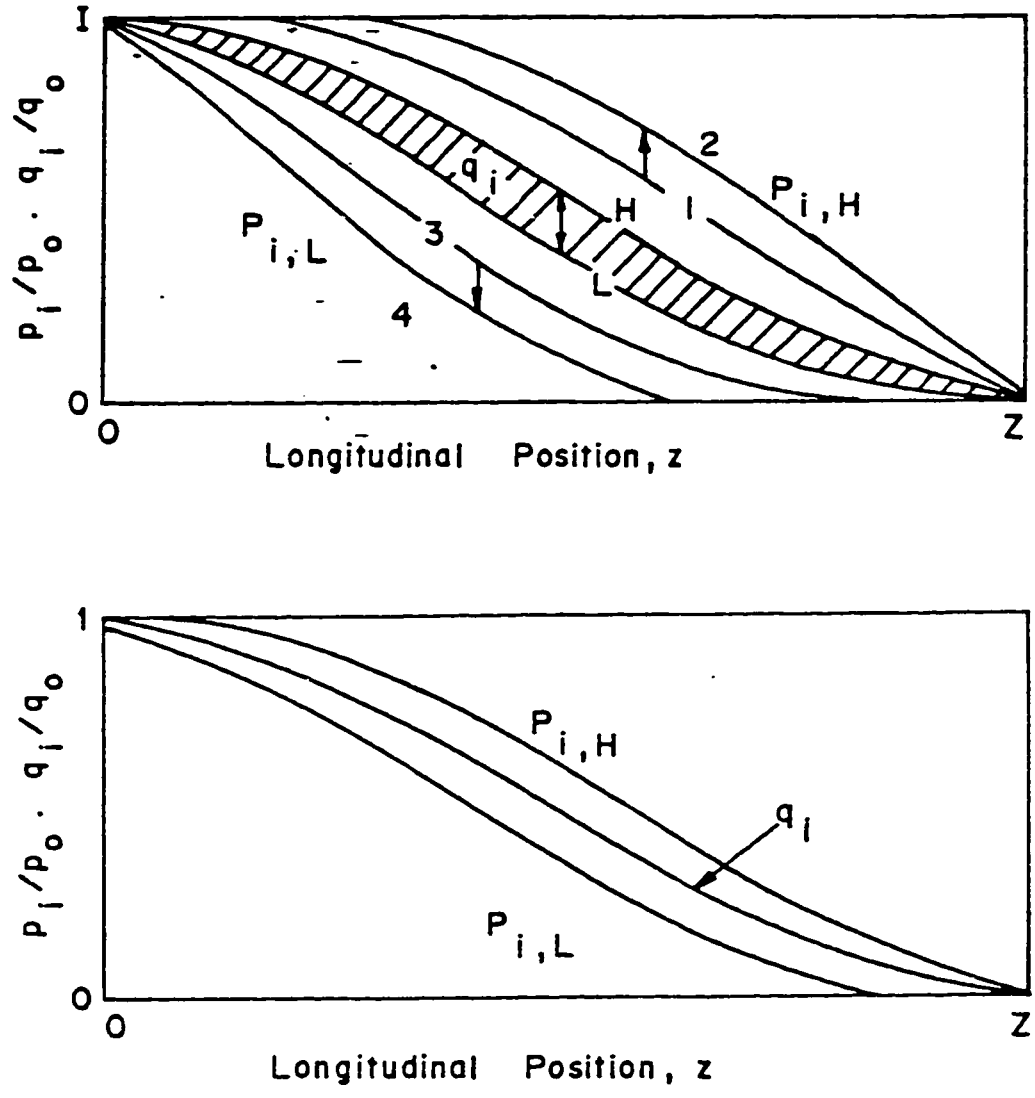

Figure 4.6 Longitudinal profile of concentration in gas phase and amount adsorbed in column during cyclic steady state of PSA operation

the corresponding CCF model. The mass flows of the adsorbates from a high pressure to the particle and from the particle to a low pressure flow take place in series.

These extreme assumptions may be realistic for a purification process; in a bulk separation process there will generally be significant excursions of the concentration profiles during the adsorption and the desorption steps. The model of Chihara and Suzuki [68], was extended recently by Farooq and Ruthven [69] to make it applicable for bulk separation processes.

4.3.1 MATHEMATICAL MODELING :

A description of the model presented by Farooq and Ruthven [69] is given below.

An isothermal, plug flow system is considered in which fractional pressure drop in the bed is negligible and the total pressure in the bed remains constant during the adsorption and desorption steps. The equations are developed for a two component system in which both the components are adsorbed and therefore the fluid velocity in the bed varies along the length of the column. Equilibrium relationship for both the components are represented by the binary Langmuir isotherm and the mass transfer rates are given by linear driving force rate expression. Development of the CCF model, subject to these assumptions, is as follows:

Mass balance (component A) :

$$j\frac{d(u_i C_{Ai})}{dz} + \frac{1-\varepsilon}{\varepsilon}(m-1+j\alpha)\frac{dq_{Ai}}{dt} = 0 \qquad \text{----------(4.1)}$$

Continuity condition :

$$C_{Ai} + C_{Bi} = C_i \quad (constant) \qquad \text{----------(4.2)}$$

Overall balance :

$$jC_i\frac{du_i}{dz} + \frac{1-\varepsilon}{\varepsilon}(m-1+j\alpha)\left(\frac{dq_{Ai}}{dt} + \frac{dq_{Ai}}{dt}\right) = 0 \qquad \text{----------(4.3)}$$

Mass transfer rates :

$$\frac{dq_{Ai}}{dt} = k_{Ai}(q^{*}_{Ai} - q_A) \qquad \text{----------(4.4)}$$

$$\frac{dq_{Bi}}{dt} = k_{Bi}(q^{*}_{Bi} - q_B) \qquad \text{----------(4.5)}$$

Adsorption equilibrium :

$$\frac{q_{Ai}^{\cdot}}{q_{AS}} = \frac{b_A C_{Ai}}{1 + b_A C_{Ai} + b_B C_{Bi}} \qquad \text{----------(4.6)}$$

$$\frac{q_{Bi}^{\cdot}}{q_{BS}} = \frac{b_B C_{Bi}}{1 + b_A C_{Ai} + b_B C_{Bi}} \qquad \text{----------(4.7)}$$

In the above equations i = H or L, j = +1 or -1, and m = 1 or 2.

If i = H, j = +1, and m = 1 represents high pressure flow, and if

i = L, j = -1, and m = 2 represents low pressure flow.

Boundary conditions for the high pressure flow are :

$$C_{AH}|_{z=0} = C_{A0} \qquad \text{----------(4.8)}$$

$$u_H|_{z=0} = u_{0H} \qquad \text{----------(4.9)}$$

Boundary conditions for the purge flow are :

$$C_{AL}|_{z=L} = C_{AH}|_{z=L}\left(\frac{p_L}{p_H}\right) \qquad \text{----------(4.10)}$$

$$u_L|_{z=L} = u_{0L} \qquad \text{----------(4.11)}$$

The velocities used in the above equation are the equivalent velocities for the CCF model and are related to the velocities in an actual PSA cycle as follows:

$$u_H = \alpha v_H \; ; \; u_{0H} = \alpha v_{0H} \qquad \text{---------- (4.12)}$$

$$u_L = (1-\alpha)\, v_L \; ; \; u_{0L} = (1-\alpha)\, v_{0L} \qquad \text{----------(4.13)}$$

$$\alpha = \frac{t_H}{t_H + t_L} \qquad \text{----------(4.14)}$$

Equation (4.10) represents the fact that part of the high pressure product is expanded to low pressure and used for purge flow. In an actual operation:

$$v_{0L} = G \times v_{0H} \qquad \text{----------(4.15)}$$

where G is the purge to feed velocity ratio. An equivalent relation for the CCF model will be :

$$u_{0L} = G\left(\frac{\alpha}{1-\alpha}\right) u_{0H} \qquad \text{----------(4.16)}$$

The factor (m-1+j α), in equations (4.1) and (4.3), has been introduced to maintain consistency in mass transfer rates between the CCF approximation and the transient simulation. The assumption of zero net accumulation in the solid phase leads to :

$$\alpha\frac{dq_{AH}}{dt} + (1-\alpha)\frac{dq_{AL}}{dt} = 0 \qquad \text{----------(4.17)}$$

$$\alpha\frac{dq_{BH}}{dt} + (1-\alpha)\frac{dq_{BL}}{dt} = 0 \qquad \text{----------(4.18)}$$

From equations (4.4) and (4.17) we get :

$$q_A = \frac{\alpha\, k_{AH}\, \dot{q}_{BH} + (1-\alpha)\, k_{BL}\, \dot{q}_{BL}}{\alpha\, k_{BH} + (1-\alpha)\, k_{BL}} \qquad \text{----------(4.19)}$$

Similarly, from equations (4.5) and (4.18) we get :

$$q_B = \frac{\alpha\, k_{BH}\, \dot{q}_{BH} + (1-\alpha)\, k_{BL}\, \dot{q}_{BL}}{\alpha\, k_{BH} + (1-\alpha)\, k_{BL}} \qquad \text{----------(4.20)}$$

Substituting equation (4.19) in (4.4) and equation (4.20) in (4.5) and rearranging yields :

$$(m-1+j\alpha)\frac{dq_{Ai}}{dt} = j\, k_{eA}\, (\dot{q}_{AH} - \dot{q}_{AL}) \qquad \text{----------(4.21)}$$

$$(m-1+j\alpha)\frac{dq_{Bi}}{dt} = j\, k_{eB}\, (\dot{q}_{BH} - \dot{q}_{BL}) \qquad \text{----------(4.22)}$$

where :

$$k_{eA} = \frac{1}{\frac{1}{\alpha k_{AH}} + \frac{1}{(1-\alpha) k_{AL}}} \qquad \text{----------(4.23)}$$

$$k_{eB} = \frac{1}{\frac{1}{\alpha k_{BH}} + \frac{1}{(1-\alpha)k_{BL}}} \qquad \text{----(4.24)}$$

Combining equations (4.1), (4.3), (4.21), and (4.22) gives :

$$u_i \frac{dc_{Ai}}{dz} + \frac{1-\varepsilon}{\varepsilon}\left[(1-X_{Ai})\, k_{eA}\,(q^{*}_{AH}-q^{*}_{AL}) - X_{Ai}\, k_{eB}\,(q^{*}_{BH}-q^{*}_{BL})\right] = 0 \qquad \text{----(4.25)}$$

Combining equations (4.3), (4.21), and (4.22) results :

$$C_i \frac{du_i}{dz} + \frac{1-\varepsilon}{\varepsilon}\left[k_{eA}\,(q^{*}_{AH}-q^{*}_{AL}) + k_{eB}\,(q^{*}_{BH}-q^{*}_{BL})\right] = 0 \qquad \text{----(4.26)}$$

Equations (4.25) and (4.26) were integrated using fourth order Runge-Kutta method to obtain C_{Ai} and u_i at different axial location in the bed. The boundary conditions at high pressure flow are known at z = 0 and those for purge are given at z = 1 and therefore, the solution procedure required iteration. Values of the dependent variables for purge flow were guessed at z=0. The integration was then performed from z=0 to L which was repeated until the known boundary conditions for purge flow at z=L were satisfied. Jacobian analysis was performed to update the trial values. Starting from the same initial guess, the convergence was much faster with Jacobian analysis than without as

expected. c_{Bi} at different locations were obtained by difference from total concentration. Steady state adsorbed phase concentrations were then calculated from equations (19) and (20).

In the present study since pure purge is being used instead of part of product the boundary condition given by equation (10) needs to be modified. This approach has been adopted to compare the experimental results with these obtained from the above theoretical model.

4.4 COMMERCIAL PSA PROCESSES:

Since the invention of the Skarstrom cycle, PSA has rapidly developed into a major technology for air drying, hydrogen purification, and small to medium scale air fractionation. Still, many more applications are being developed. Table 4.2 gives a history of PSA processes that have been commercialized. In the following sections, a brief description of the most widely used PSA processes in industry is given.

4.4.1 AIR DRYING:

Dry compressed air is widely used in industry. The original Skarstrom PSA cycle has been used for this purpose with almost no process modifications [1]. The original two bed unit is shown in Figure 4.2. Each bed undergoes the four steps of the cycle: repressurization, adsorption, counter current blowdown, and purge. The cycle time is usually between 1 and 10 minutes and the preferred

Table 4.2 History of commercial PSA processes.

Year	*Process*
1960	Air separation using Skarstrom cycle
1961	n-paraffin solvent production
1964	Kerosene range n-paraffin recovery
1966	Hydrogen production
1970	Oxygen production
1975	medical oxygen concentrators
1975	Octane improvement
1976	Nitrogen production using CMS
1977	large scale PSA hydrogen system
1980	Rapid pressure swing adsorption
1983	nitrogen production using zeolite adsorbent

sorbents are silica gel and activated alumina although zeolites are also used.

4.4.2 HYDROGEN PURIFICATION AND RECOVERY:

Hydrogen purification is an important step in the production of hydrogen. Presently, the production of hydrogen is carried out by catalytic steam reforming of natural gas, naphtha, or refinery gases. Hydrogen is also recovered from catalytic reformer effluent gas, ethylene plant effluent gas, and from other sources [47].

The first commercial PSA unit for hydrogen purification was installed at the effluent of a steam reformer by Union Carbide in Toronto in 1966. Presently, the capacity of PSA systems for hydrogen purification exceeds 1 billion SCF/day worldwide [70].

Hydrogen purification was successful because of the high selectivity of the impurity gas over hydrogen. As a result all commercial sorbents can be used in the purification process. In practice, a combination of activated carbon and zeolites are used [1].

4.4.3 AIR SEPARATION FOR O_2 AND N_2 PRODUCTION :

The standard procedure for obtaining oxygen from air is liquefaction followed by distillation. The process is complex and energy intensive. Separation of oxygen and nitrogen from air by PSA is a relatively simple process which is particularly useful for smaller scale installation for production of both nitrogen

and oxygen. Separation can be achieved either on the basis of equilibrium selectivity, as in the case of 5A zeolite where nitrogen is preferentially adsorbed or alternatively, on the basis of kinetic selectivity as in the case of CMS, where oxygen diffuses faster than nitrogen. The operating conditions and performances are quite different for the two types of systems.

4.4.4. OTHER SEPARATIONS :

Processes such as isotope separation in the nuclear reprocessing industry, recovery of helium from blast furnace gases, and hydrocarbon separation are some other examples where PSA can be utilized successfully.

CHAPTER 5

DESCRIPTION OF THE PSA UNIT

5.1 APPARATUS:

The pressure swing adsorption apparatus used in this work consists of one adsorption column of stainless steel of 3.45 cm internal diameter and 36 cm length, an oxygen analyzer 540A, Matheson solenoid valves, programmable cycle timer, and Matheson multiple mass flow controller Model 8209. A schematic diagram of the PSA unit is shown in Figure 5.1, and details of column are given in Table 5.1.

High pressure air was introduced to the column during steps 1 and 2. Product was withdrawn at a constant rate during during step 2. Bed pressure was controlled in step 2 by pressure regulator. A programmed timer controlled solenoid valves to achieve the desired cyclic operation. Product purity was determined by withdrawing gas samples from the product stream and analyzing in a oxygen analyzer. Prior to 4 and 5A-zeolite PSA experiment, the bed was regenerated at 250 °C in He flow for approximately 12 hours and then allowed to cool to room temperature.

5.1.1 LOADING OF THE ADSORPTION COLUMN:

In this step, the adsorption column is loaded with the desired adsorbent. A

Table 5.1 Details of PSA Column and Adsorbents.

Length of Column	=	36.0 cm	
Internal Diameter of Column	=	3.43	*cm*
Cross-sectional Area of Column	=	9.24	cm^2

ADSORBENT	CMS (Bergbau Forschung)	4A-Zeolite (Linde)	5A-Zeolite (Linde)
Voidage	0.403	0.398	0.384
Wt. of Wet Adsorb.(gm)	242.9	292.0	263.0
Pellet Density (gm/cc)	1.210	1.150	1.130

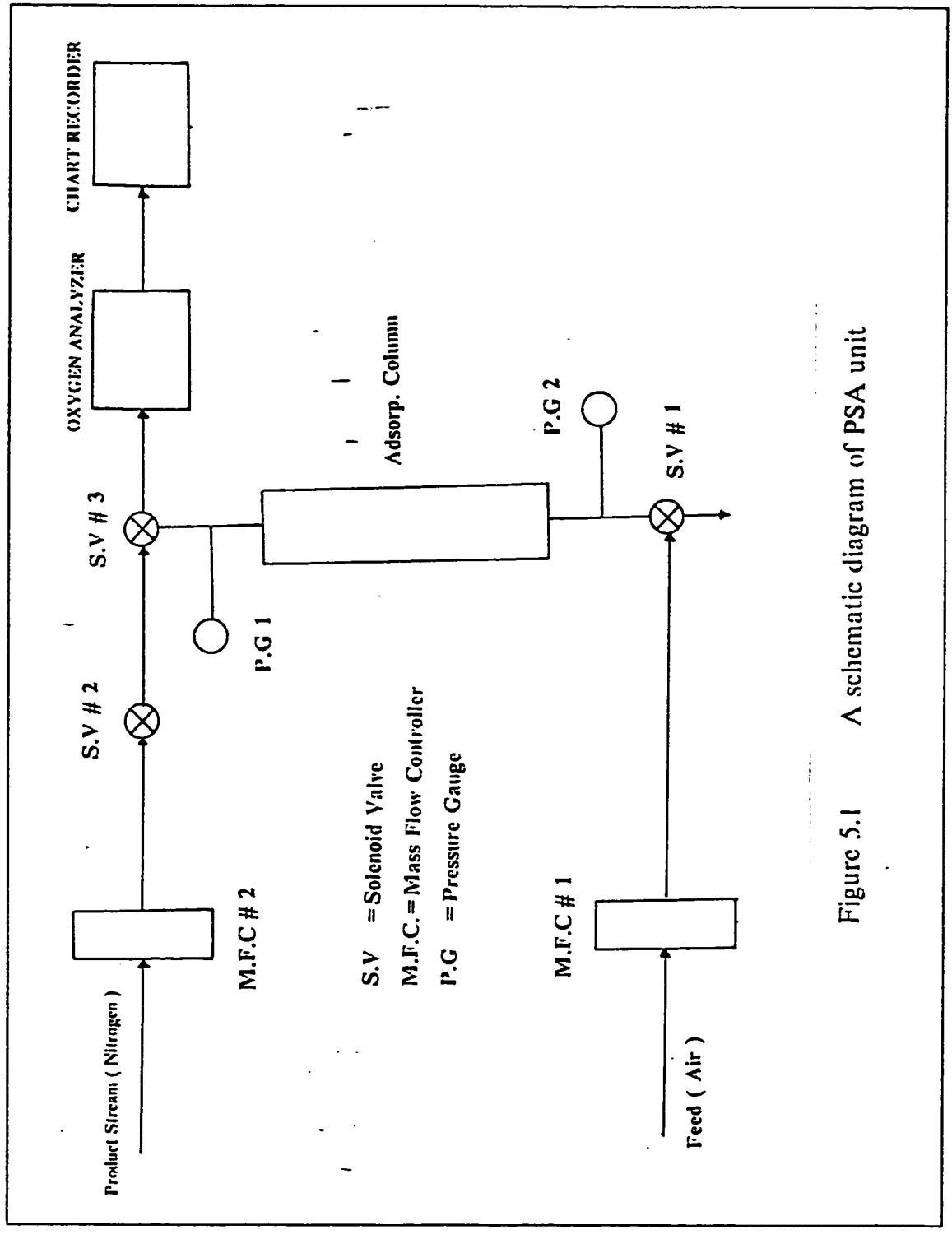

Figure 5.1 A schematic diagram of PSA unit

careful procedure is followed in packing the column to insure a constant density distribution of the adsorbent throughout the whole length of the column. Prior to the packing of the columns, the top flange of column is removed carefully. An accurate balance was used to measure the quantity of adsorbent used to fill the column. The top flanges are then mounted. The screws holding the flanges to the columns are tightened with a new set of seals with equal pressure to avoid leaks.

5.1.2 PRESSURE TESTING:

Pressure testing for possible leaks is normally carried out after loading the adsorption column with the new adsorbent. In systems with adsorbent material, it is always advisable to pressure test using an inert gas. Since inert gas is not adsorbed, any pressure changes may be attributed directly to leaks from the system, provided that no significant temperature changes occur. In the PSA unit, the column and pipes are pressurized with helium gas up to a pressure of 60 psig. The adsorption column is then isolated by closing valves at the top of the column. Closing these valves isolates different sections of the unit, which makes it easier to detect leaks and identify their origin. Leaking joints once detected, are fixed and the unit is then repressurized. The pressure testing is completed when no significant changes of pressure occurs.

5.1.3 REGENERATION OF THE ADSORBENT:

Zeolite adsorbents are generally known to be hydrophilic material except for the silicalite family. When exposed to the atmosphere, the sieve adsorbs large

quantities of water and equilibrium is quickly achieved between the moisture content of the air and that of the sieve. The first four water molecules in the zeolite cavity are normally adsorbed on the pore mouth of the void structure making it almost impossible for any other gas molecule to penetrate through and be adsorbed in the available internal active sites. Obviously, this will result in considerable reduction in the sieve activity for adsorption. The molecular sieve bed is dried by regenerating at a considerably high temperature. In this work, the adsorption bed is heated at 200 to 250°C for about 12 to 13 hours and purged with helium. The column is then cooled to the room temperature and saturated with feed air at high pressure before the PSA experimental run.

5.2 EXPERIMENTAL PROCEDURE :

The whole process may be summarized in four steps:

Step 1 : PRESSURIZATION

In the pressurization step, the feed is introduced at the bottom of the column, while the upper end of column is closed in order to pressurize the column.

Step 2 : ADSORPTION

The feed air is introduced at high pressure through the bottom end of the column, while the top end of the column is opened through which the product stream comes out and then passes through the oxygen analyzer for monitoring

the concentration.

Step 3 : BLOWDOWN

In this step the column pressure is reduced by opening the bottom end of the column while keeping the top end closed.

Step 4 : DESORPTION OR PURGE

During this step, which is the fourth step, a pure purge gas is introduced from the top end of the column at atmospheric pressure to clean the previously loaded column. The purge gas flows out of the column from the bottom end. This completes one full cycle of PSA and the column is ready for the next cycle.

The solenoid valves are switched on or off by a Xanadu universal programmable cycle timer, through which the flow direction through the valves can be controlled. The flow rates of feed and purge gas are monitored by mass flow controllers.

The above procedure is followed for experimental runs conducted at different sets of operating parameters, such as the cycle time, purge and feed flow rates, pressure ratio, length/velocity ratio. The results obtained from the experimental work are presented in chapter 6.

CHAPTER 6

RESULTS AND DISCUSSION

In this chapter the results obtained from the experimental work on PSA air separation on CMS, 5A and 4A zeolites are presented and analyzed.

There are many operating parameters involved in the operation of the PSA unit. The parameters include cycle time, high to low pressure ratio, feed and purge flow rates, length of column/velocity ratio, desorption time and type of adsorbent used. Every operating parameter has a considerable effect on the separation performance of the unit. In order to study the effect of the operating parameters on the separation performance of the unit, more than one experimental run is carried out. Prior to all experimental run the column was saturated with feed air at high pressure to establish a well defined initial condition. A typical output starting from the initial conditions to the cyclic steady state condition is shown in Figure 6.1.

The separation performance of the unit is rated on the basis of the steady state product concentration. The composition of the desired gas in the product stream is considered to be a measure of the separation performance of the unit. The effect of various operating parameters on the separation of air is given in the following section.

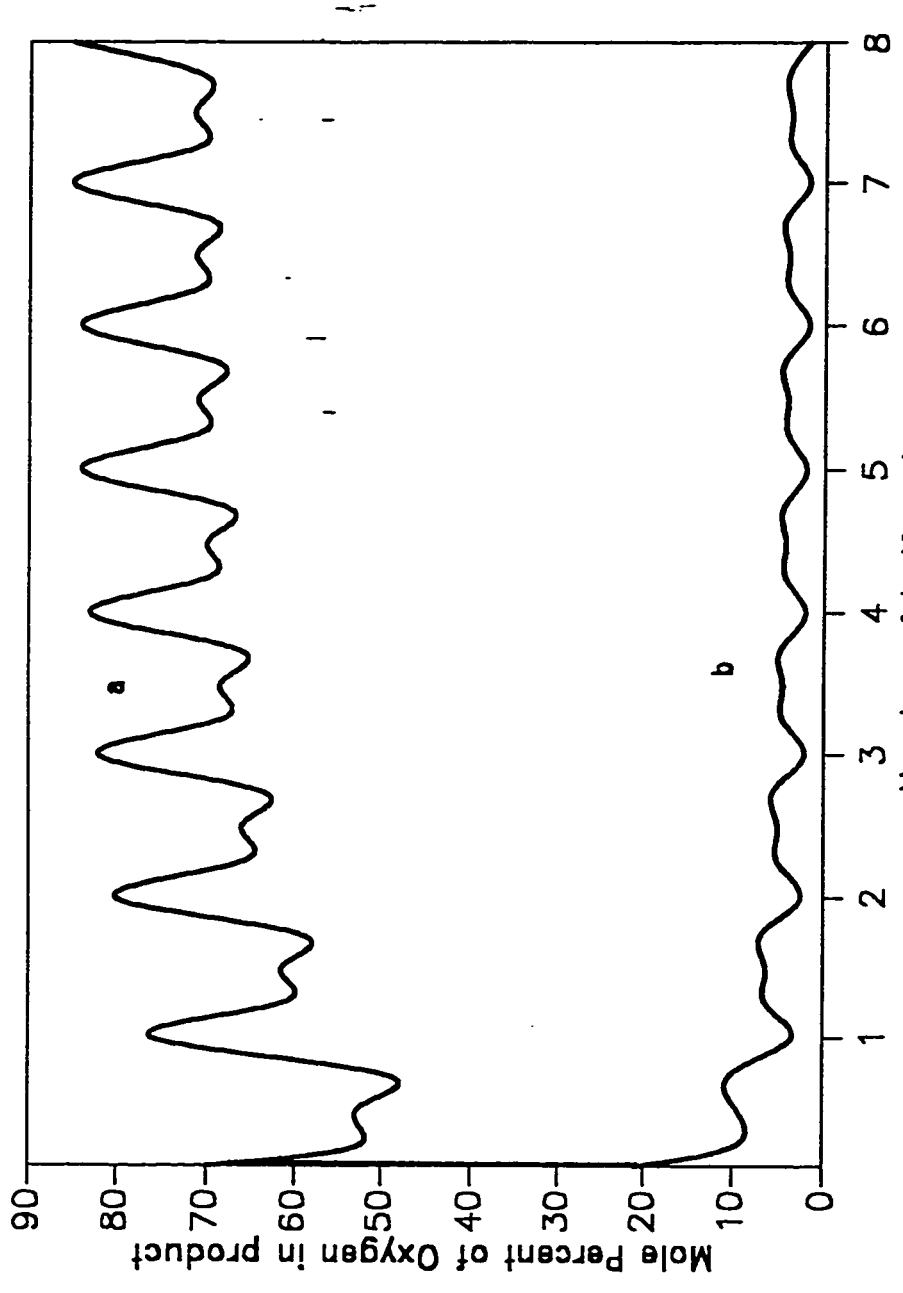

Figure 6.1 Typical Output from the Chart Recorder for PSA air Separation (a) 4A-zeolite (b) CMS

6.1 SEPARATION OF AIR ON PSA USING CMS AS ADSORBENT :

Air separation by pressure swing adsorption (PSA) on carbon molecular sieve (CMS) has emerged recently as one of the more interesting processes. Most adsorptive separation processes are based on equilibrium selectivity where the equilibrium capacity of the preferentially adsorbed component is substantially larger in the sorbent. However, the separation of air on carbon molecular sieve is based on the kinetic selectivity since the micropore diffusivity of O_2 is much larger than that of N_2. The faster diffusing species oxygen is therefore preferentially adsorbed and by using properly selected conditions it is possible to obtain a fairly high purity nitrogen product. The summary of the present experimental results is shown in Table 6.1.

(i) EFFECT OF LENGTH/VELOCITY RATIO (L/ v_H) :

It is always desirable from a practical point of view, to operate PSA units at the highest possible feed flow rates. This will increase the amount of product and hence the yield of the unit. However, in PSA processes, an increase in the feed flow rate may limit the separation efficiency of the unit.

The effect of L/ v_H on the separation of N_2 and O_2 from air using CMS adsorbent is indicated on Figure 6.2, for L/ v_H of 13.58 to 23.52 s . The cycle time, pressure ratio and purge to feed ratio are held constant the purge being pure N_2. As the L/ v_H increases, the percentage of O_2 in the product decreases,

the concentration of N_2 increases, hence improving the separation performance of the unit.

(ii) EFFECT OF PRESSURE RATIO (P_H / P_L) :

The effect of cycle high to low pressure ratio on separation of air using CMS adsorbent is shown in Figure 6.3. The increase in the high to low pressure ratio from 2.02 to 3.04 decreases the percentage of oxygen in the product from 3.30 to 2.00. Further increase in pressure ratio beyond 3.04 results in an increase in the percentage of oxygen in the product stream. It is apparent that oxygen concentration in the product stream reaches a minimum at a pressure ratio of about 3.04. This value may be considered optimum for the specified set of operating conditions.

(iii) EFFECT OF CYCLE TIMES:

Cycle time is the elapsed time during which one of the adsorption columns undergoes all steps of the PSA cycle and returns to its original condition. The incentive for operation a PSA unit at a long cycle time is to maximize the quantity of the product. However, too large cycle time causes the adsorption waves to frequently break out of the column, which results in impurities in the product stream. Alternatively, too small value of cycle time results in less efficient utilization of the adsorption column, and less volume of gas available for purging, resulting in a decrease in the degree of regeneration, and hence a lower performance of the unit is expected. Optimum cycle time is a highly

sensitive function of stream size, composition, and product purity.

The effect of cycle time on the separation of oxygen from air at purge to feed ratio of 0.85, L/ v_H =20.50 s , high and low pressure ratio of 3.04, using CMS adsorbent, is shown in Figure 6.4. From Table 6.1 we conclude that a slight increase of the cycle time from 80 to 90s results in the decrease of the oxygen concentration. However, beyond a cycle time of 90s, oxygen concentration in the product increases. Therefore a cycle time of 90s may be considered optimum for the present set of conditions.

(*iv*) ***EFFECT OF PURGE TO FEED RATIO*** (v_L/v_H) :

The purge step in the PSA processes may be characterized as the reflux step in distillation operations. The higher the purge rate, the purer the product. This is owing to the availability of sufficient quantity of gas for better regeneration of the adsorbent. The use of high purge rate will increase the unit operating cost. Similar to the reflux ratio, there is a minimum purge flow rate below which the desired product purity may not be obtained. An approximate rule valid for linear adsorption isotherms, is that the minimum purge rate for a pure product is such that the volume of the purge is equal to the volume of feed calculated at the specific pressure of each step.

The effect of purge to feed ratio on separation of oxygen from air using CMS as adsorbent is shown in Figure 6.5. The cycle time, high to low pressure ratio and L/ v_H are held constant. An increase in the purge to feed ratio

decreases the oxygen concentration, and hence gives a purer product stream of N_2.

(v) *EFFECT OF DESORPTION TIME*:

The time used for desorption has a significant effect on the product purity. In order to see the effect of desorption time, several runs were performed by varying the proportion of desorption and blowdown timings of the low pressure half cycle, while keeping the cycle time fixed. The results are reported in Figure 6.6, from which it is evident that the oxygen concentration decreases as the desorption time is increased indicating purer nitrogen in the product.

(vi) *COMPARISON WITH THEORETICAL MODEL PREDICTION*:

The predictions from the theoretical model described in section 4.3.1 were computed for some runs and have been compared with the present experimental data and results are reported in Table 6.2. The theoretical models predicts slightly higher concentration of nitrogen in the product as compared to the experimental data. However, considering the complexity of the process and the simplified assumptions made in the model the agreement is good.

Table 6.1 Operating conditions of experimental runs for O_2 and N_2 separation on CMS, using pure N_2 as purge.

	Cycle Time (s)	P_H/P_L	L/v_H (s)	v_L/v_H	% of O_2 in prod.
Effect of Cycle Time (s)	80	3.04	19.56	0.84	2.40
	90	3.04	21.42	0.89	1.60
	110	3.04	20.80	0.87	2.00
	120	3.04	20.22	0.83	3.75
	140	3.04	19.56	0.80	4.90
Effect of v_L/v_H	110	3.04	21.42	0.87	2.00
	110	3.04	21.42	1.51	1.25
	110	3.04	21.42	2.23	1.00
Effect of L/v_H (s)	110	3.04	13.58	2.65	2.60
	110	3.04	22.78	2.76	0.50
	110	3.04	22.00	2.87	0.40
	110	3.04	23.52	2.90	0.20
Effect of P_H/P_L	110	2.02	19.56	0.83	3.30
	110	2.36	20.23	0.87	2.70
	110	3.04	20.80	0.87	2.00
	110	3.38	20.68	0.87	2.50
	110	3.22	19.83	0.83	3.40

Table 6.2 Comparison of experimental and theoretical results for PSA separation on CMS.

p_H/p_L	Ads/Des (time)	v_L/v_H	L/v_H (s)	Percentage of Nitrogen in the Product	
				Experimental	Theoretical model
3.04	44/44	2.23	21.42	99.00	100.0
3.04	44/44	1.51	21.42	98.75	100.0
3.04	44/44	2.65	23.52	99.98	100.0
3.04	44/44	2.87	15.38	98.25	100.0
3.04	56/56	0.80	19.56	95.10	99.99
2.36	44/44	0.83	20.00	97.30	99.95
3.04	44/32	0.87	20.80	98.00	99.99
3.04	32/32	0.84	19.56	97.60	99.98

Saturation concentration for O_2 and N_2 = $q_{AS} = q_{BS} = 0.00264$ mole/cm^3[71]

Equilibrium constant for Oxygen = $K_A = b_A q_{AS} = 10.92$

Equilibrium constant for Oxygen = $K_b = b_B q_{BS} = 8.93$

D/r_c^2 for Oxygen = 5.4×10^{-3} s^{-1}

D/r_c^2 for Nitrogen = 7.3×10^{-4} s^{-1}

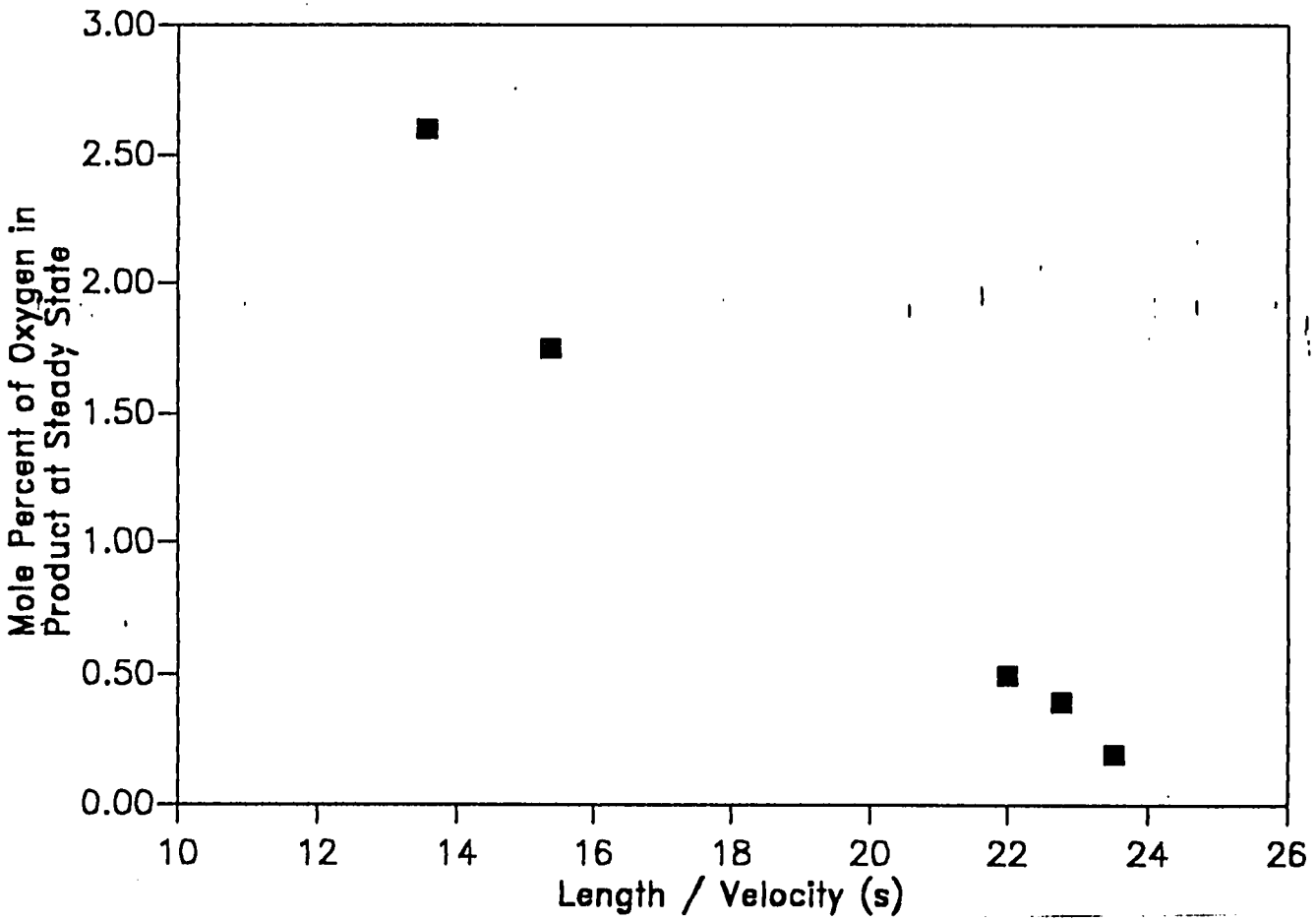

Figure 6.2 Effect of L/ v_H on Separation of O_2 and N_2 using CMS as Adsorbent. (Cycle Time = 110s, P_H/P_L = 3.04, v_H/v_L = 2.70)

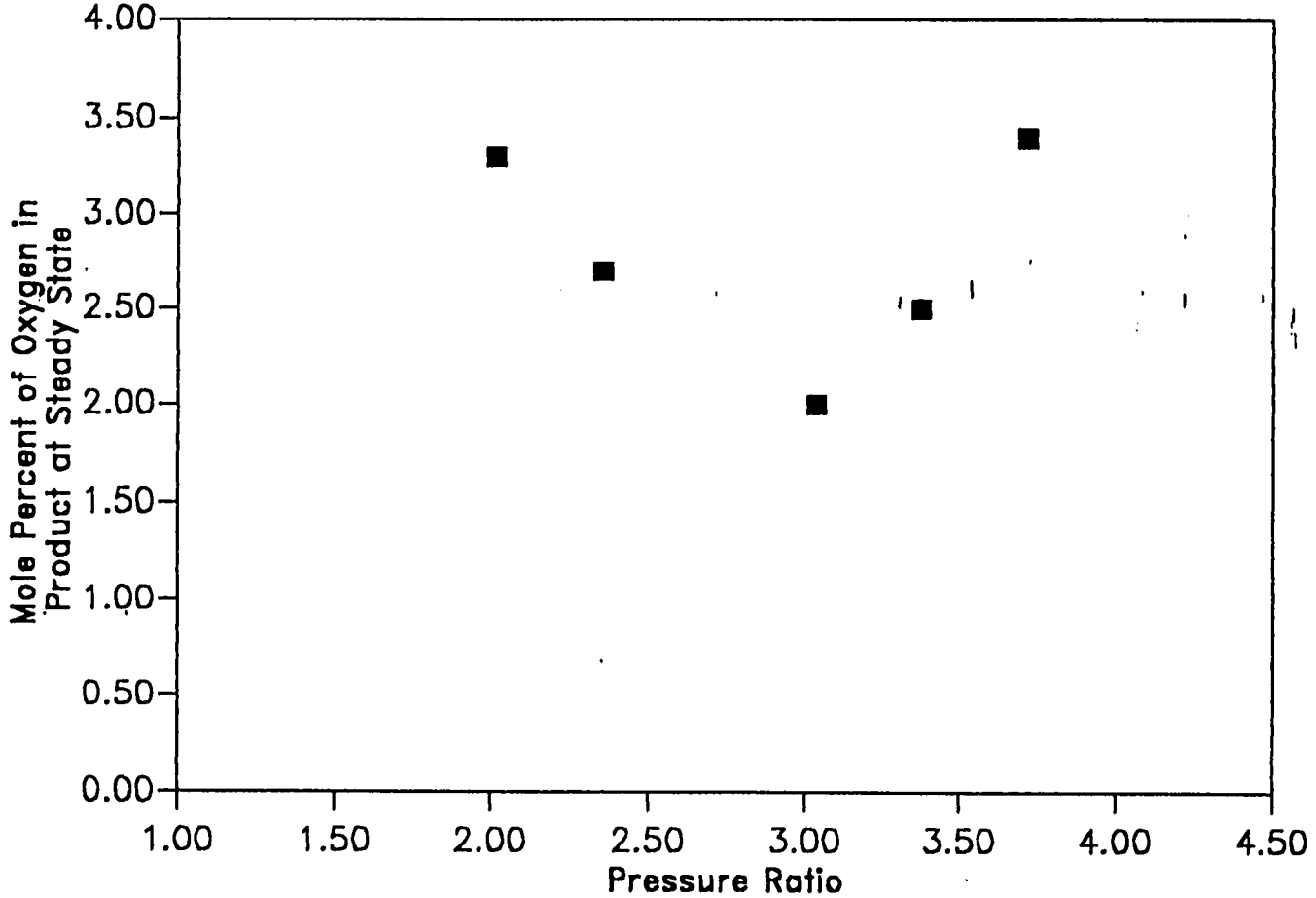

Figure 6.3 Effect of Pressure Ratio on Separation of O_2 and N_2 using CMS as Adsorbent. (Cycle Time = 110s, L/v_{II} = 20.0 s , v_I/v_{II} = 0.87)

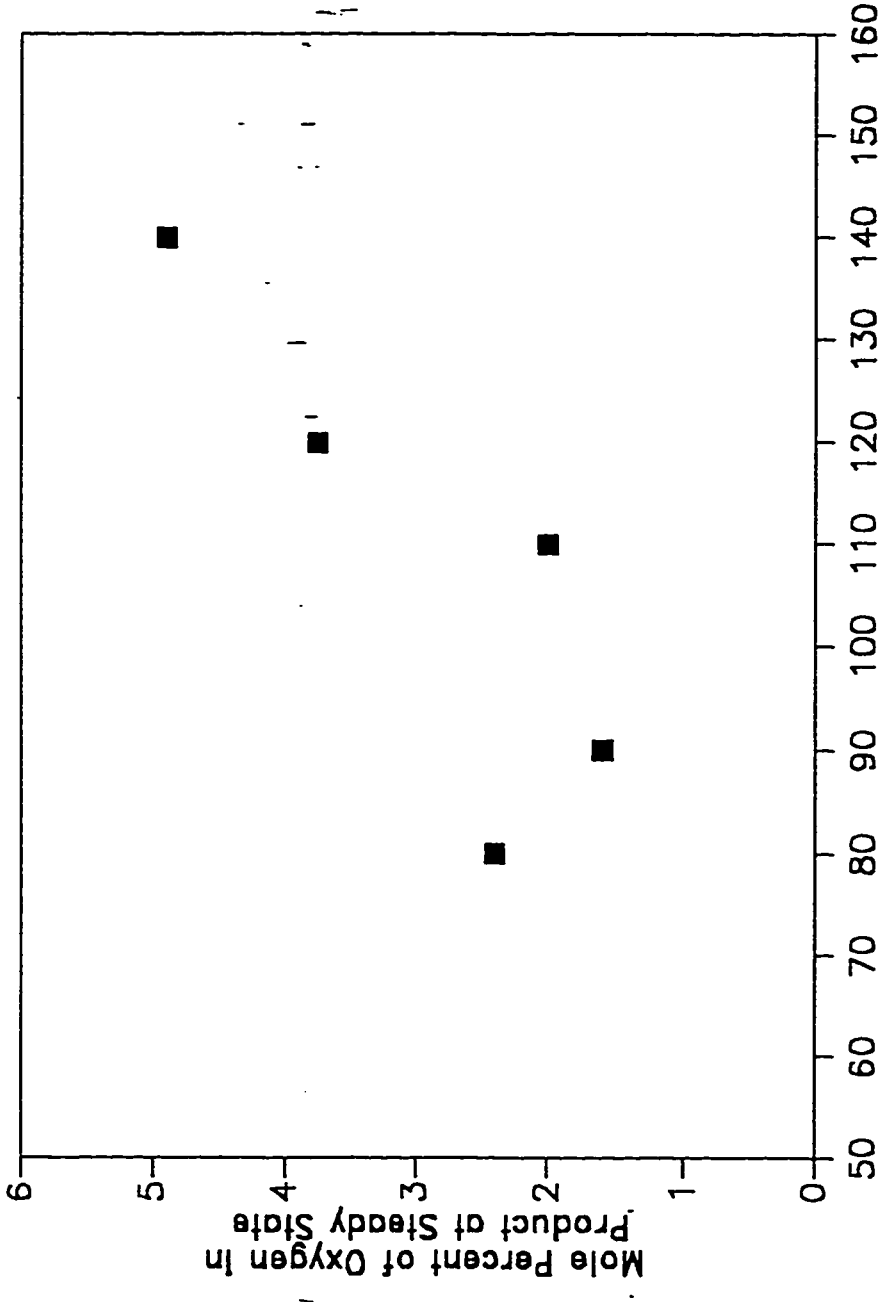

Figure 6.4 Effect of Cycle Time on Separation of O_2 and N_2 using CMS as Adsorbent. ($P_H/P_L = 3.04$, $L/v_H = 20.0\ s$, $v_H/v_L = 2.70$)

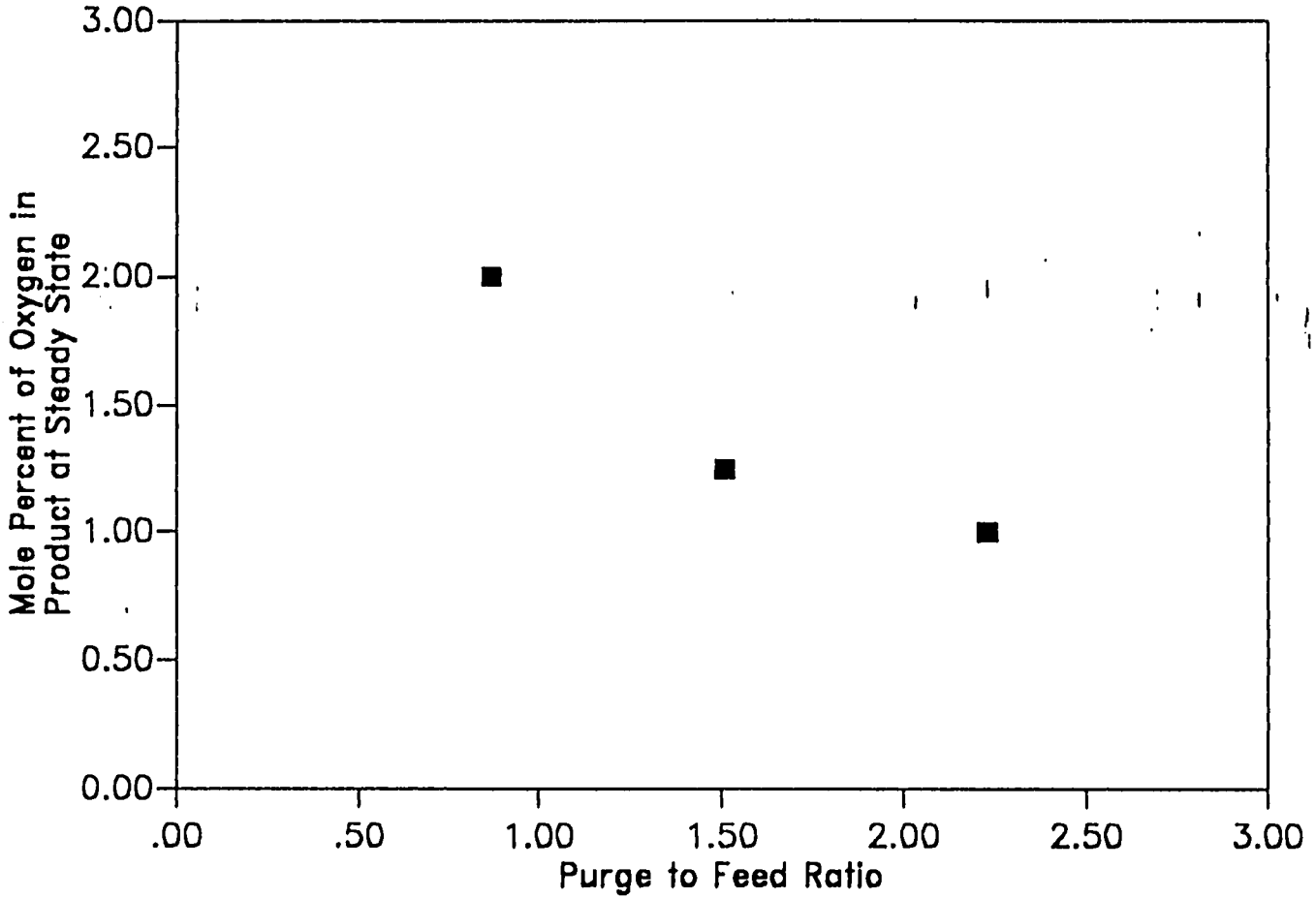

Figure 6.5 Effect of Purge to Feed Ratio on Separation of O_2 and N_2 using CMS as Adsorbent. (Cycle Time = 110s, $P_H/P_L = 3.04$, $L/v_H = 20.0$s)

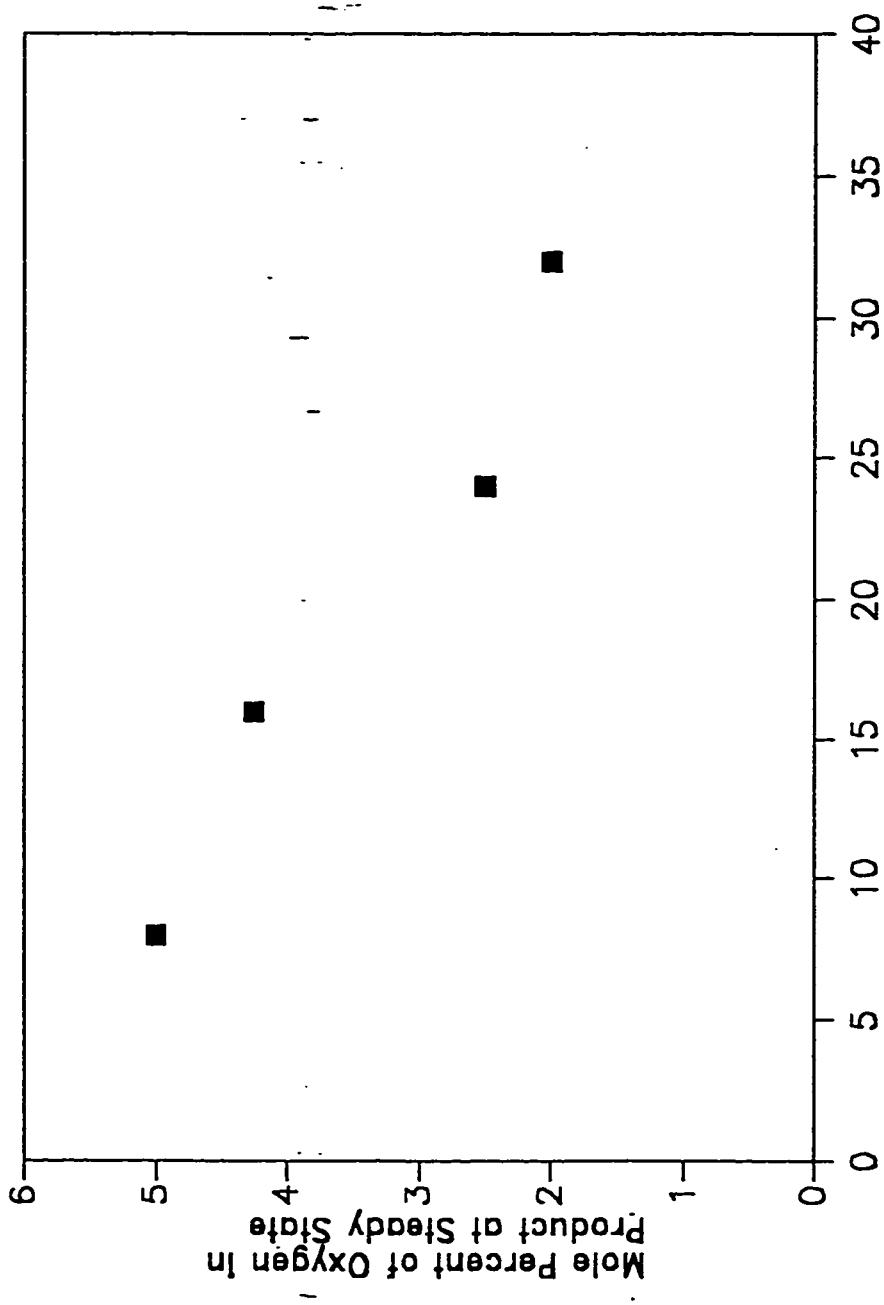

Figure 6.6 Effect of Desorption Time on Separation of O_2 and N_2 using CMS as Adsorbent with Cycle Time Maintained Constant. ($P_H/P_L = 3.04$, $L/v_H = 20.0$s $v_L/v_H = 0.87$)

6.2 SEPARATION OF AIR ON PSA USING 5A-ZEOLITE AS ADSORBENT :

In 5A-zeolite both oxygen and nitrogen diffuse very easily in the wider lattice of 5A-zeolite indicating negligible intracrystalline diffusional resistance. Nitrogen being more strongly adsorbed on 5A as compared to oxygen serves as the basis for equilibrium separation. This process is used to generate pure oxygen from air. The summary of the present experimental data is shown in Table 6.3.

(*i*) *EFFECT OF LENGTH TO VELOCITY RATIO* (L/ v_H) :

The effect of L/ v_H on the separation of air mixture at cycle time of 120s, pressure ratio $P_H / P_L = 3.04$, purge to feed ratio $v_L / v_H = 0.87$ on 5A-zeolite adsorbent is shown in Figure 6.7. In the Figure the effect of six different L/ v_H ratios 7.28,8.75, 9.40, 10.72, 11.57, 15.72 s , on the product concentration is shown. The oxygen concentration sharply rises between L/ v_H of 7.28 s and 8.75 s beyond which the change in the product concentration is relatively small.

(*ii*) *EFFECT OF PRESSURE RATIO* (P_H / P_L) :

The effect of high and low pressure ratio on the separation of air at purge to feed ratio of 0.868 , $L/v_H = 11.96$ s , and cycle time of 120s, using 5A-zeolite is shown in Figure 6.8. From the Figure, it is apparent that an increase in the high to low pressure ratio above 4.4 results in a decrease in the percentage of oxygen

in the product stream. No significant change in the oxygen concentration was observed between pressure ratios of 1.34 and 4.4.

(iii) EFFECT OF CYCLE TIMES :

The effect of cycle time on the separation of air at a purge to feed ratio of 0.866, L/ v_H =11.96 s , high to low pressure ratio of 3.04, using 5A zeolite is shown in Figure 6.9. The effect of six different cycle times ranging from 80 to 150s on the product concentration is shown in the Figure. An increase of the cycle time from 80 to 140s slightly decreases the oxygen concentration. However at a cycle time of 150s the oxygen concentration decreases sharply.

(iv) EFFECT OF PURGE TO FEED RATIO (v_L/v_H) :

The effect of purge to feed ratio on separation of oxygen from air at L/ v_H =11.96 s , high to low pressure ratio =3.04, and cycle time =120s, using 5A-zeolite adsorbent is shown in Figure 6.10. The increase in the purge to feed ratio causes the product concentration to increase. This indicates an improvement in the separation performance of the unit. It may be noted that large purge to feed ratio indicates lower recovery. Further, very little improvement in the product concentration is observed beyond a purge to feed ratio of 0.36.

(v) EFFECT OF DESORPTION TIME :

The effect of desorption time in the case of 5A-zeolite can be seen by varying the desorption time and blowdown timing of the low pressure half cycle,

while keeping the cycle time fixed, as shown in Figure 6.11. From the figure we conclude that as the desorption time increases the percentage of oxygen also increases but beyond 16s there appear to be little change.

Table 6.3 Operating conditions of experimental runs for O_2 and N_2 separation on 5A-zeolite, using pure O_2 as purge

	Cycle Time (s)	P_H/P_L	L/v_H (s)	v_L/v_H	% of O_2 in prod.
Effect of Cycle Time (s)	80	3.04	11.95	0.86	96.00
	100	3.04	11.96	0.86	96.00
	120	3.04	11.96	0.86	95.75
	130	3.04	12.40	0.86	95.50
	140	3.04	11.96	0.86	95.00
	150	3.04	11.96	0.86	89.00
Effect of v_L/v_H	120	3.04	11.96	0.11	55.00
	120	3.04	11.96	0.23	89.50
	120	3.04	11.96	0.36	94.25
	120	3.04	11.96	0.49	94.90
	120	3.04	11.96	0.74	94.90
	120	3.04	11.96	1.00	95.00
	120	3.04	11.96	1.49	95.10
Effect of L/v_H (s)	120	3.04	7.28	0.84	44.00
	120	3.04	8.71	0.84	91.75
	120	3.04	9.40	0.84	92.50
	120	3.04	10.72	0.84	95.10
	120	3.04	11.57	0.84	94.80
	120	3.04	15.72	0.84	95.00
Effect of P_H/P_L	120	1.34	11.96	0.868	95.00
	120	1.68	11.96	0.868	95.00
	120	2.02	11.96	0.868	95.00
	120	2.36	11.96	0.868	95.25
	120	3.72	11.96	0.868	95.10
	120	4.40	11.96	0.868	94.50
	120	5.08	11.96	0.868	52.50

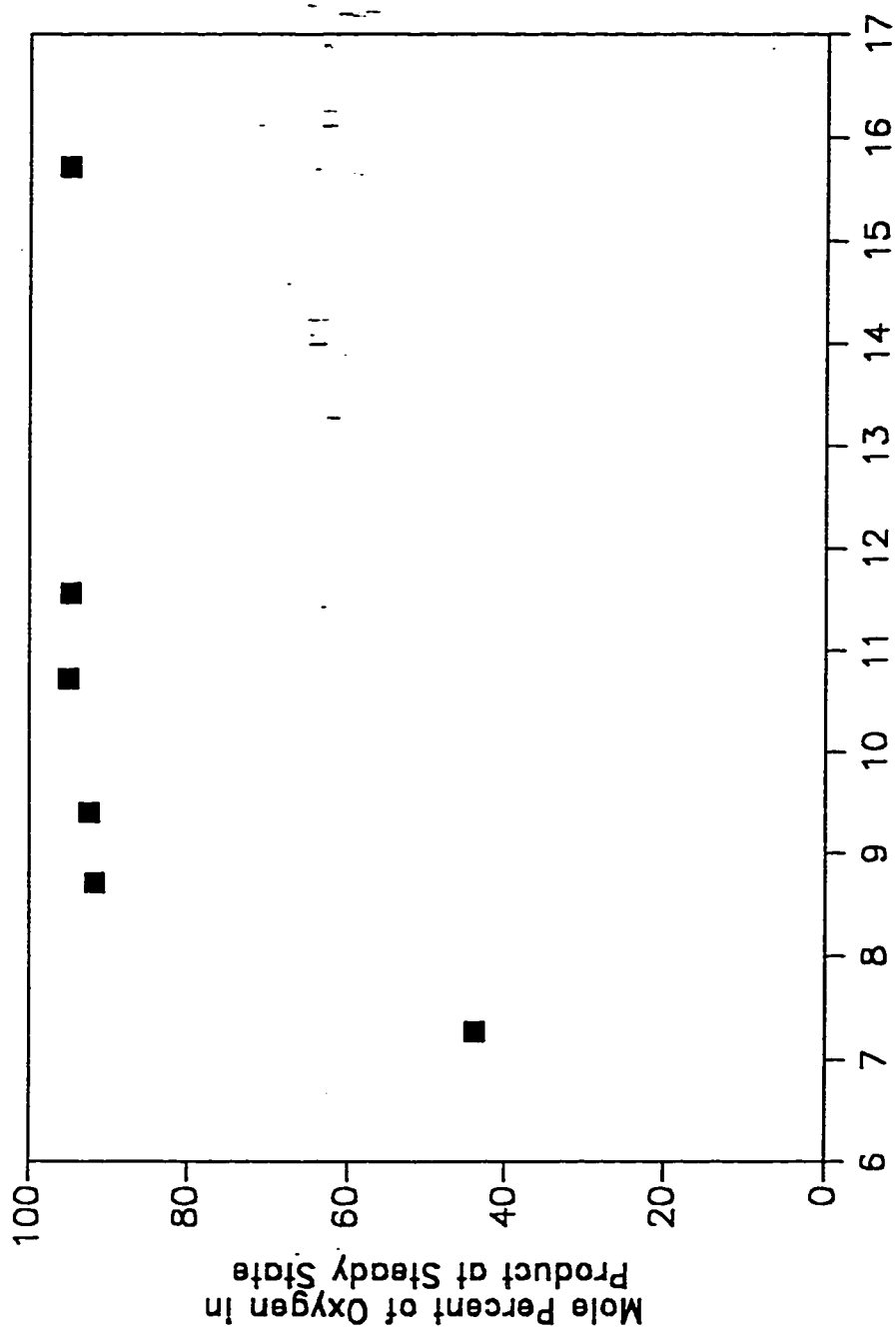

Figure 6.7 Effect of L/ v_{II} on Separation of O_2 and N_2 using 5A-zeolite. (Cycle Time = 120s, $P_{II}/P_L = 3.04$, $v_{II}/v_L = 0.84$)

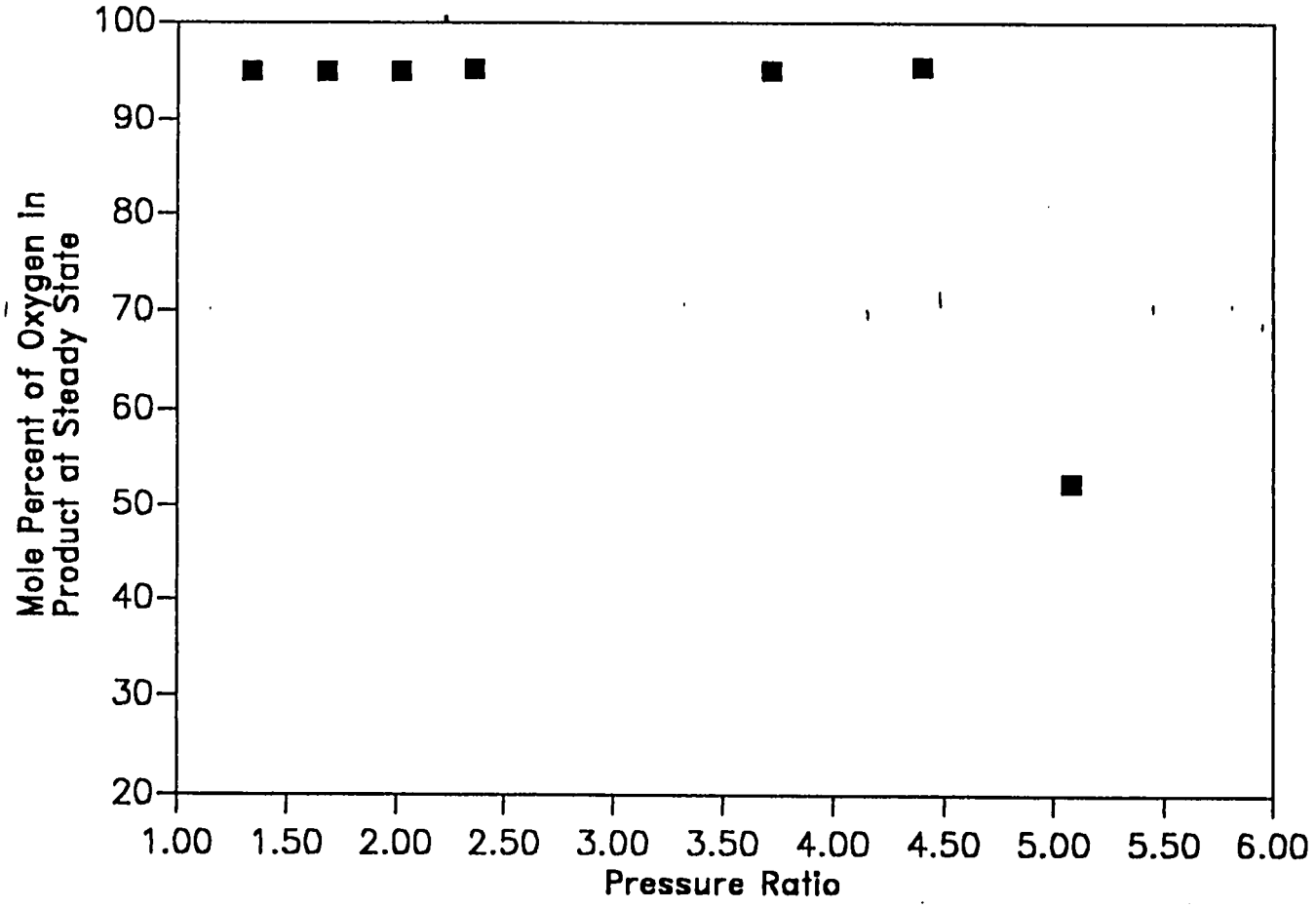

Figure 6.8 Effect of Pressure Ratio on Separation of O_2 and N_2 using 5A-zeolite. (Cycle Time = 120s, L/v_{II} = 11.96s, v_I/v_{II} = 0.87)

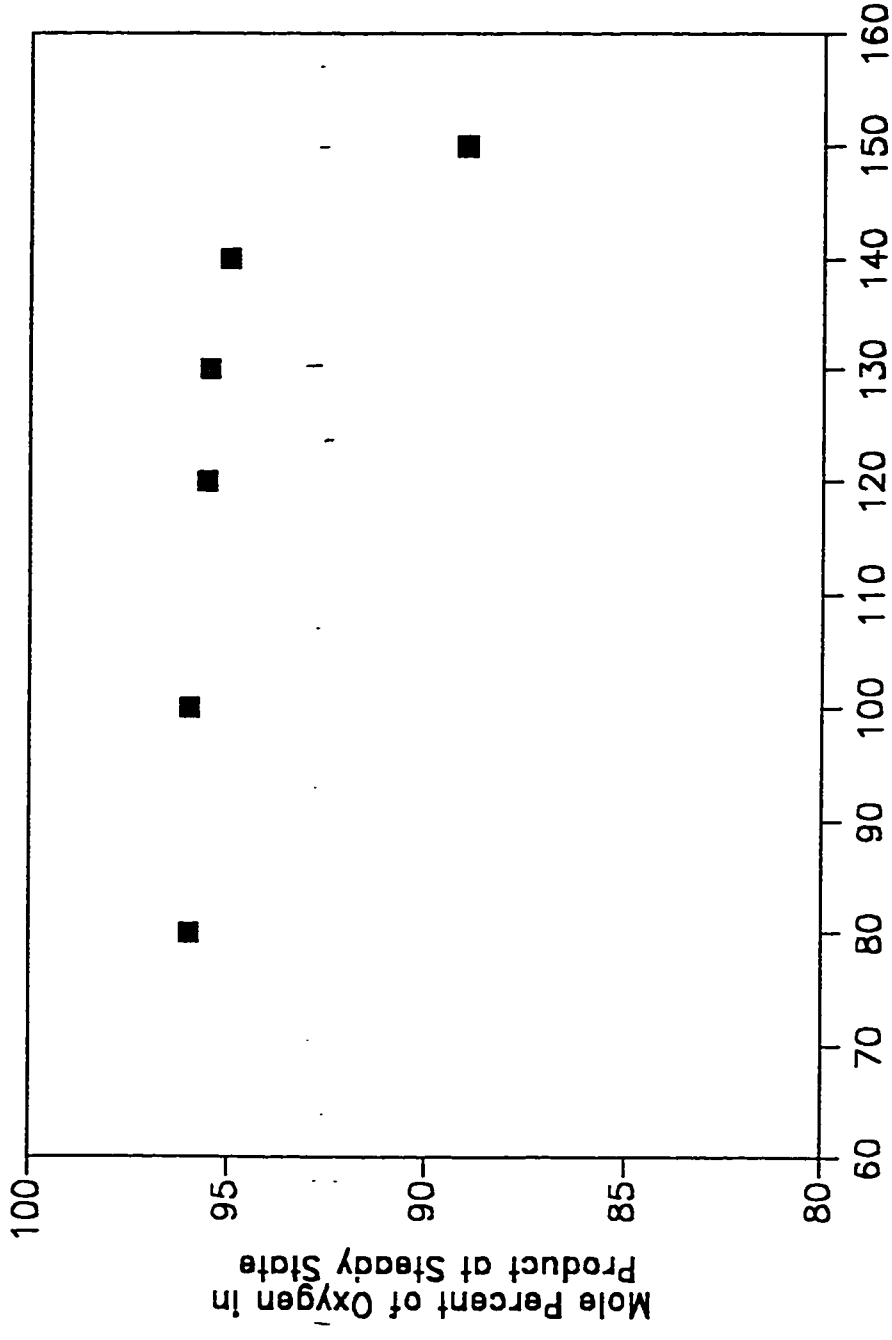

Figure 6.9 Effect of Cycle Time on Separation of O_2 and N_2 using 5A-zeolite. ($P_H/P_L = 3.04$, $L/v_H = 11.95$s, $v_H/v_L = 0.86$)

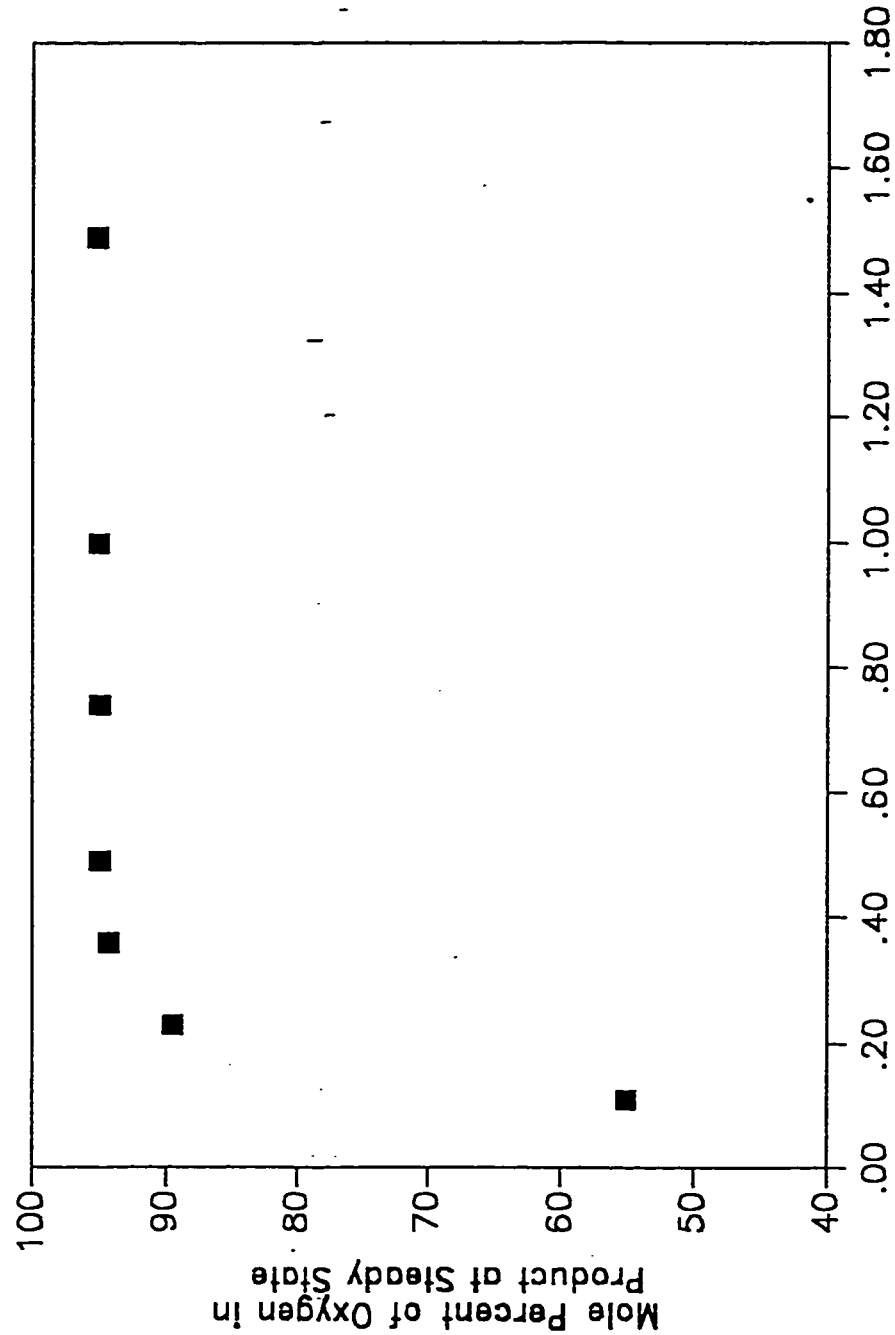

Figure 6.10 Effect of Purge to Feed ratio on Separation of O_2 and N_2 using 5A-zeolite. (Cycle Time = 110s, P_H/P_L = 3.04, L/v_H = 11.96s)

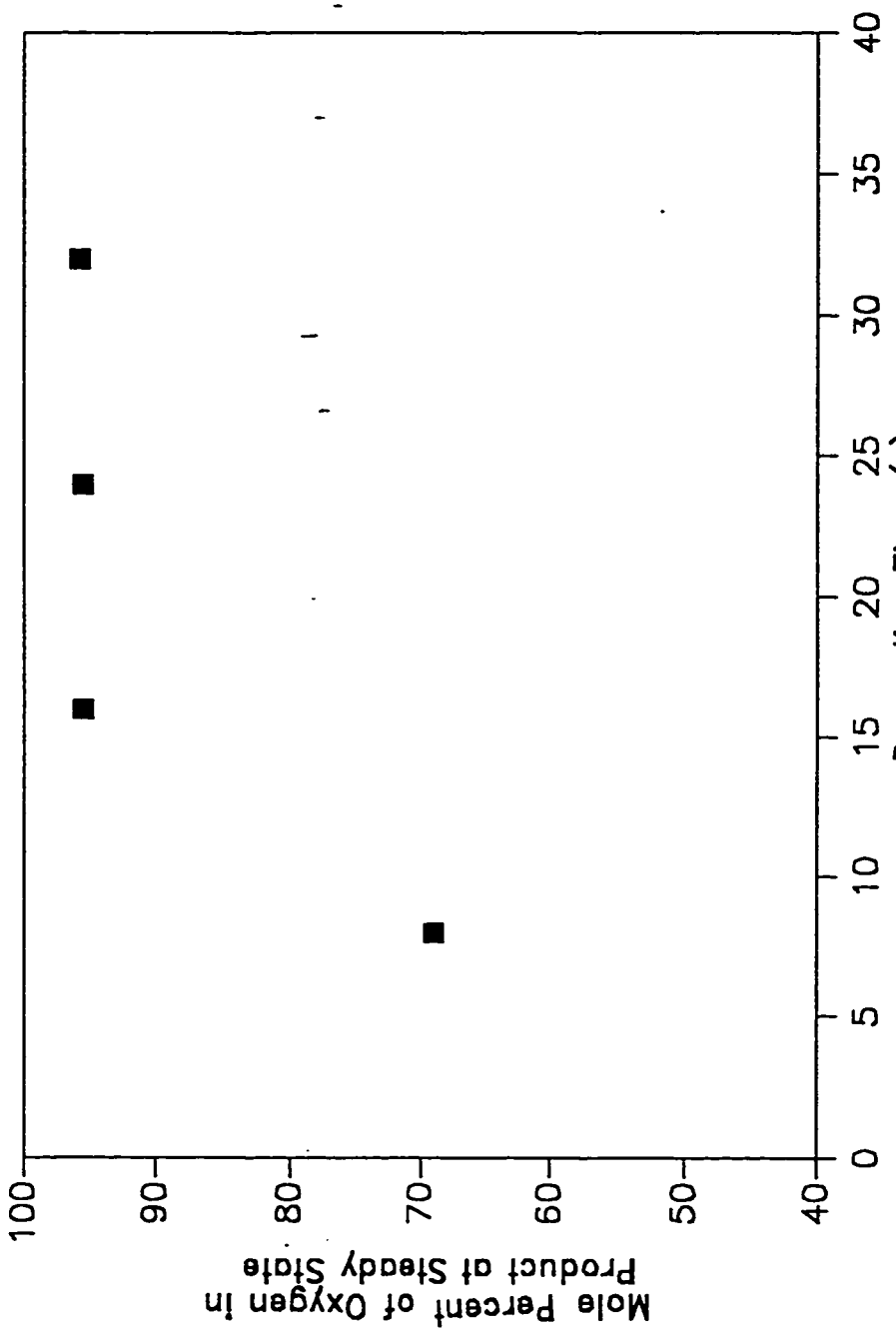

Figure 6.11 Effect of Desorption Time on Separation of O_2 and N_2 using 5A-zeolite. ($P_H/P_L = 3.04$, $L/v_H = 11.96$s, $v_L/v_H = 0.87$)

6.3 SEPARATION OF AIR ON PSA USING OXYGEN AS PURGE AND 4A-ZEOLITE AS ADSORBENT :

In case of adsorption of air on 4A-zeolite the equilibrium favours the sorption of nitrogen while the kinetics favours the diffusion of oxygen and therefore either of these selectivities can be utilized to separate oxygen and nitrogen.

For the production of pure oxygen, the equilibrium selectivity of the relatively strongly adsorbed nitrogen is utilized. This case is similar to the case of air separation on 5A zeolite. Nitrogen is preferentially adsorbed and pure oxygen product can be obtained. In this case, therefore, pure oxygen is used as a purge to clean the previously loaded adsorbent beds. The effect of various parameters on the separation performance were studied and are reported in Table 6.4.

(*i*) *EFFECT OF LENGTH TO VELOCITY RATIO* (L/ v_H) :

The effect of L/ v_H ratio on the separation of nitrogen and oxygen from air at purge to feed ratio =0.97, cycle time =80s, pressure ratio =2.02 using 4A-zeolite is seen in Figure 6.12. It is shown that by increasing the L/ v_H from 21.32 to 34.40s , the percentage of oxygen increases from 68% to 84.50% .

(*ii*) *EFFECT OF PRESSURE RATIO* (P_H / P_L) :

The effect of pressure ratio on the separation of nitrogen and oxygen from air by using the 4A-zeolite is shown in Figure 6.13. It may be seen that by increasing the pressure ratio, the percentage of oxygen decreases and hence the product purity decreases.

(iii) EFFECT OF CYCLE TIMES :

The effect of varying the cycle time is illustrated in Figure 6.14. The residual oxygen concentration is found to decrease by increasing the cycle time. It may be noted however that too short cycle times on the otherhand could probably decrease the oxygen concentration since the time allowed for adsorption in that case could be insignificant. Therefore, a cycle time of about 80s could well be around the optimum value for this system.

(iv) EFFECT OF PURGE TO FEED RATIO (v_L/v_H) :

The effect of varying the purge to feed ratio is shown in Figure 6.15. It is apparent that product purity increases with purge to feed ratio but, there is a limit beyond which increasing the purge rate is uneconomical.

(v) EFFECT OF DESORPTION TIME :

The effect of varying the proportion of desorption and blowdown time is shown in Figure 6.16. It was found that the concentration of oxygen achieved was higher at longer desorption time.

Table 6.4 Operating conditions of experimental runs for O_2 and N_2 separation on 4A-zeolite, using pure O_2 as Purge.

	Cycle Time (s)	P_H/P_L	L/v_H (s)	v_L/v_H	% of O_2 in prod.
Effect of Cycle Time (s)	80	2.02	30.04	1.23	83.00
	100	2.02	30.04	1.23	74.50
	110	2.20	30.04	1.23	73.00
	120	2.02	30.04	1.23	72.00
	130	2.02	30.04	1.23	71.50
	150	2.02	30.04	1.23	58.00
Effect of v_L/v_H	80	2.02	30.09	0.60	76.00
	80	2.02	30.09	0.79	81.00
	80	2.02	30.09	0.97	82.00
	80	2.02	30.09	1.23	86.00
	80	2.02	30.09	1.40	88.00
Effect of L/v_H (s)	80	2.02	21.23	0.97	68.00
	80	2.02	24.56	0.97	72.25
	80	2.02	27.44	1.00	79.00
	80	2.02	30.09	1.00	82.00
	80	2.02	34.40	1.00	84.50
Effect of P_H/P_L	80	2.02	30.00	1.00	83.00
	80	2.36	30.00	1.00	74.00
	80	2.70	29.98	0.98	67.50
	80	3.04	29.92	0.97	65.00
	80	3.38	30.00	1.00	59.50

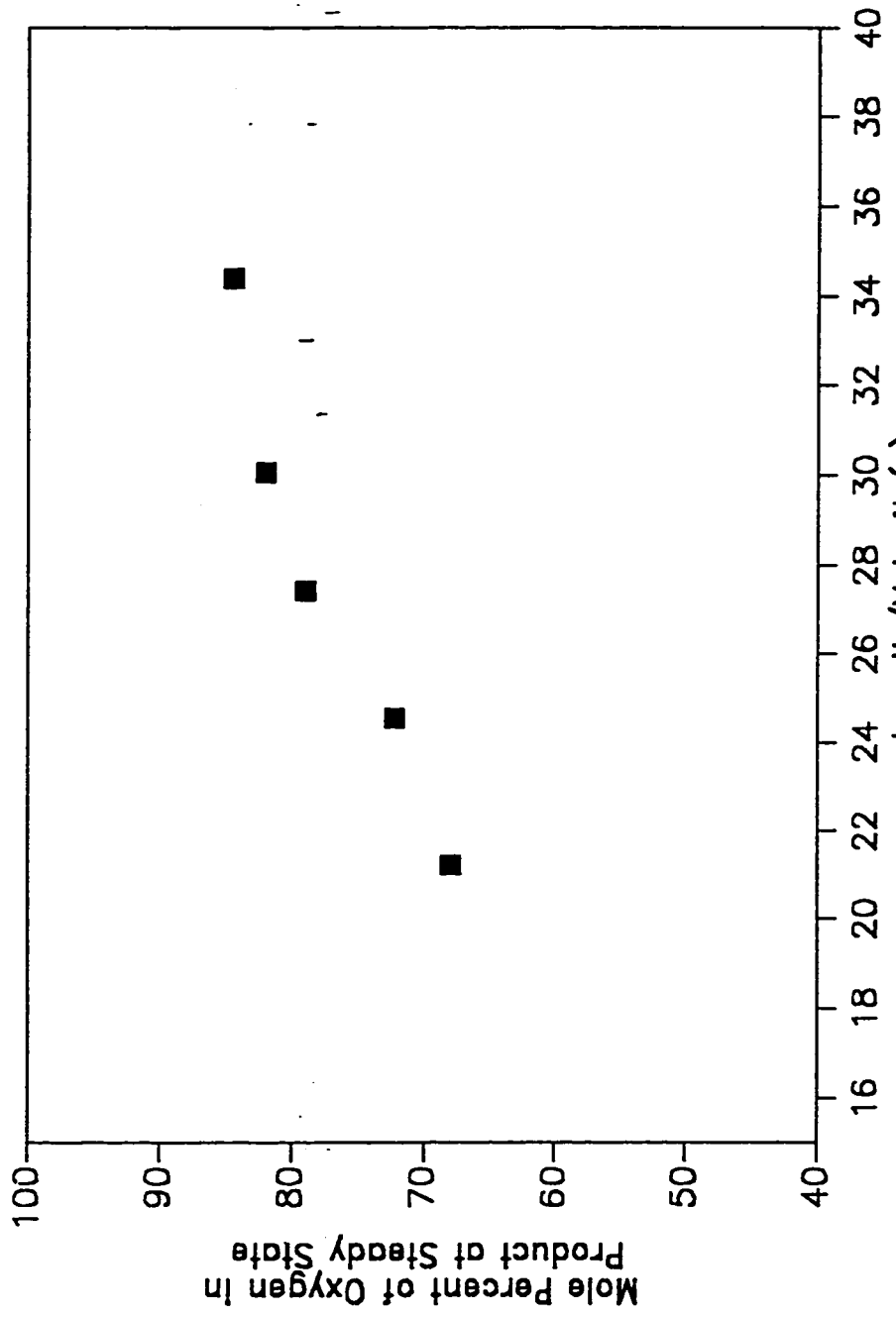

Figure 6.12 Effect of L/ ν_{II} on Separation of O_2 and N_2 using 4A-zeolite and O_2 as Purge. (Cycle Time = 80s, $P_{II}/P_L = 2.02$, $\nu_{II}/\nu_L = 0.97$)

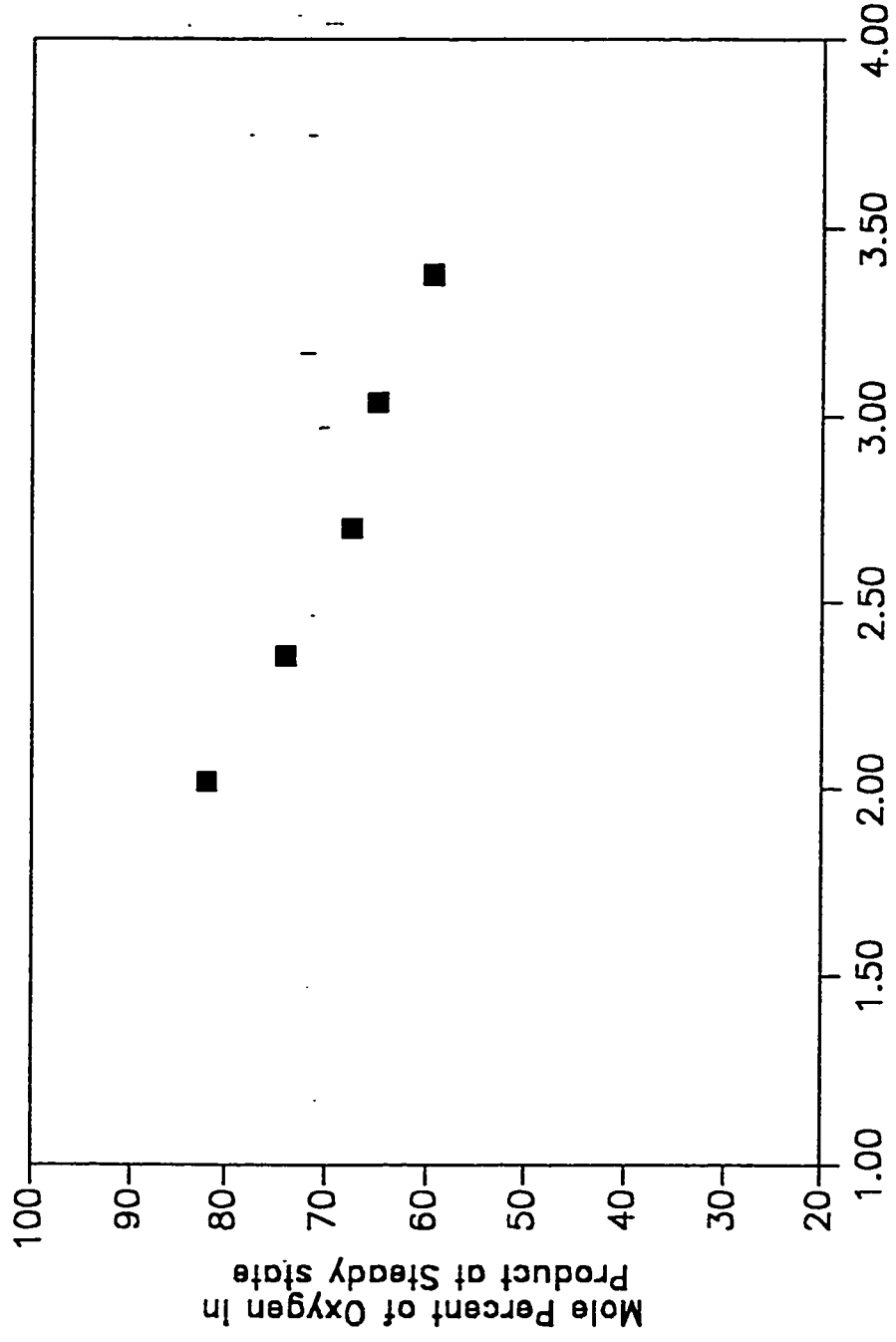

Figure 6.13 Effect of Pressure Ratio on Separation of O_2 and N_2 using 4A-zeolite and O_2 as Purge. (Cycle Time = 80s, $L/v_{II} = 30.0$s, $v_L/v_{II} = 1.00$)

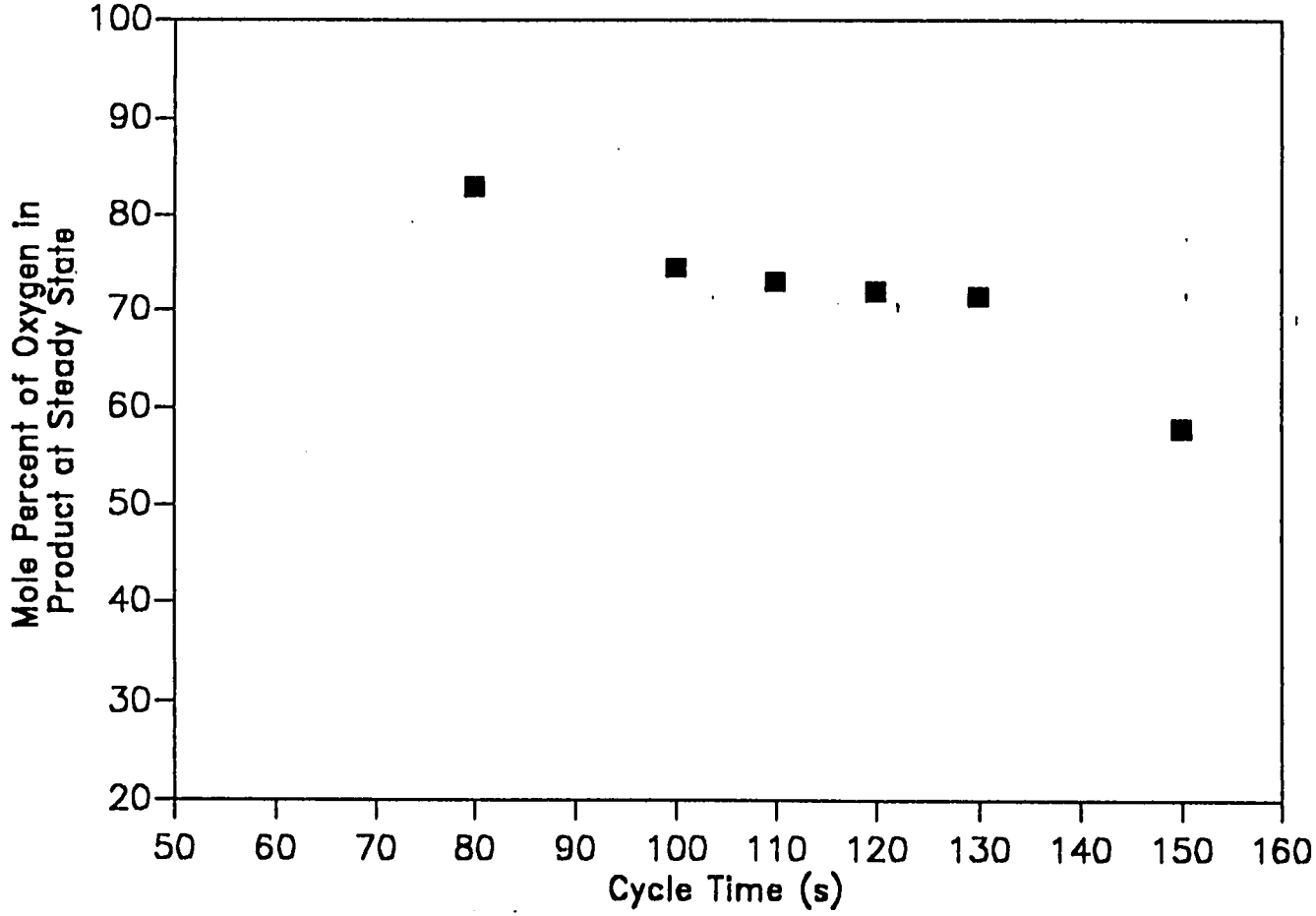

Figure 6.14 Effect of Cycle Time on Separation of O_2 and N_2 using 4A-zeolite and O_2 as Purge. (P_H/P_L =2.02, L/v_H =30.04s, v_H/v_L =1.23)

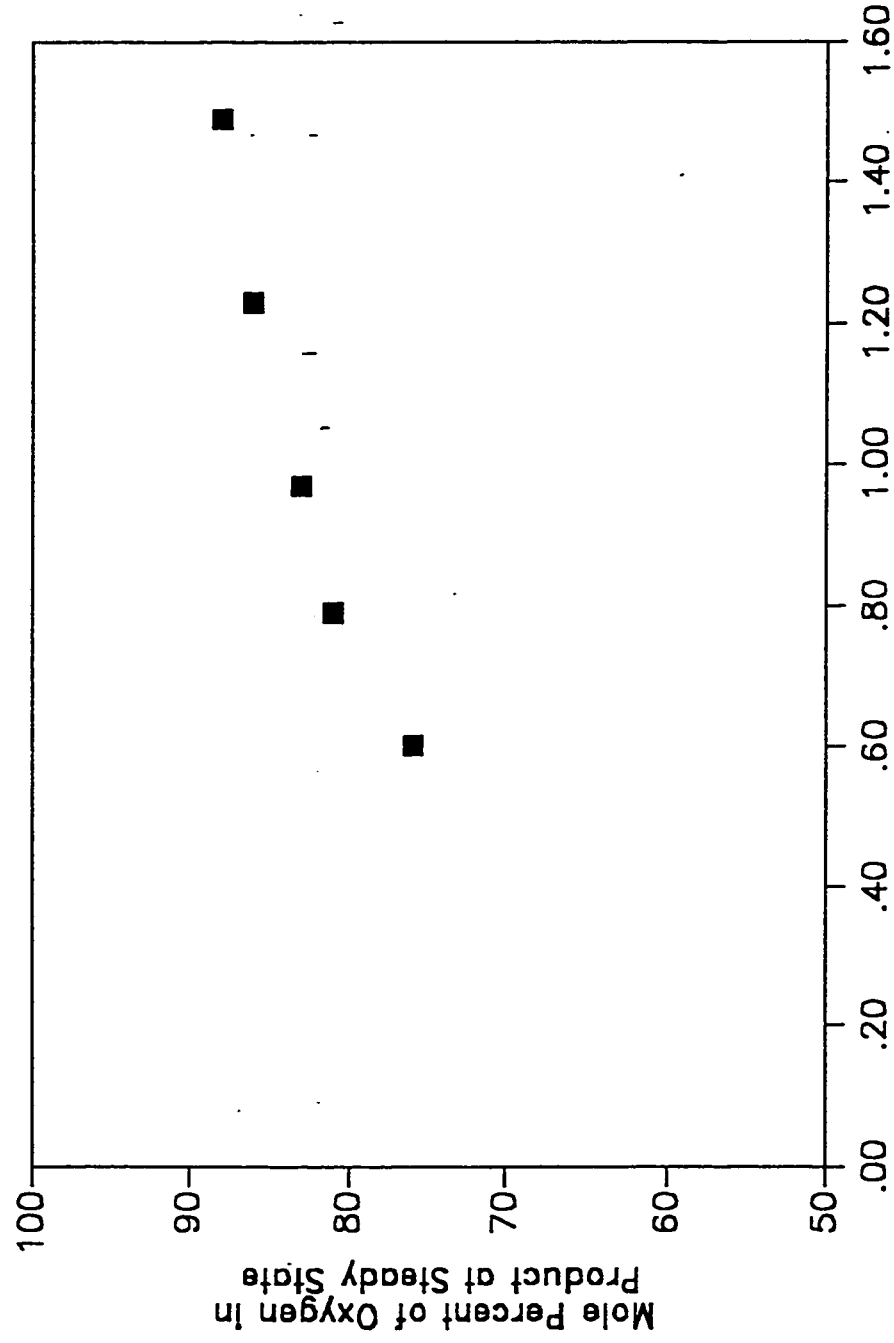

Figure 6.15 Effect of Purge to Feed ratio on Separation of O_2 and N_2 using 4A-zeolite and O_2 as Purge. (Cycle Time = 80s, $P_H/P_L = 2.02$, $L/v_H = 30.09$s)

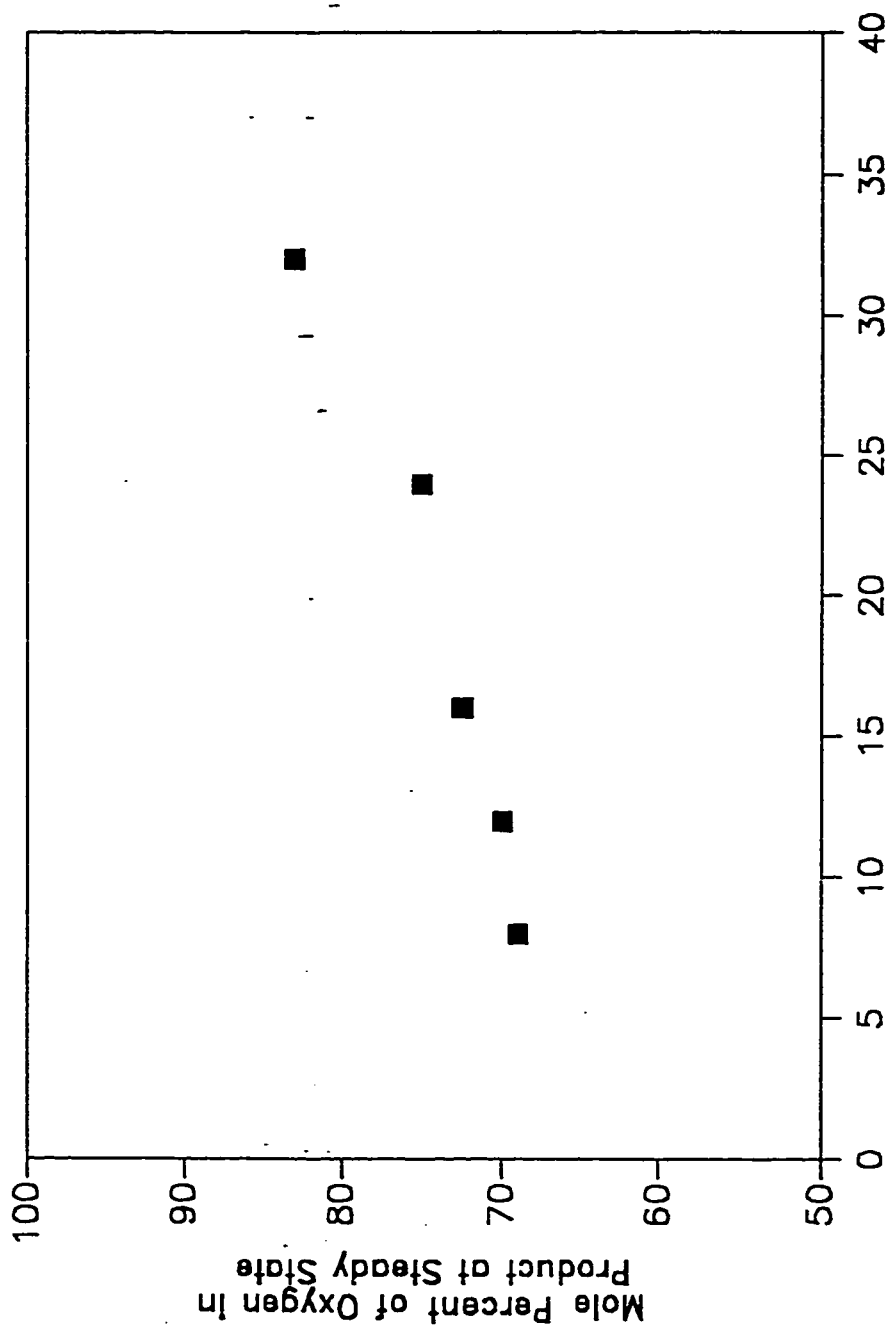

Figure 6.16 Effect of Desorption Time on Separation of O_2 and N_2 using 4-A Zeolite and O_2 as Purge. ($P_H/P_L = 2.02$, $L/\nu_H = 30.00$ $s_p\nu_L/\nu_H = 1.00$)

6.4 SEPARATION OF AIR ON PSA USING NITROGEN AS PURGE AND 4A-ZEOLITE AS ADSORBENT :

For the production of pure nitrogen the kinetic selectivity of the faster diffusing oxygen is utilized. Oxygen is preferentially adsorbed in the sorbent at a relatively much faster rate as compared to nitrogen and therefore pure nitrogen product can be expected. In this case, pure nitrogen is used for purging the adsorbents beds during desorption mode. The results of the experimental runs under various operating conditions for this case are summarized in Table 6.5.

(*i*) *EFFECT OF LENGTH TO VELOCITY RATIO* (L/ v_H) :

The effect of varying the L/ v_H ratio is illustrated in Figure 6.17. It may be noticed that low oxygen concentration is accomplished by applying large L/ v_H , which increases the nitrogen concentration in the product. However, the rate of decrease in the oxygen concentration in the product decreases at higher L/ v_H ratio.

(*ii*) *EFFECT OF PRESSURE RATIO* (P_H / P_L) :

The effect of high and low pressure ratio on the separation of air at purge to feed ratio of 1.0, L/ v_H =27.28 s , and cycle time=80s, using 4A zeolite as adsorbent is shown in Figure 6.18. It is seen that an increase in pressure ratio results in an increase in the percentage of oxygen, therefore the percentage of nitrogen decreases in the product stream.

(*iii*) *EFFECT OF CYCLE TIME* :

The effect of varying the cycle time is shown in Figure 6.19. It is apparent that if the cycle time increases, while the other parameters are held constant, the percentage of oxygen increases, and therefore the product concentration of nitrogen decreases.

(*iv*) *EFFECT OF PURGE TO FEED RATIO* (v_L/v_H) :

The effect of purge to feed ratio is shown in Figure 6.20, and the relevant parameters are given in Table 6.5. It is clear that the percentage of oxygen decreases with the increase in the purge to feed ratio. However, using this strategy to increase the product purity is not economical in an industrial process, because large amount of the product will have to be used as purge.

(*v*) *EFFECT OF DESORPTION TIME* :

A similar results are obtained as discussed in case of 4A-zeolite using oxygen as purge. Figure 6.21 shows that higher desorption time gives a purer product.

Table 6.5 Operating conditions of experimental runs for O_2 and N_2 separation on 4A-zeolite, using pure N_2 as purge.

	Cycle Time (s)	P_H/P_L	L/v_H (s)	v_L/v_H	% of O_2 in prod.
Effect of Cycle Time (s)	80	2.02	26.66	0.98	0.80
	90	2.02	26.66	0.98	2.00
	100	2.20	26.66	0.98	3.00
	110	2.02	26.66	0.98	4.10
	120	2.02	26.66	0.98	7.75
Effect of v_L/v_H (s)	80	2.02	26.66	0.47	2.50
	80	2.02	26.66	0.75	1.50
	80	2.02	26.66	1.00	0.80
	80	2.02	26.66	1.20	0.70
	80	2.02	26.66	1.49	0.50
Effect of L/v_H (s)	80	2.02	16.14	1.00	6.75
	80	2.02	18.75	1.00	3.75
	80	2.02	20.80	1.00	2.00
	80	2.02	23.37	1.00	1.00
	80	2.02	26.66	1.00	0.80
Effect of P_H/P_L	80	2.02	27.28	1.00	0.80
	80	2.36	27.28	1.00	1.75
	80	2.70	27.28	1.00	2.25
	80	3.04	27.28	1.00	3.00
	80	3.38	27.28	1.00	4.00

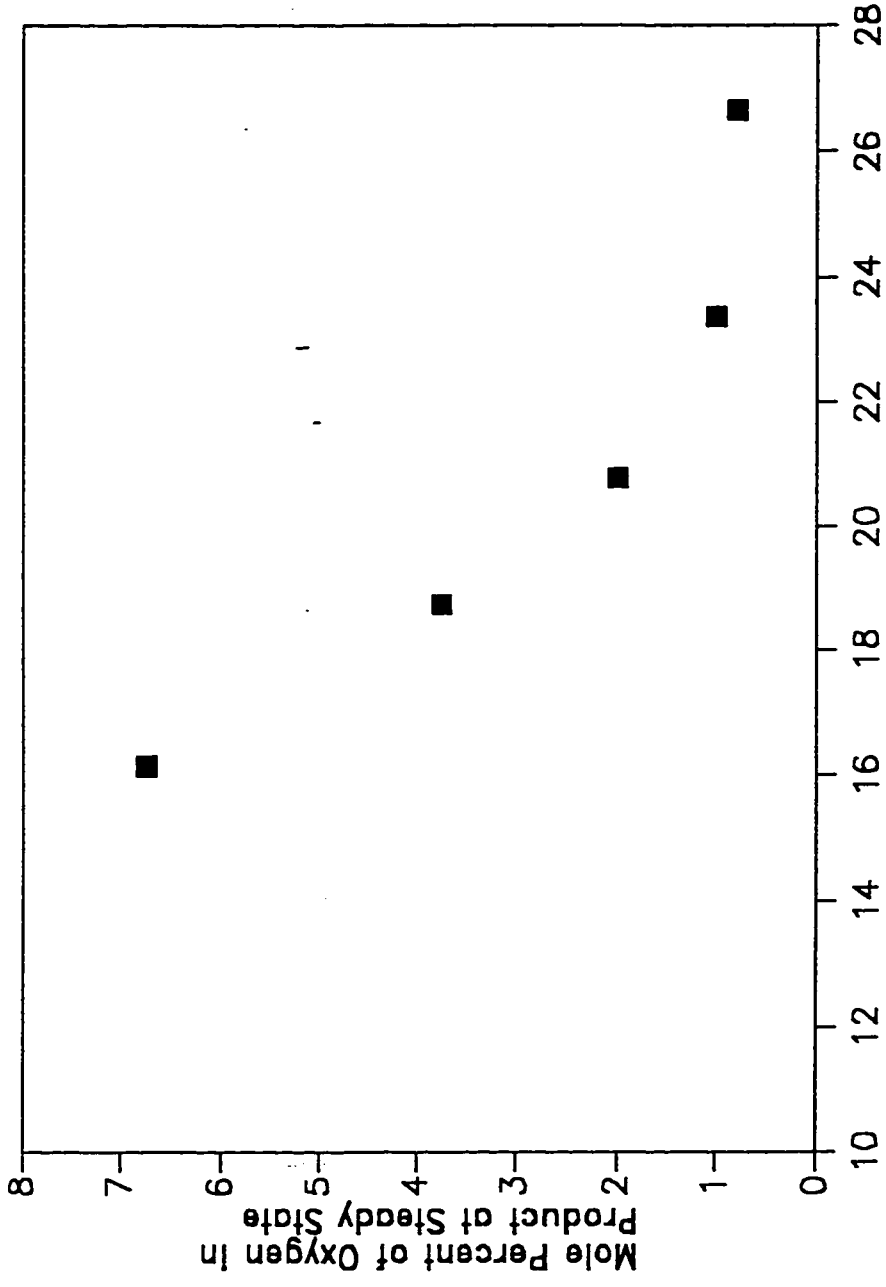

Figure 6.17 Effect of L/ v_{II} on Separation of O_2 and N_2 using 4A-zeolite and N_2 as Purge. (Cycle Time = 80s, P_{II}/P_I = 2.02, v_{II}/v_I = 1.00)

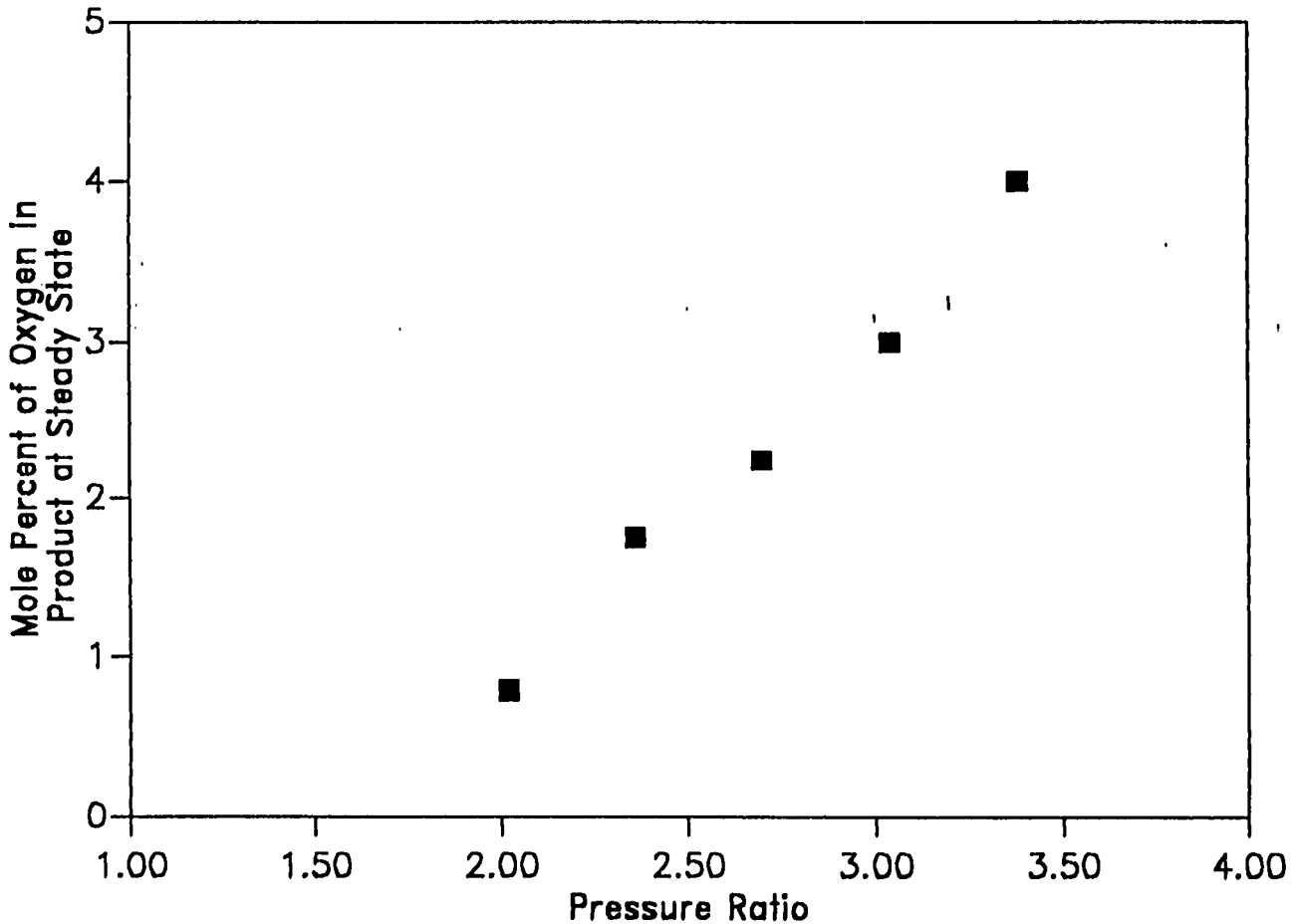

Figure 6.18 Effect of Pressure Ratio on Separation of O_2 and N_2 using 4A-zeolite and N_2 as Purge. (Cycle Time = 80s, L/v_{II} = 27.28s, v_I/v_{II} = 1.00)

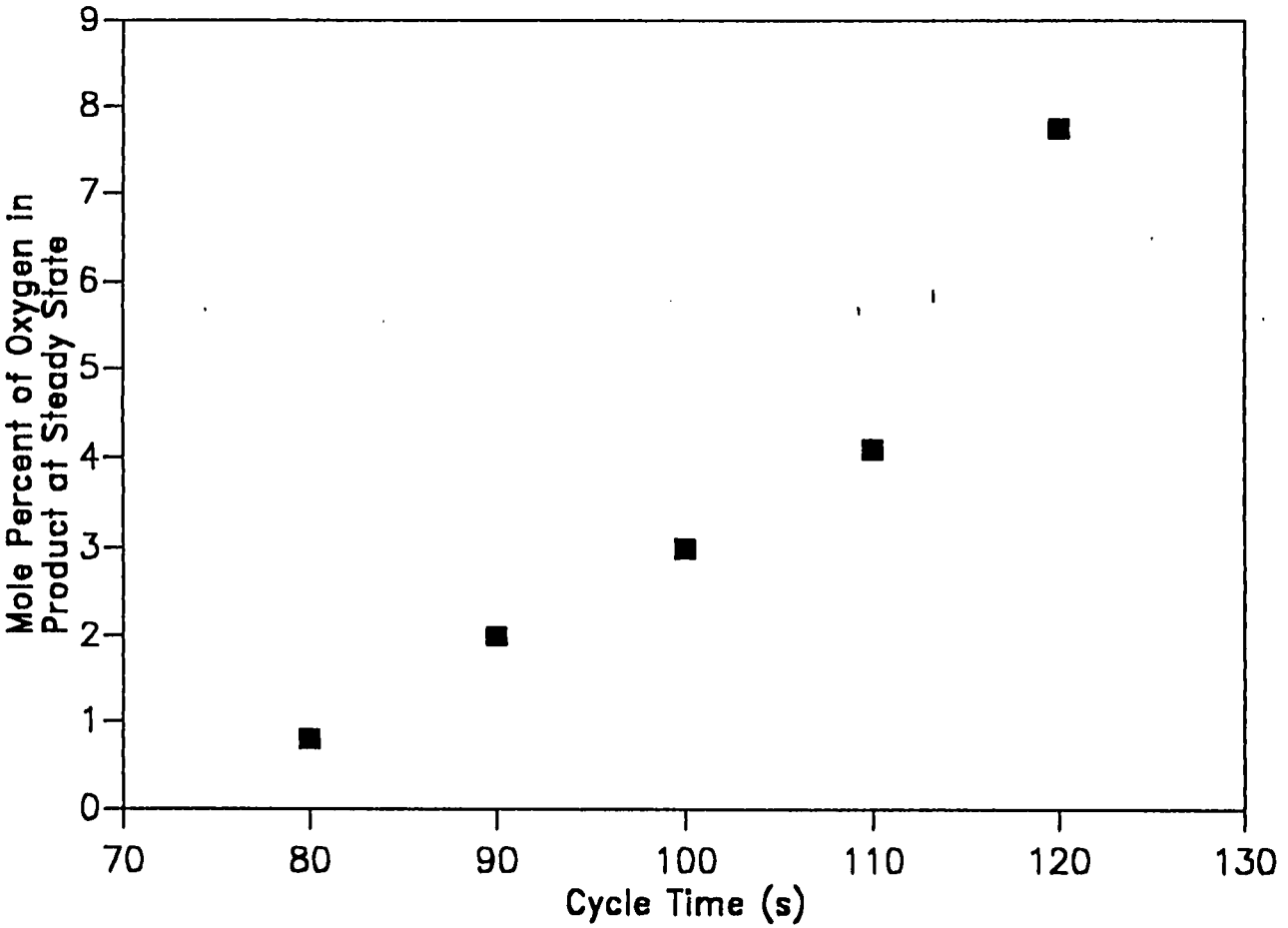

Figure 6.19 Effect of Cycle Time on Separation of O_2 and N_2 using 4A-zeolite and N_2 as Purge. ($P_H/P_L = 2.02$, $L/v_H = 26.66s$, $v_H/v_L = 0.98$)

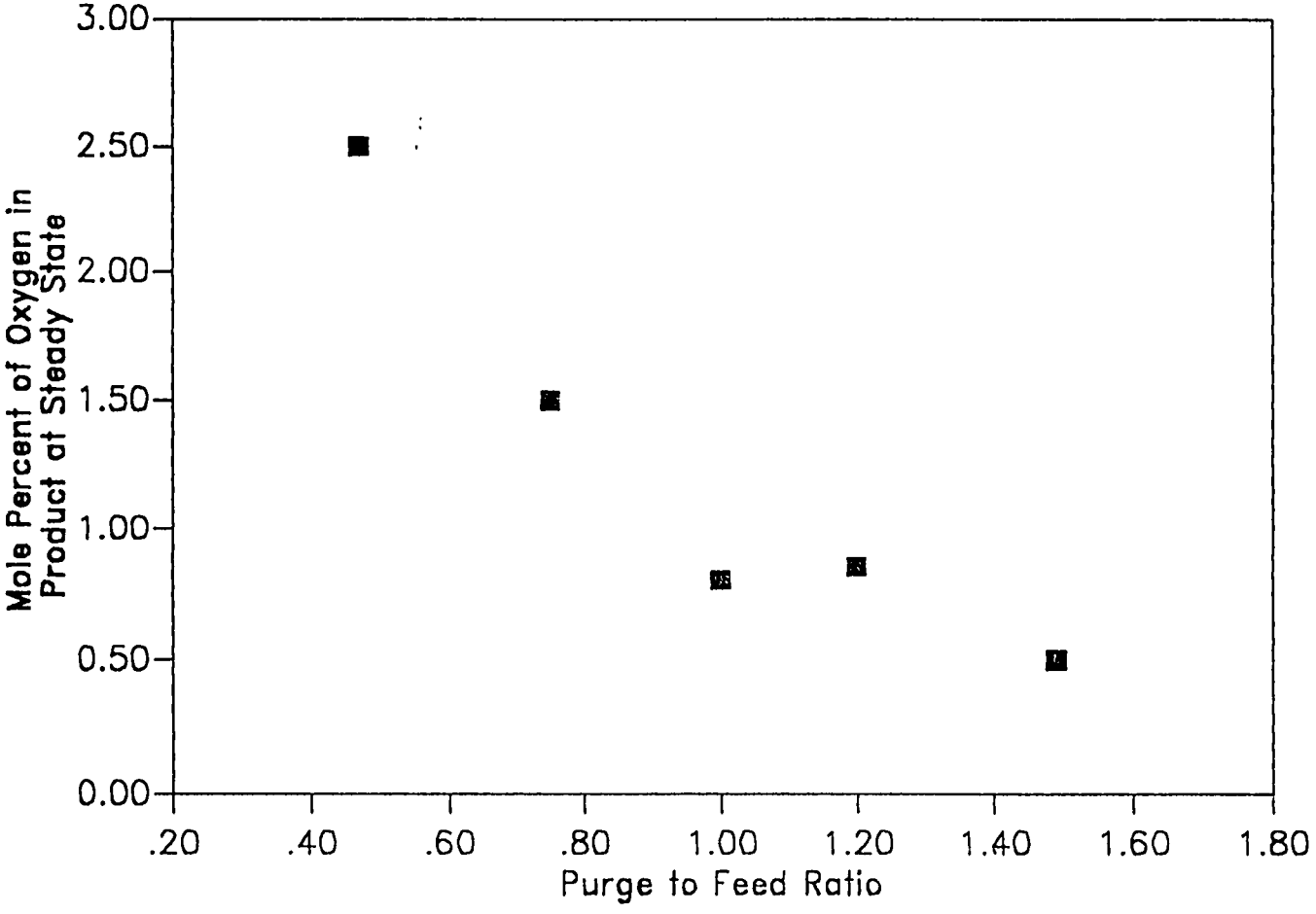

Figure 6.20 Effect of Purge to Feed ratio on Separation of O_2 and N_2 using 4A-zeolite and N_2 as Purge. (Cycle Time = 80s, P_H/P_L = 2.02 L/v_H = 26.66s)

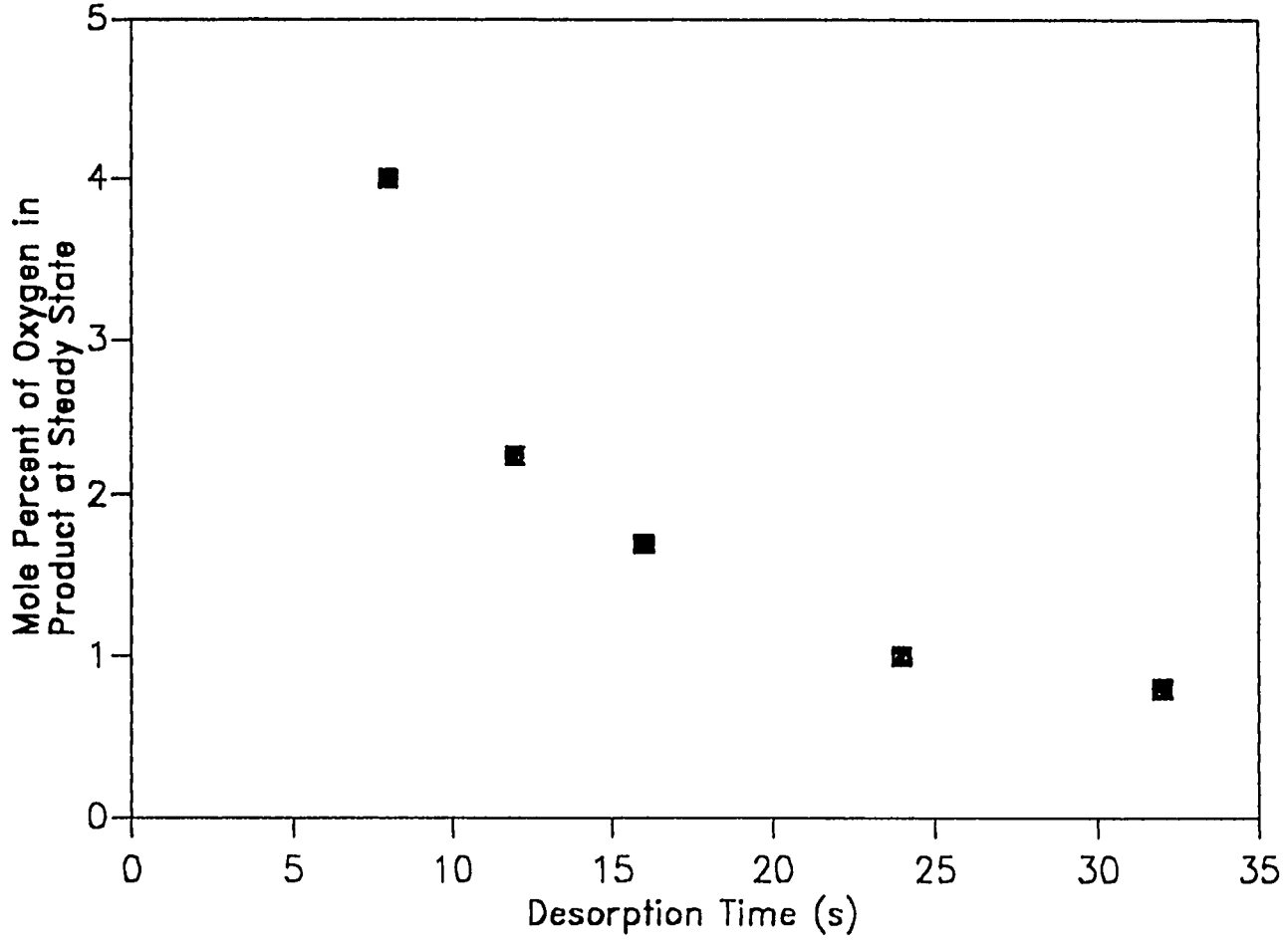

Figure 6.21 Effect of Desorption Time on Separation of O_2 and N_2 using 4A-zeolite and N_2 as Purge. (P_H/P_L = 2.02, L/v_H = 26.66s, v_L/v_H = 1.00)

6.5 CONCLUSIONS OF PSA STUDY :

The effect of L/r_{μ} , purge to feed ratio, cycle time, desorption time on air separation over CMS, 4A and 5A zeolite using a single column PSA process were investigated and the results have been summarized in Figures 6.1-6.21 and in Tables 6.1-6.5.

The results from the analysis of air separation of PSA on a CMS show that a fairly high purity nitrogen product (> 98%) can be easily obtained. The oxygen concentration in the product is found to decrease with increase in desorption time, purge to feed ratio and L/r_{μ} ratio. The residual oxygen concentration is found to pass through a minimum value of about 1.60% at a cycle time of 90s. Similar type of behavior is seen in pressure ratio the minimum value of oxygen is found to be about 2.0% at a pressure ratio of 3.04. If the pressure ratio is increased or decreased from this value the oxygen concentration in the product increases indicating lower concentration of residual nitrogen and hence lower separation performance.

The theoretical model of Farooq and Ruthven [69] was used after minor modification to predict the results for air separation on Carbon Molecular Sieve. The model predictions agree reasonably well with the experimental data.

Experimental studies of PSA air separation on a 5A-zeolite reveal that efficient separation can be achieved to yield a oxygen product containing 4-5 % residual nitrogen. The oxygen concentration in the product stream increases with

increase in desorption time, purge to feed ratio and L/ r_p ratio. On the other hand increase in the cycle time and high and low pressure ratio decreases the concentration of oxygen in the product.

In case of 4A-zeolite using oxygen as purge the results are evident that a product containing 88 % oxygen can be obtained. Increase in cycle time or pressure ratio decrease the percentage of oxygen in the product, while increase in purge to feed ratio, L/ r_p and desorption time increases the percentage of oxygen. Hence increase of purge to feed ratio, L/ r_p and desorption time favour the product purity. If we use nitrogen as purge for the production of nitrogen on 4A-zeolite, it is found that increasing either the L/ r_p , desorption time or purge to feed ratio decreases the percentage of oxygen and we get purer product stream, whereas increasing the cycle time or pressure ratio increases the percentage of oxygen in the product and therefore decreases the purity of product.

CHAPTER 7

RECOMMENDATIONS OF FURTHER STUDY

In light of the results from the present study the following recommendations are made for future work.

(*i*) The present study was restricted to a single column PSA process. In practice two columns or even multibed systems are quite often used and therefore the work can be extended to study such systems.

(*ii*) In real systems vacuum desorption is used for purging many PSA systems. The effect of vacuum on process performance can be studied for various adsorption pressures.

(*iii*) The present system can be easily used to test the separation of other gas mixtures (e.g. $CH_4 - N_2$ on CMS, $CH_4 - N_2$ on 4A zeolite).

(*iv*) The theoretical model used in the present study is over simplified and can not be applicable at large cycle times. A detailed simulation model should be prepared for a single column PSA process to make better predictions.

(*v*) The present system was operated under isothermal conditions at room temperature. Some systems may require studies at high temperatures, which can be very easily done with the present system.

LIST OF SYMBOLS

A°	:	Angstrom, unit , 10^{-8} cm
a	:	Activity of the sorbate at a point where its concentration is C
a_p	:	External area per unit volume of the particle.
b	:	Langmuir constant, g. mol/cc
c	:	gas phase concentration, g. mol/cc
C	:	Sorbate concentration in bulk phase, g. mol/cc
$\overline{C}$	:	Average concentration in gas phase, g. mol/cc
C_o	:	Initial inlet concentration, g. mol/cc
C_L	:	Transformed concentration variable at column outlet.
C^*	:	Concentration of labelled species at a point where the concentration of the unlabelled species is C, g. mol/cc
D	:	Intrinsic diffusion coefficient, cm^2 / sec
D^*	:	Trace Diffusion coefficient, cm^2 / sec
D_{AB}	:	Mutual Diffusion coefficient, cm^2 / sec
D_A, D_B	:	Intrinsic or Self Diffusion Coefficient for Component A, B cm^2 / sec
D_A^*, D_B^*	:	Two tracer diffusion coefficients for component, A, B. cm^2 / sec
D_c	:	Micropore diffusivity, cm^2 / sec

D_k	:	Knudsen diffusion coefficient, cm^2 / sec
D_L	:	Axial dispersion coefficient, cm^2 / sec
D_m	:	Molecular diffusivity , cm^2 / sec
D_p	:	Pore diffusivity, cm^2 / sec
D_o	:	Preexponential factor, cm^2 / sec
E	:	Diffusional activation energy, kcal mole
G	:	Purge to feed velocity.
$-\Delta H_o$	:	Limiting heats of adsorption at low coverage, kcal mole
K_c, K_p	:	Dimensionless Henry's law adsorption equilibrium constant
k_f	:	External fluid film mass transfer coefficient, cm sec
K_F	:	Langmuir type equilibrium coefficient
K_o	:	Preexponential factor
L	:	Column length, cm
L_{AA}	:	Straight coefficient in irreversible thermodynamic formulation
L^*_{AA}	:	Cross coefficient between traced and untraced molecule of A.
M	:	Cation of valence n
M_A, M_B	:	Molecular weight of two species of gases, A, B
m_n	:	nth moment of peak, defined by equation (3.19).
n	:	Valence number
N	:	Nusselt number
P	:	Total pressure, atm
P_H	:	High pressure (Adsorption) flow, atm

P_L	:	Low pressure (Desorption) flow, atm
P_i^*	:	Equilibrium partial pressure, atm
q_i	:	Amount adsorbed of component 'i', g.mol/cc
q	:	Local adsorbed sorbate concentration in particle, g.mol cc
$\overline{q}$	:	Average sorbate concentration in particle, g.mol cc
$\overline{Q}$	:	Sorbate concentration averaged over a particle, g.mol/cc
r_c	:	Crystal radius, cm
r_A	:	Macropore radius, cm
R_e	:	Reynold number
R_p	:	Radius of particle, cm
R	:	Gas constant, cal/mole °K
S	:	Laplace transform variable
t	:	Time, s
T	:	Absolute temperature, °K
u	:	Equivalent interstitial velocity for CCF model, cm/s
Sc	:	Schmidt number
Sh	:	Sherwood number
t_H	:	Duration time for high pressure flow, s
t_L	:	Duration time for low pressure flow, s
u	:	Superficial velocity, cm/sec.
$-\Delta U_o$	:	Internal energy change on sorption, kcal/mole
v	:	Interstitial velocity, cm/sec

W	:	Number of water molecules
x,y	:	Number of aluminium and silicon tetrahedron respectively
X_A	:	Mole fraction of component 'A' in adsorbed phase at equilibrium.
X_B	:	Mole fraction of component 'B' in adsorbed phase at equilibrium.
Y_A	:	Mole fraction of component 'A' in fluid phase at equilibrium.
Y_B	:	Mole fraction of component 'B' in fluid phase at equilibrium.

Greek Symbols

α	:	Defined by equation (4.14).
α_{AB}	:	Separation factor
γ_1,γ_2	:	Constant in equation (3.6).
$\delta(t)$	:	Pulse function.
ε	:	Bed voidage
ε_p	:	Pellet porosity
μ	:	First moment of chromatographic response
μ'	:	Apparent residence time, sec
σ^2	:	Variance of response peak
σ	:	Force constant in the Lennard-Jones potential function
τ	:	Tortuosity factor
Ω	:	Collision integral

Subscripts

A	:	Equivalent for CCF model for component A.
$A0$	:	Component A in feed.
AH, AL, AS	:	Component A at high pressure, purge pressure, saturation.
B	:	Equivalent for CCF model for component B.
BH, BL, BS	:	Component B at high pressure, purge pressure, saturation.
H	:	High pressure flow
L	:	Purge flow
OH	:	At the inlet of high pressure flow.
OL	:	At the inlet of purge flow.

REFERENCES

[1] Yang, R.T., *'Gas Separation by Adsorption Process'*, Butterworths, New York, (1984).

[2] Ruthven, D.M., *'Principle of Adsorption and Adsorption Process'* John Wiley, New York, (1987).

[3] Milton, R.M., *'Molecular Sieve Adsorbents'*, U.S. Patent 2, 882, 244 (1959).

[4] Skarstrom, C.W., *'Method and Apparatus for Fractionating Gaseous Mixtures by Adsorption'*, U.S. Patent 2, 944, 627 (1960).

[5] Skarstrom, C.W. *'Heatless Fractionating of Gases over Solid Sorbents'*, Recent Development in Separation Science, 2, Cleveland, CRC Press (1972).

[6] Barkhordar, P.M., *SRI report No. 18, Energy Tech. Econ. Prog.* (1981).

[7] Ruthven D.M., M.M. Hassan and N.S. Raghavan, *Chem. Engg. Sci.*, 41(5), 1325, (1986).

[8] Chihara, K. and Suzuki. M., *Carbon.*, 17, 339, (1979).

[9] Knoblauch. K., *Chem. Eng. Sci.*, 5, 87, (1978).

[10] M. W. Ackley and R. T. Yang, *AIChE J.*, 36, 8, 1229, (1990).

[11] S.P Nandi and R.L Walker, *Fuel* 54, 169, (1975).

[12] J. Koresh and A. Saffer *J. Chem. Soc. Faraday Trans. I.*, 76, 2472, (1980).

[13] R.L Patel, S.P Nandi, and R.L Walker, *Fuel*, 51, 47, (1972).

[14] H. Juntgen, Ber. Bunsenges., ***Physik. Chem.*** 79, 747, (1975).

[15] D.L. Trimn, ***Carbon***, 15, 273, (1977).

[16] H. Juntgen, ***Carbon***, 15, 273, (1977).

[17] Barrer, R.M., ***'Zeolite and Clay Minerals as Sorbents and Molecular Sieves'***, Academic Press, London (1978).

[18] Breck, D.W., ***'Zeolite Molecular Sieves, Structure, Chemistry and Use'*** John Wiley and Sons, New York, (1974).

[19] Shoemaker, D.P. and Seff, K. ***Acta Cryst***, 22, 162, (1967).

[20] Reed, T.B and Breck, D.W., ***J. Amer. Chem. Soc.*** 78, 23, 5972, (1956).

[21] Shoemaker, D.P., and Broussard, L., ***J. Amer. Chem. Soc.*** 82, 1041, (1960).

[22] Smith, T.V., ***Amer. Mineral Soc. Spec.***, Paper 1, 281, (1963).

[23] N. Haq., ***Ph. D Thesis, University of New Brunswick, Canada***, June, (1983).

[24] Yanagida, R.Y., Amaro, A. and Seff, K., ***J. Phys. Chem***, 77b, 805, (1973).

[25] Satterfield, C.N., ***'Mass Transfer Heterogeneous Catalysis'***, M.I.T. Press (1975)

[26] Bird, R.B., Stewart, W.E. and Lightfoot, E.N. ***'Transport Phenomena'***, John Wiley and Sons, New York, (1960).

[27] Treybal, R.E., ***'Mass Transfer Operation'***, McGraw-Hill, 2nd Ed., (1968).

[28] Crank, J., ***'The Mathematics of Diffusion'***, Oxford, (1956).

[29] Ash, R. and R.M. Barrer., ***J. Surface Sc.***, 8, 461, (1967).

[30] Karger., ***J. Surface Sc.***, 36, 797, (1973).

[31] Darken,L.S., ***Trans. AMIE.***, 175, 184, (1948).

[32] Lapidus, L. and Amundson, N.R., ***J. Phys. Chem.***, 56,984, (1952).

[33] Kubin, M., ***Cllect. Czech. Chem. Commun.***, 30, 1104, (1965).

[34] Kucera, E. ***J. Chromatog.***, 19, 237, (1965).

[35] Suzuki, M. and Smith, J.M., ***Chem. Sci.***, 26, 221, (1971).

[36] Hashimoto, N. and Smith, J.M., ***Ind. Eng. Chem. Fund.***, 12, 353, (1973).

[37] Haynes, W.H. and Sharma,P.N., ***Adv. Chem. Ser.***, 133, 205, (1974).

[38] Haynes, W.H. and Sharma P.N., ***AIChE J.***, 193, 5 1043, (1973).

[39] Ruthven, D.M. and Shah, D.B., ***AIChE J.***, 23, 6, 804, (1977).

[40] Roberts, P.V. and York, R., ***Ind. Eng. Chem. Proc. Des. Develop.***, 6, 516, (1967).

[41] Sargent, R.W.H., and Whitford, C.J., ***Adv. Chem. Ser.***, 102, 247, (1971).

[42] Lee L.K. and Ruthven D.M., ***Ind. Eng. Chem.Fund.***, 16, 290, (1977).

[43] M.J. Martin and R.L.M. Synge., ***Biochem.J.***, 35, 1359, (1941).

[44] W. Boetsma-Klin and J.A Moulijin., ***Chem. Eng. Sci.***, 34, 959, (1982).

[45] T.S. Chou. and L.L. Hedgedus., ***AIChE J.***, 24, 255, (1978).

[46] A. Rasmuson., ***Chem. Eng. Sci.***, 37, 787, (1982).

[47] Edward, M.F and Richardson J.F., ***Chem. Eng. Prog.***, 23, 109-123, (1968).

[48] Stewart H. A., and Heck J.L., ***Chem. Eng. Prog.***, 65 (9), 78, (1969).

[49] G.E Keller and R.L.Jones., *'In Adsorption and Ion Exchange with Synthetic Zeolites, W.H Flank(ed)'*. Am. Soc. Washington D.C. 225. (1980)'

[50] P.H Turnockand R.H Kadlec., *AIChE J.*, 17, 335, (1971).

[51] Mitchell, J.E and Shendalman, L.H., *AIChE Symp. Ser.*, 69 (134), 25, (1973).

[52] Lee H. and Stahl, D.E., *AIChE Symp. Ser.*, 69, (134), (1973).

[53] Landolt, G. R., and Kerr, G.T., *'Separation and Purification Methods'* Ed. Perry, E.S., et al., 2, 283, Marcel Dekker, N.Y (1974).

[54] Wankat P.C., *Separ. Sci.* 9, 2, 85, (1974).

[55] Bird, G., and Granville, W.H., *Adv. Cryog. Eng.*, 19, 463, (1974).

[56] Weaver, K., and Hamrin, C. E., *Chem. Eng. Sci.*, 29, 9, 1873, (1974).

[57] Wong, Y.W., and Hill, F.B., *Chem. Eng. Commun.*, 15, 5-6, 343, (1980).

[58] Wong, Y.W., Hill, F.B., and Chan Y.N., *Sep. Sci. Tech.*, 15, 3, 423, (1982).

[59] Fernandez, F.G, and Kenney, C.N., *Chem. Eng. Sci.*, 38, 6, 827, (1983).

[60] Carter, J.W., and Wyszynski, *Chem. Eng. Sci.*, 38, 7, 1093, (1983).

[61] Cheng, H.C., and Hill, F.B., *AIChE J.*, 31, 1, 95, (1985).

[62] Whitley, M.D., and Hamrin, *J. ACS. Symp. Ser.*, 135, 261, (1980).

[63] Tondeur, D., and Wankat, P.C., *Sep. and Pur. Methods.*, 14, 2, 157-212, (1985).

[64] Cen, P.L., Chen, W.N., and Yang, R.T., *Ind. Eng. Chem. Pr. Design.*

Dev., 24, 1201-1208, (1985).

[65] Raghavan, N.S., M.M Hassan, and D.M. Ruthven., *AIChE J.*, 31, 3851, (1985).

[66] Hassan M.M., N.S. Raghavan, D.M Ruthven, and H.A Boniface., *AIChE J.*, 31, 2008, (1985).

[67] Raghavan, N.S., and D.M. Ruthven., *AIChE J.*, 31, 2017, (1986).

[68] Chihara, M. and Suzuki, M., *AIChE Symp. Ser.*, 81, 67-737, (1985).

[69] S. Farooq and Ruthven, D.M., *Chem. Eng. Sci.*, 45, 1, (1990).

[70] Cassidy, R.T., Holmes, E.S., *AIChE Symp. Ser.*, 80, 233, 68, (1984).

[71] M.M Hassan, N.S. Raghavan and D.M Ruthven., *Chem. Eng. Sci.*, 41, 5, 1333, (1986).

APPENDIX-A

SAMPLE CALCULATIONS

CALCULATION OF BED VOIDAGE

Bed voidage (ε) for CMS can be calculated by the following method :

Length of the column = 49.0 cm

Diameter of the column = 1.0 cm

Weight of empty column = 287.7 gm

Weight of empty column + CMS = 315.8 gm

Weight of CMS = 28.1 gm

Volume of column = V = 41 cm^3

Density of CMS = 1.21 gm/cc

$$\varepsilon = \frac{V - (\textit{weight of CMS} / \textit{density of CMS})}{V}$$

$$\varepsilon = \frac{41.0 - (28.1 / 1.21)}{41.0}$$

$$\varepsilon = 0.433$$

SAMPLE CALCULATION OF SORPTION PARAMETERS USING MOMENT METHOD

The first moment, μ and the variance σ^2 were calculated by equation 3.21 and 3.22 from the pulse response curve using a computer program as given in Appendix-B. The equilibrium constant, K_p was calculated from the slope of the plot μ vs $1/v$. using equation 3.23.

The micropore diffusivity D_c/r_c^2 can be obtained from the plot of $(\sigma^2/2\mu^2)L/v$ vs $1/v^2$ by using the equation 3.25.

I. CALCULATION OF K_p VALUE :

The value of K_p was calculated at 50° C of nitrogen by using the Figure 3.3, and equation 3.23. From the slope of the plot μ vs 1/v , the equilibrium constant, K_p was extracted.

$$\text{Slope} = L\left[1 + \frac{1-\varepsilon}{\varepsilon}K_p\right]$$

$$522.35 = 49\left[1 + \left(\frac{1 - 0.433}{0.433}\right)K_p\right]$$

$$K_p = 7.38$$

II. CALCULATION OF DIFFUSIVITY CONSTANT

(a) From the Plot of $(\sigma^2/2\mu^2)L/v$ vs. $1/v^2$:

Equation 3.25 was used for calculating diffusivity. The values of slope and intercept of plots $(\sigma^2/2\mu^2)L/v$ vs. $1/v^2$ for this system were obtained from Figure 3.3, at temperature 50° C of Nitrogen.

$$\text{Intercept} = \frac{\varepsilon}{15K_p(1-\varepsilon)(D_c/r_c^2)}$$

$$D_c/r_c^2 = \frac{\varepsilon}{15K_p(1-\varepsilon)} \div \textit{Intercept}$$

$$D_c/r_c^2 = \frac{0.764}{15*7.38*4.90}$$

$$D_c/r_c^2 = 1.40\text{E-}3\ s^{-1}$$

(b) From the Plot of HETP vs. v :

The value of D_c/r_c^2 was calculated from equation 3.26, by using the Figure 3.9, at 50° C of Nitrogen.

$$\text{HETP} = A + 2v\frac{\varepsilon}{15K_p(1-\varepsilon)(D_c/r_c^2)}$$

$$\text{Slope} = \frac{2\varepsilon}{15K_p(1-\varepsilon)(D_c/r_c^2)}$$

$$(D_c/r_c^2) = \frac{2\varepsilon}{15K_p(1-\varepsilon)*slope}$$

$$(D_c/r_c^2) = \frac{2*0.763}{15*7.38*9.71}$$

$$(D_c/r_c^2) = 1.435\text{E-}3\ s^{-1}$$

III. CALCULATION OF ΔU_o, ΔH_o, K_o.

The values of ΔU_o, ΔH_o, K_o, were calculated from a plot of ln K_p vs. 1/T as shown in Figure 3.5 on semi-logarithmic scale for nitrogen.

(*i*) $K_p = K_o e^{-\Delta U_o / RT}$

$\ln K_p = \ln K_o - \Delta U_o/RT$

$Slope = -\Delta U_o/R$

$941.17 = -\Delta U_o/1.987$ (*By Regression*)

$-\Delta U_o = 1.87$ *kcal/mole*

Intercept = $\ln K_o$

$\ln K_o = -0.916$ (*By Regression*)

$K_o = 0.40$

$K_p = 0.40\, e^{941.17/T}$

(*ii*) $-\Delta H_o = -\Delta U_o + RT$ (T = Average Temperature)

$-\Delta H_o = 1870.10 + 1.987 * 340$

$-\Delta H_o = 2.54$ *kcal/mole*

IV. CALCULATION OF D_o/r_c^2 and E .

The values of D_o/r_c^2 and E were calculated from a plot of ln D_c/r_c^2 vs. 1/T as shown in Figure 3.8 on semi-logrithimic scale for nitrogen.

$$D_c/r_c^2 = D_o/r_c^2 e^{-E/RT}$$

$$Slope = \frac{-E}{R} \approx \frac{ln(D_2/D_1)}{(1/T_2 - 1/T_1)} = -2766 \text{ (By Regression)}$$

E = 5.496 kcal/ mole

Intercept = ln (D_o/r_c^2) =1.82 (By Regression)

$D_o/r_c^2 = 6.82\ s^{-1}$

$D_c/r_c^2 = 6.82\ e^{-2.76/T}$

APPENDIX-B

COMPUTER PROGRAM

Computer Program for Calculation of First and Second Moment from the Chromatographic Peak.

```
      DIMENSION
           D(400),F(400),C(400),T(400),CT(400),CTMU(400)
           REAL V(99),SM(99),HETP(99),ID,L
           DOUBLE                                    PRECISION
     FSL,FIN,FM(99),FMF(99),VIN(99),EQ(99)
           DOUBLE PRECISION SSL,SIN,LHS(99),VIN2(99)
C    L IS THE COLUMN LENGTH IN CM
C    TEMP IS THE TEMPERATURE IN DEGREE C
C    EPSI IS THE BED VOIDAGE
C    ID IS INSIDE DIAMETER OF THE COLUMN
C    JT IS THE TOTAL NUMBER OF RUNS
C    COLUMN#3
C    MESH = 425 MICRON
C    TEMP = 50C
C
           L = 49.0
           TEMP = 50.0
           EPSI = 0.433
           ID = 1.0
           FAC = 1.0
```

```
      JT=4
C
C     WRITE  GAS SOLID PAIR
C
      WRITE(6,*)'SIEVE  TYPE:CARBON  MOLECULAR
SIEVES:'
      WRITE(6,*)'SAMPLE GAS:NITROGEN'
      WRITE(6,*)'TEMP=50.0'
C     NR IS THE RUN NO.
C     N IS NUMBER OF DATA POINTS FOR EACH RUN
C     Q IS THE VOLUMETRIC FLOWRATE IN CU.CM PER
SECOND
C     RECD IS RECORDER SPEED IN CM PER MINUTE
      DO 777 J=1,JT
      READ(5,*)NR,N,Q,RECD
      WRITE(6,*)'      NR      N      Q
     &   RECD'
      WRITE(6,*)
      WRITE(6,*)NR,N,Q,RECD
      SPEED=RECD
      AREA=3.1416*((ID/2.0)**2)
      N1=N-1
      TK1=273.0+21.0
```

```
      TK2=273.0+TEMP
      QS=Q*FAC*60.0
      QA=QS*TK2/TK1
      V(J)=QA/AREA/EPSI/60.0
      VIN(J)=1/V(J)
      VIN2(J) =1/(V(J)**2)
C
C     READ DATA AS DISTANCE AND CONCENTRATION
C     D(I) DISTANCE IN CM
C
      DO 300 I=1,N
      READ(5,*)D(I),F(I)
 300  CONTINUE
      EM= (F(N)-F(1))/(D(N)-D(1))
      CM= (F(1)*D(N)-F(N)*D(1))/(D(N)-D(1))
      DO 302 I=1,N
 302  C(I)= F(I) - (EM*D(I)+CM)
C
C     CONVERTING  DISTANCES TO TIME UNITS AND
      CALCULATING
C     C*T VALUES
C
      DO 301 I=1,N
```

```
      T(I) = D(I)/(SPEED/60.0)
301   CT(I) = C(I)*T(I)
C
      WRITE(6,*) '
      WRITE(6,*) '
      WRITE(6,*) '
      WRITE(6,*) '
      WRITE(6,*) RUN NO:',J
      WRITE(6,*) SIEVE TYPE: CARBON MOLECULAR
SIEVE'
      WRITE(6,*) SAMPLE GAS: NITROGEN'
      WRITE(6,*) CARRIER GAS: HELIUM'
      WRITE(6,*) CARRIER GAS FLOW:',QS,'SSCM MIN'
      WRITE(6,*) '
      WRITE(6,*) '
      WRITE(6,*) '
      WRITE(6,*)          D(I)          T(I)
      &TIME          CONCENTRATION'
      WRITE(6,*)'
      &(SECS)'
      DO 111 I = 1,N
 111  WRITE(6,*)D(I),F(I),T(I),C(I)
C
```

```
C     CALCULATION OF FIRST AND SECOND
MOMENTUM
C     FIRST MOMENT
C
      SUM1 =0.0
      SUM2 =0.0
      DO 10 I = 1,N1
      SUM1 =SUM1 + (T(I + 1)-T(I))*(C(I + 1) + C(I)) 2.0
      SUM2 =SUM2 + (T(I + 1)-T(I))*(CT(I + 1) + CT(I)) 2.0
10    CONTINUE
      EME(J) = SUM2 SUM1
      EMC =(34.06*VIN(J)) + 3.75
      EM(J) = EME(J)-EMC
C
C     SECOND MOMENT
C
      DO 20 I = 1,N
      CTMU(I) = C(I)*((T(I)-EM(J))**2)
 20   CONTINUE
      SUM3 = 0.0
      DO 30 I = 1,N1
      SUM3 = SUM3 +
(T(I + 1)-T(I))*(CTMU(I + 1) + CTMU(I)) 2.0
```

```
 30   CONTINUE
      SM(J)=SUM3/SUM1
C
C     CALCULATION OF HETP AND LHS
C
      HETP(J)=(SM(J)*1.)/(FM(J)**2)
      LHS(J) = (SM(J)*1.)/((FM(J)**2)*2.0*V(J))
777   CONTINUE
      WRITE(6,*)
      WRITE(6,*)
      WRITE(6,*)
      WRITE(6,*)
      DO 201 I=1,IT
 201  EQ(I)=((FM(I)*V(I).L)-1.0)*EPSI/(1.0-EPSI)
C
      DO 202 I=1,IT
C
 202          WRITE(6,*) FOR          RUN ,I,EQUILIBRIUM
CONSTANT = ,EQ(I)
      WRITE(6,104)
 104  FORMAT(1X,'      V          1/V       1ST  MOMENT
2ND
     & HETP       LHS      1/V**2',/)
```

```
      DO 333 I = 1,JT
 333
WRITE(6,105)V(I),VIN(I),FM(I),SM(I),HEIP(I),LHS(I),VIN2(I)
 105  FORMAT(1X,7(3X,E10.3))
 999  CONTINUE
      STOP
      END
```